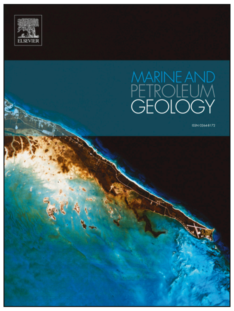

Reef building and carbonate production modes in the west-central Tethys during the Cenozoic

Luis Pomar, Juan I. Baceta, Pamela Hallock, Guillem Mateu-Vicens, Daniela Basso

PII: S0264-8172(17)30101-0

DOI: 10.1016/j.marpetgeo.2017.03.015

Reference: JMPG 2853

To appear in: *Marine and Petroleum Geology*

Received Date: 9 August 2016

Revised Date: 28 February 2017

Accepted Date: 13 March 2017

Please cite this article as: Pomar, L., Baceta, J.I., Hallock, P., Mateu-Vicens, G., Basso, D., Reef building and carbonate production modes in the west-central Tethys during the Cenozoic, *Marine and Petroleum Geology* (2017), doi: 10.1016/j.marpetgeo.2017.03.015.

Reef building and carbonate production modes in the west-central Tethys during the Cenozoic

Luis Pomar[a,*], Juan I. Baceta[b], Pamela Hallock[c], Guillem Mateu-Vicens[a,e], Daniela Basso[d]

a: Catedra Guillem Colom, University of the Balearic Islands, Ctra. Valldemossa km 7.5; E-07122 Palma de Mallorca, Spain (luis.pomar@uib.es)

b: Dpt. Stratigraphy and Paleontology, The University of the Basque Country, E48940 Leioa, Bizkaia, Spain. (juanignacio.baceta@ehu.eus)

c: College of Marine Science, University of South Florida, 140 Seventh Ave. S., St. Petersburg, FL 33701-5016, U.S.A (pmuller@usf.edu)

d: Dept. of Earth and Environmental Sciences, University of Milano-Bicocca , Piazza della Scienza 4, 20126 Milano, Italy (daniela.basso@unimib.it)

e: Dept. of Biology, University of the Balearic Islands, Ctra. Valldemossa km 7.5; E-07122 Palma de Mallorca, Spain (guillem.mateu@uib.es)

Corresponding author: Luis Pomar,
Catedra Guillem Colom, University of the Balearic Islands, Ctra. Valldemossa km 7.5, E-07122 Palma de Mallorca, Spain (luis.pomar@uib.es)
Fax: 0034 971 173 184
Phone: 0034 971 173 160

CONTENT

ABSTRACT

Changing components, rock textures, lithofacies, platform types and architecture throughout time are unique characteristics of carbonate rocks. Characterizing these attributes has been approached by 1) building reference models for specific Phanerozoic intervals, 2) recognizing the climatic impact in modulating carbonate production, and 3) analyzing the influence of changing bio-geochemical conditions. The reference-model approach is mostly based on biological evolution, the climatic-impact approach emphasizes temperature, and the bio-geochemical approach considers the changes in Mg/Ca ratios and Ca^{++} concentrations in the oceans. To date, however, an analysis integrating all of these factors is still missing. The analysis presented here includes all these factors but also CO_2, which is fundamental for both photosynthesis and $CaCO_3$ precipitation.

Here we analyze the waxing and waning of Cenozoic reef limestones from the central Tethys region through several steps: 1) on the basis of rock volume, rock textures, associated sediments and light-dependent skeletal components, as records of light penetration and wave energy (depth); 2) on global environmental conditions ($\delta^{13}C$, $\delta^{18}O$, pCO_2, temperature); and 3) on the basis of functionality, nutritional requirements and available resources.

Through the Cenozoic, water motion, whether induced by surface or internal waves or by currents, increased as the thermal gradients strengthened, both with depth and with latitude. Active water motion is essential for plankton catchers such as corals, but less so for many larger benthic foraminifers (LBF). Pycnoclines in the meso-oligophotic zone would then favor the benthic plankton catchers such as corals, but would be detrimental for many LBF. Warm temperatures favored LBF. The Eocene LBF families predominated during lowering of atmospheric pCO_2 by using respiratory CO_2 to enhance the symbiont production of photosynthates under oligotrophic conditions and limited turbulence, whereas the Miocene families had to adapt to a progressive increase in turbulence. The eurythermal coralline red algae, however, became preponderant producers in the mesophotic zone during times when the $\delta^{13}C$ was relatively high. This explains two apparent paradoxes: 1) corals thrive best when the Earth's high latitudes cool, and 2) the dominance of corals and LBF is inversely correlated, despite they both require tropical conditions and have similar trophic strategies (mixotrophy).

Key words: Cenozoic; coral buildups; LBF; red algae; seagrass; carbonate production

1 - Introduction

The evolution of reefs, reef organisms and reef attributes though time has long been a focus of research (e.g., Heckel, 1974; James, 1983; Fagerstrom, 1987; Wood, 1998, 1999; Stanley Jr., 2003; Kiessling et al., 1999, 2002; Flügel, 2004; Kiessling, 2009). Heckel (1974) reviewed the changing character and composition of buildups through the Phanerozoic and characterized buildups and reefs. Buildups were defined as carbonate bodies with a topographic relief above surrounding sediments, and reefs as buildups showing clear evidence of accretion in the zone of waves. Wilson (1975) differentiated three main types of carbonate buildups: framework reefs that build in a zone of turbulence, slightly deeper knoll reefs on outer slopes or ramps, and downslope mud mounds, emphasizing differences between high-energy and low-energy reefs. James (1983) expanded those categories to include stromatolites, emphasizing that the shapes of the reef-building organisms, the metazoan zonation and relative diversity, all exhibit notable differences with time.

Kiessling and co-authors applied a quantitative approach to study carbonate buildups through time. Based on a wide compilation of paleogeographic positions, ages, reef types, dimensions, environmental settings, paleontological features, and reservoir quality of the buildups, they have attempted to capture the major trends in reef evolution and properties of reef carbonates (e.g., Kiessling et al., 1999). Major challenges are inherent weaknesses in the database: 1) bias by both geological history and research intensity (Kiessling, 2006); 2) time windows that do not necessarily coincide with the changes in the biotic composition or in the buildup type; and 3) interpretative bias, as buildups were often interpreted by using models based on modern coral reefs, which are presently considered as a particular case rather than a rule in the Earth history (Wood, 1999). These semi-quantitative approaches revealed that the boom and bust character of Phanerozoic reefs does not indicate linear responses to physico-chemical changes (e.g., Kiessling et al., 2002; Flügel, 2004). Rather, threshold effects appear to influence both reef crises and expansions (Kiessling, 2009).

Even more ambitious is the “Carbonate Analogs Through Time hypothesis” (CATT hypothesis), in which Markello et al. (2008) seek to develop high-confidence, age-specific models for carbonate systems. Their goals include prediction of reservoir occurrence, composition, stratal attributes, and reservoir properties by summing the ambient conditions of the carbonate processes and Earth processes at any geologic age.

Focusing on the Cenozoic, several studies have shown the relative abundance of reef builders and other major carbonate producers through the Paleogene and Neogene (e.g., Kiessling and Baron-Szabo, 2004; Baceta et al., 2005; Pomar and Hallock, 2008; Wilson, 2008, Scheibner and Speijer, 2008; Perrin and Kiessling, 2010; Zamagni et al., 2012; Höntzsch et al., 2013). These studies have revealed several steps in the rise of coralgal associations as chief reef builders: (1) Coralgal reef communities survived the crisis at the Cretaceous-Paleogene (K-Pg) transition, and were able to construct substantial buildups by the middle Danian, only 1.5-2 Ma after the K-Pg boundary. (2) The hyperthermal event at the Paleocene-Eocene boundary resulted in a short-lived, major reef hiatus, which is now considered a global reef crisis (Kiessling and Simpson, 2011). (3) Coralgal reefs were scarce during the early-middle Eocene, coevally to the maximum spread of the Paleogene larger benthic foraminifers (LBF). (4) Reef development increased worldwide during the late Eocene and Oligocene. (5) The closure of the Tethys seaway, coeval to late Miocene global cooling, induced a latitudinal retraction of the coral reef zone and the splitting of the cosmopolitan tropical reef realm into three major reef provinces: Mediterranean, Caribbean and Indo-Pacific.

Shallow coralgal reefs disappeared in the Mediterranean province during the Messinian salinity crisis and did not recover thereafter. Although global climatic conditions are generally known, a rationale linking them with the reef types and their boom and bust pattern is still missing. Within this conceptual frame, the goal of this paper is to analyze the evolution of the coral buildups and shallow carbonate factories through the Cenozoic in the Mediterranean region.

The Cenozoic was the period of emergence of modern coral reefs, and its interpretation is enhanced by detailed knowledge of the ecological requirements of modern biotas. The abundance and quality of the outcrops in the Mediterranean region, many with almost continuous exposure along dip, reduces interpretative uncertainties and permits an unbiased study of the buildup shape and size, internal-facies architecture and position along the depositional profile. Although there are numerous examples, many with objective descriptions, we primarily base our comparative analysis on “first-hand” studies that have been directly investigated or revised by some of the authors.

Cenozoic coral buildups from the central Tethys are here analyzed through three consecutive steps: 1) on the basis of rock volume, textures, associated sediments, and light-dependence of organisms, as a proxy for water depth (i.e., light penetration and wave energy); 2) in the context of global environmental conditions (e.g., temperature gradients and carbon cycling derived from oxygen and carbon isotope records); and 3) through discussion of key processes that might constrain the waxing and waning of coral buildups (e.g., relief functionality, water chemistry and trophic requirements). This approach recognizes a fundamental aspect: carbonate producers are organisms and therefore should meet their energetic requirements for growth, metabolism, reproduction, and calcification. Moreover, the size and type of buildup depends primarily upon the accumulation of biologically controlled or induced carbonates.

2 – Methods

2.1 - Proxies for global environmental conditions

Standard proxies for climatic parameters include oceanic planktic and benthic foraminiferal oxygen (δ^{18}O) and carbon (δ^{13}C) isotopic trends, compiled from multiple sites throughout the oceans. δ^{18}O in planktic foraminifers can be used to interpret sea-surface and subsurface temperatures, while δ^{18}O in deep-sea benthic foraminifers reflects a combination of surface temperatures at deep-water source regions (e.g., high latitudes), with global ice volume as an additional influence. δ^{13}C reflects global carbon-cycle perturbations, first-order changes in deep-sea circulation patterns, and/or changes in biological productivity (Bijl et al., 2009; Cramer et al., 2009, 2011; Zachos et al., 2010; Vandenberghe et al., 2012). Despite the inherent uncertainties in these proxies (e.g., Cramer et al., 2009) and although the age estimations for the examples we present are relatively broad, some clear trends can be seen. To frame the global conditions in which different buildups predominated, we use the oxygen (δ^{18}O) and carbon (δ^{13}C) isotopes from Cramer et al. (2009), recalibrated to GTS2012 (in Vandenberghe et al., 2012) for the Paleogene, and from Zachos et al. (2001) for the Neogene.

Also important and often neglected is ambient CO_2, which directly impacts the food web. The combination of warm temperature and ample light with high atmospheric CO_2 provides potential for high rates of photosynthesis (e.g., Riebesell et al., 1993; Hein and Sand-Jansen, 1997; Riebesell, 2004). Proxies for ambient CO_2 are very diverse. Although it is accepted the atmospheric CO_2 concentrations in the early Cenozoic were higher than at present, there is disagreement regarding their magnitude (particularly during the Paleocene), the timing of the subsequent long-term decline and the mechanisms that are most important for the control of CO_2 concentrations over geological timescales (Royer et al., 2012).

Beerling and Royer (2011), when claiming reconstructions are heading towards consensus, present a highly variable data set based on compilation of four proxies. Two are terrestrial-based; abundance of stomatal pores on fossil leaves and carbon isotope composition of carbonates in fossil soils. The other two are marine-based, carbon isotope composition of phytoplankton and the boron isotope composition of fossil foraminifers. Such a mixture of proxies produces a complex data set in which multiple CO_2 values can occur in the same time intervals. These inconsistencies hamper a straightforward application of such data. Nevertheless, different proxies, taken separately, do show the same pattern of change, although details and absolute values are not comparable. Particularly useful proxies include the boron-isotope ratios of ancient planktic foraminifers to estimate the pH of surface-layer seawater (Pearson and Palmer, 2000), the secular oscillation of Mg/Ca ratio in seawater and in the mineralogy of primary oceanic carbonate sediments (Demicco et al., 2003); and the stable carbon isotopic values of di-unsaturated alkenones extracted from deep-sea cores (Pagani et al., 2005).

2.2 – Paleodepth

The bathymetric position of buildups has been constrained using light-dependent communities and lithofacies distribution within the buildups. In wave-dominated systems, both hydraulic competence and light penetration decrease exponentially with depth. The lower limit of light penetration (base of the photic zone) also co-varies with latitude; it is deeper in the tropics and sub-tropics and shallower at higher latitudes due to changes in the angle of solar irradiance (Liebau, 1984; Lüning, 1990). Because of their different light requirements that influence depth ranges, red and green calcareous algae tend to develop distinct distribution patterns with depth and thus become the best paleobathymetric indicators (Flügel, 2004). The depth range of modern seagrasses and non-dasyclad green algae can be used to define the euphotic zone. The term “chlorocline” (sensu Liebau, 1984) is defined as the lower limit of in situ green algae. Rhodophyceae grow at greater depths than other algae, thus we use the term “rhodocline” (sensu Liebau, 1984), the deepest occurrence of in situ coralline red algae (**Fig.** 1), to identify the lower limit of the oligophotic zone. Consequently, the distinction between “euphotic” (good light and, in open seas, commonly high wave energy), “mesophotic” (sufficient light for coral growth, commonly below normal wave base), “oligophotic” (sufficient light for coralline red algal growth), and “dysphotic” (absence of sufficient light for photosynthesis) and “aphotic” zones becomes a useful tool in analyzing carbonate platforms and reef buildups (Pomar, 2001a, b).

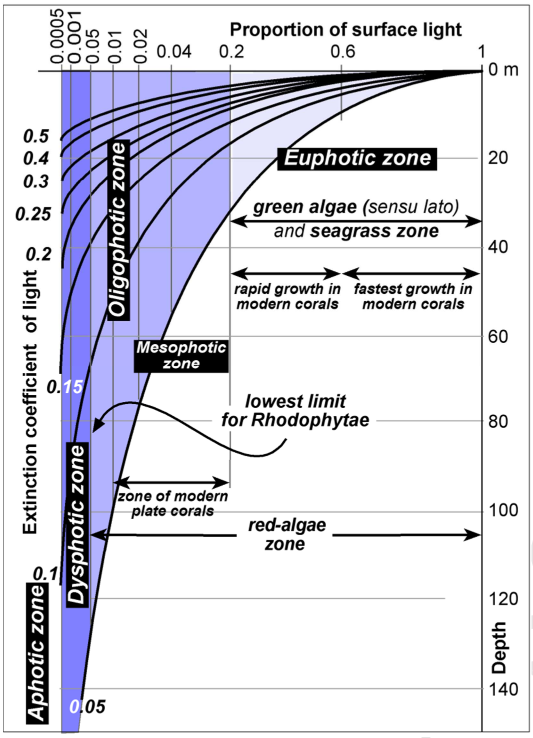

Fig. 1. - Bathymetric light zones and their lower boundaries based on the presence of in situ photoautotrophs (adapted from Hallock, 1987). Bathymetric extent of these light zones depends on the extinction of light. Curves of light penetration for different extinction coefficient of light based on: Kanwisher and Wainwright (1967), Huston (1985), Hallock and Schlager (1986) and Kahng et al. (2010).

The changing character of the shape of larger benthic foraminifers (LBF) with depth, especially for *Amphistegina* spp. (Larsen, 1976; Larsen and Drooger, 1977; Hallock, 1979; Hallock and Glenn, 1986; Drooger, 1993; Renema, 2005; Bernoulli et al., 2007; Mateu-Vicens et al., 2009), has been widely used to infer paleobathymetry. The thickness to diameter ratio (T/D) has also been used to constrain the paleobathymetry of recent nummulitids such as *Operculina* and *Heterostegina* (Reiss and Hottinger, 1984; Yordanova, 2004) and for extinct nummulitids (Beavington-Penney and Racey, 2004).

2.3 – Terminology

Most fossil Cenozoic reefs are skeletal rich buildups, dominated by associations of scleractinian corals and calcareous algae, with bryozoans, sponges, foraminifers and/or mollusks as secondary contributors (Perrin, 2002). Numerous definitions of coral reefs, reef frameworks, and reef communities exist in the literature (e.g., see reviews by Riegl and Piller, 2000; Riding, 2002; Flügel, 2004; many others). “Coral buildup” and “coral bioherm” are generic terms that denote carbonate bodies with depositional relief above the seafloor at the time of deposition, in which many coral skeletons are in living position.

For architectural fabric we follow Riding's (2002) nomenclature, which identifies three main types among skeletal buildups: "frame", "segment" and "cluster" reefs (**Fig. 2**). These categories are differentiated in terms of skeleton-matrix ratio; skeleton abundance, shape, rate of overgrowth and in place character; development of primary cavities, matrix grain size and early cementation, which are attributes that together provide substantial information about potential depositional relief and hydrodynamic energy levels, and when combined with compositional and growth-fabric characteristics, also allow important inferences about facies zonation and distribution with depth. Other categories differentiated by Riding (2002), such as cement and microbial reefs, were relatively uncommon during the Cenozoic, although it is important to note that both early cementation and microbial binding/encrustation are conspicuous in many reported examples.

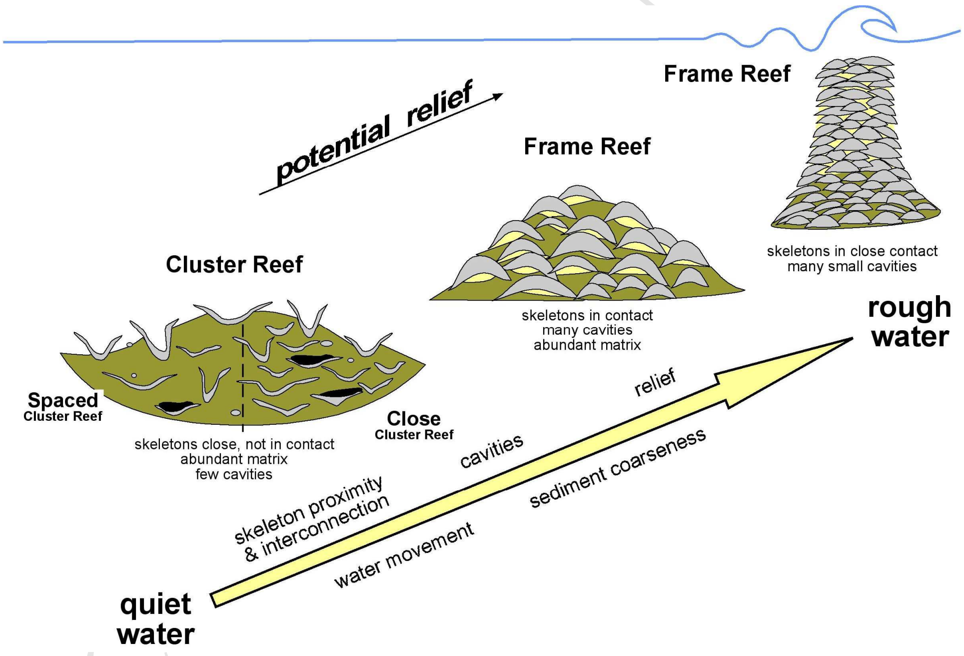

Fig. 2. Structure–relief relationships in skeletal reefs, and quiet–to-rough water skeletal reef spectrum. From Riding (2002)

Growth-fabric descriptors follow Insalaco (1998), according to the dominant growth form: *platestone* (platy to tabular skeletons), *sheetstone* (sheet-like and lamellar skeletons), *domestone* (domal and irregular massive skeletons), *pillarstone* (branching, rod and tubular solitary forms with relatively restricted lateral growth), and *mixstone* (not dominated by one growth form and including a variety of growth forms). Boundstone is used as a generic term for autochthonous limestones without specific growth-fabric differentiation.

A *pycnocline* represents a boundary layer between two water masses of different density. In most mid- and low-latitude modern oceans, the surface ocean water temperatures are relatively warm above depths of ~50–200 m (~10–30°C depending upon location and season). In contrast, by ~1000 m in depth, ocean temperature is typically ~4°C. This depth change creates strong gradients in temperature (the thermocline) and density (the pycnocline). Mixing by winds and currents, which can change with season, controls the upper limit of the thermocline. Warm summer temperatures and weak winds can produce a shallow seasonal pycnocline, while strong winter winds in temperate latitudes produce a much deeper winter thermocline/pycnocline. Several pycnoclines separating different water masses, however, may exist at a given locality. This is particularly true in small interior seas, where pycnoclines can be strongly influenced by riverine discharge, fetch of the basin, wind regimes and seasonal temperature changes.

Any disturbance of a pycnocline will propagate as an internal wave. Perturbation of the pycnocline can be induced by tides, storms and a number of other factors still not fully understood. Breaking internal waves produce sediment remobilization on the seafloor at the depth where the pycnocline intersects the seafloor (see Pomar et al., 2012b, and references therein).

3 – Case studies: Cenozoic platforms in the Mediterranean Tethys

This section describes the main compositional-architectural features of 22 “first-hand” case studies used as the database, grouped at the epoch level: five in the Paleocene, six in the Eocene, four in the Oligocene and six in the Miocene. Descriptions are complemented with comparisons with other known, coeval examples from the same or other areas across the western-central Tethys **(Table 1 and Fig. 3**).

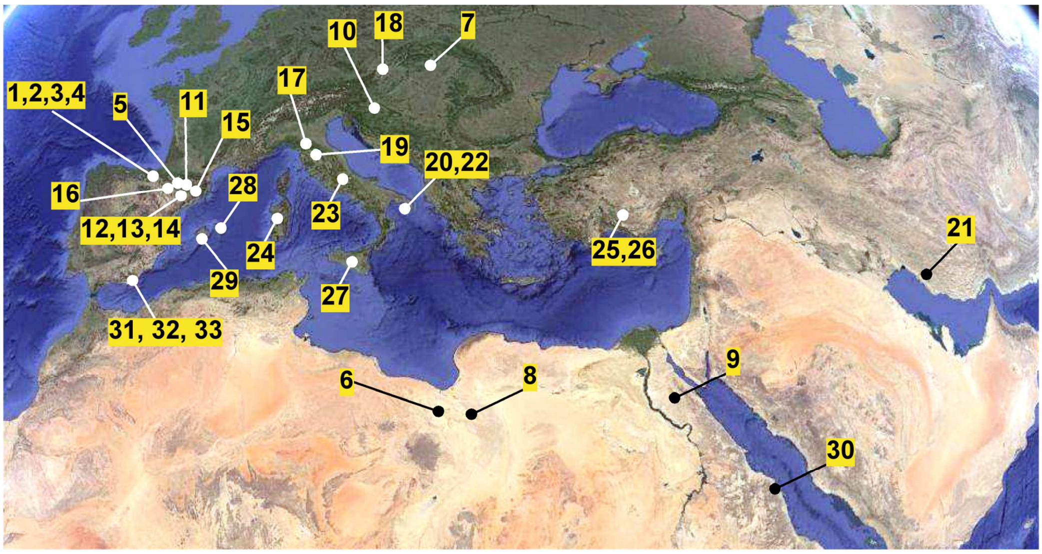

PALEOCENE

- **1,2,3** *Urbasa-Andia plateau (Danian)*
- **4** *Urbasa-Andia plateau (Selandian-Thanetian)*
- **5** *Campo section (upper Thanetian)*
- **6** upper Satal platform (Danian)
- **7** western Carpathians (Danian)
- **8** Nasser buildup (Selandian-Thanetian)
- **9** Galala mountains (Selandian-Thanetian)
- **10** Treslj Formation (upper Thanetian)

EOCENE

- **11** *Merli, Berganui, Iscles - Tremp (lower Ypresian)*
- **12, 13, 14** *Grustan, Meson de Liguerre, Buil (Lutetian)*
- **15** Vic-Igualada buildups (Bartonian-lower Priabonian)
- **16** *Rasal-Yeste (Bartonian)*
- **17** Nago Limestone (Bartonian-Priabonian)
- **18** Eisenrichterstein Limestone (Priabonian)

OLIGOCENE

- **19** *Castelgomberto, Vicentin area (Rupelian)*
- **20** *Castro Limestone (lower Chattian)*
- **21** Asmari Formation (Rupelian-Chattian)
- **22** *Porto Badisco (upper Chattian)*

MIOCENE

- **23** Latium-Abruzzi (Burdigalian)
- **24** Sedini platform (Burdigalian)
- **25,26** Mut-Ermenek (Burdigalian-Langhian)
- **27** Ragussa platform (lower Tortonian)
- **28** *Migjorn ramp (upper Tortonian)*
- **29** *Cap Blanc reef margin (Tortonian-Messinian)*
- **30** Abu Shaar platform (Langhian-Serravallian)
- **31,32,33** Nijar, Sorbas & Las Negras bioherms & fringing reefs (Tortonian-Messinian)

Fig. 3 – Location of the case studies reported in this study. In italics are the examples worked out or revisited by the authors. Background map is from GoogleEarth.

3.1. Paleocene

The Paleocene was a time of recovery and diversification, with continuous changes in the style of tropical shallow-water carbonate production. The Danian was defined by carbonates with strong Cretaceous affinities, as evidenced by the abundance of solenoporaceans, dasyclads and typical Mesozoic microproblematica. Danian coral associations mainly thrived in platform margin to slope settings and included both Cretaceous survivors and new taxa (Baron-Szabo, 2006, 2008). During the Selandian and Thanetian, red corallines, dasyclads and Halimedales increased in abundance and diversity, becoming dominant components of reefal and level-bottom communities (Aguirre et al., 2000 and 2007; Barattolo, 2002; Dragrastan and Herbig, 2007). Strikingly, this proliferation of calcareous algae parallels a marked global increase in $\delta^{13}C$ (**Fig. 4**). By the late Selandian, the first nummulitids, orthophragminids and alveolinids, plus some large rotalids (*Miscellanea*), appeared in shallow tropical seas.

These LBF groups occur in moderate abundance and low specific diversity, but already exhibit depth zonation (Hottinger, 1983, 1997; BouDagher-Fadel, 2008). Through the late Paleocene, scleractinian corals expanded into lagoons and littoral zones, probably shaded under incipient seagrass canopies, but only formed knobs and carpets, revealing moderate building capacity at euphotic depths. By the late Thanetian, when global temperature was rising (Fig. 4), coral buildups declined significantly across the west-central Tethys domain, prior to the hyperthermal event at the Paleocene-Eocene boundary (Scheibner and Speijer, 2008). It is important to note that, although well-preserved Paleocene platform exposures are scarce, reef buildups were more common and sizeable during the Paleocene than during either the Maastrichtian or the early Eocene (Kiessling and Baron-Szabo, 2004).

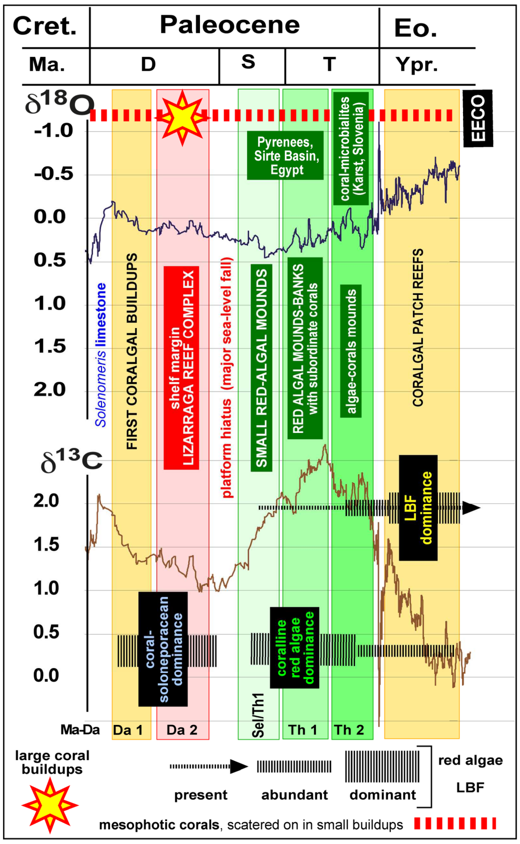

Fig. 4 – Paleocene platforms and buildup types. Oxygen and carbon isotopic curves are from Cramer et al. (2009), recalibrated to GTS201 in Vandenberghe et al. (2012).

3.1.1- Danian coral buildups (reef recovery after the K/Pg boundary)

The Urbasa-Andia plateau, in the western Pyrenees (N Spain) exposes the largest and most complete remnant of Paleocene tropical carbonate platforms in Europe, from small isolated patch reefs and mounds to large reef complexes (**Fig. 5a**), which developed in the paleo-Bay of Biscay (Baceta et al., 2005, 2011). The Danian succession forms a 150–250 m thick and 40–50 km wide land–attached platform with broad, shallow and restricted (sabkha-like) interiors. This ramp to flat-topped platform consists of three successive depositional sequences (Ma–Da, Da–1 and Da–2) and records a progressive reef-building recovery.

The Ma–Da (lower Danian) sequence (**Fig. 5a**), also known as the *Solenomeris limestone*, forms a homoclinal ramp dominated by open subtidal heterozoan carbonates (bryozoans, echinoderms, bivalves, serpulids). The few m-thick biostromes in outer ramp position consist of encrusting foraminifers (*Solenomeris* and *Nubecularia)*, serpulids, red algae (*Mesophylum, Sporolithon*) and, very locally, thin laminar actinacid corals (Aguirre et al., 2007; Baceta et al., 2011).

The first significant coral buildups occur within the middle Danian Da-1 initial shelf succession (**Fig. 5a)**. They occur as 5–10 m thick bioherms along the bioclastic margin and consist of scleractinian corals (mainly *Actinacis*) and encrusting coralline red algae, foraminifers and bryozoans, forming a cluster fabric in a medium- to coarse-grained matrix rich in solenoporaceans, peyssonnelids, echinoderms, coral debris and variable amounts of peloidal micrite (Baceta et al., 2005). The biotic association and the position within the ramp profile indicate meso-oligophotic conditions (**Fig. 6c**).

Reef growth peaked in the upper Danian with the Lizarraga reef complex (Da-2 sequence, **Fig. 5a**), developed during the lowest temperature interval of the Paleocene and a relative minimum value in $\delta^{13}C$ (**Fig.** 4). This 120–180 m-thick progradational reef complex consists of stacked sigmoidally-bedded cluster reefs (**Fig. 5b**) made of corals (up to 19 coral taxa), calcareous algae and heterozoan components showing an ecological zonation, seemingly controlled by light and hydrodynamic conditions. The sigmoidal reefs lack a wave-resistant elevated rim. Instead, they are capped by a smoothed and slightly seaward inclined package of solenoporacean-dasyclad gravels and cross-bedded foraminiferal sands with sparse coral colonies. Within the cluster reefs, similar proportions of encrusting sporolithaceans and melobesioid algae and the abundance of peyssonnelids (20-25% of the total coralline-red algal assemblage; Aguirre et al., 2007) suggest peak coral development at mesophotic depths (**Fig. 6b**). Comparable facies architecture has been recognized in coeval Danian platform margins from the Syrte Basin (upper Satal Formation, Pawelek, 2009), and the western Carpathians (Kholer et al., 1993). The upper Satal Fm. also represents a 300 m-thick reef-rimmed flat-topped shelf with a broad, very shallow evaporitic interior. According to core descriptions and stratigraphic correlations, coral facies are largely “reworked” and, as in the Lizarraga reef complex, occur concentrated at the upper slope, below bioclastic shoals rich in solenoporaceans, dasyclads and miliolid foraminifers characterizing the shelf edge.

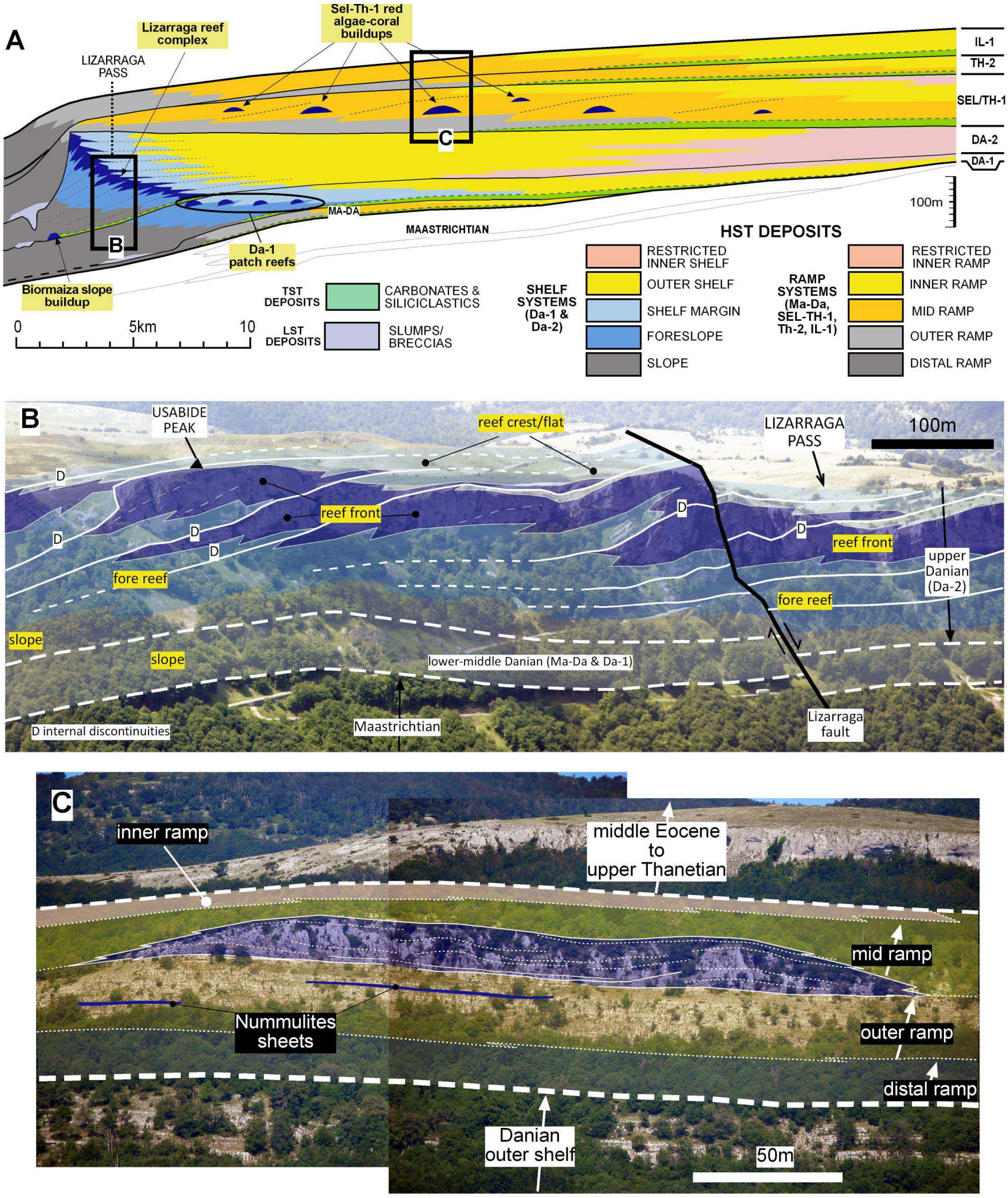

Fig. 5. A: Synthetic reconstruction of the Paleocene-lower Eocene platform succession of the Urbasa-Andia plateau, with indication of depositional sequences, facies belts, depositional settings and main reef buildups (from Baceta et al., 2005 and 2011). B: The progradational Lizarraga reef complex exposed near Lizarraga pass (northern Urbasa-Andia plateau), with differentiation of six internal sigmoidal reef units and constituent facies belts. C: Panoramic view of the largest red algae-dominated reef buildup within the Sel/Th-1 progradational ramp sequence preserved in the Zanabe ridge (southern Urbasa-Andia plateau).

3.1.2- Selandian-Thanetian buildups

In the southern Pyrenees, Selandian-Thanetian algal-dominated buildups occur in two homoclinal-ramp sequences (the *Sel/Th-1* and *Th-2* ramp sequences of Baceta et al., 2004, 2005), which developed landwards from the Danian shelf margins (Fig. 5a). All reported Selandian-Thanetian buildups occur within open-subtidal deposits, with coralline red algae as main components and corals, bryozoans and various encrusters as subordinate builders. Micritic matrix is conspicuous in most buildups, some of microbial origin (Baceta et al., 2005).

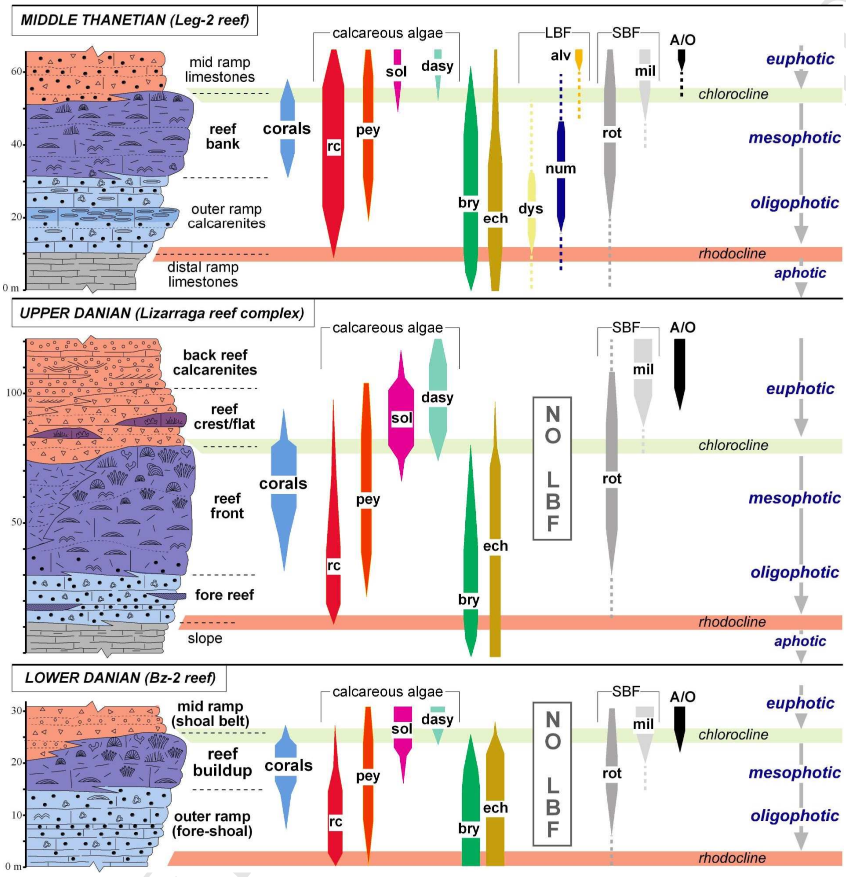

Fig. 6. Distribution of main skeletal components through three distinct Paleocene coral buildups from the Urbasa-Andia plateau. Abbreviations: **rc**: coralline red algae, **pey**: peyssonnelids; **sol**: solenoporaceans, **dasy**: dasyclads, **bry**: bryozoans, **ech**: echinoderms, **dys**: dyscociclinids, **LBF**: larger benthic forams, **SBF: small** benthic forams, **num**: nummulitids, **alv**: alveolinids, **rot**: rotalids, **mil**: miliolids, **A/O**: aggregate grains and ooids (adapted from Baceta et al., 2005).

In the Sel/Th-1 sequence (upper Selandian-middle Thanetian), low-relief buildups, 5–35 m thick and few hundred meters wide, occur within foramol deposits in mid- to outer-ramp settings (**Fig. 5a and c**; Baceta et al., 2005, 2011). The basal part of these buildups consists of red-algal bindstones to floatstones of multi-layered foliose non-geniculate corallines and peyssonnelids, with sparse laminar corals within a bioclastic matrix rich in bryozoans and small and larger benthic foraminifers. Vertically, these facies evolve into massive limestones made of laminar-platy corals and calcareous algae, with small thickets of phaceloid corals and, less frequently, knobs of domal corals with encrusting foraminifers (**Fig. 6c**, Baceta et al., 2005, 2011; Aguirre et al., 2007). Bioerosion is abundant and micritic matrix may locally reach up to 40% of the rock. In some of the largest examples, rudstones-floatstones rich in peyssonnelids, solenoporaceans, geniculate red corallines and minor amounts of dasyclads, indicate the top of these cluster reef type to have eventually reached lower euphotic depths.

Low-relief coralgal buildups are also common along the margins of the Selandian-Thanetian upper Sabil-Zelten platforms and ramps of the Syrte basin (Gumati, 1992; Spring and Hansen, 2004). The best known example occurs in the Nasser (Zelten) oilfield (Bebout and Pendexter, 1975) and consists of several tabular to mounded coral-algal biomicrite limestone bodies overlying or interfingering both landwards and seawards with argillaceous molluskan micrites and bioclastic limestones, and calcarenites with *Discocyclina* and flat *Nummulites*. Based upon these compositional features, the buildup likely developed at mesophotic-oligophotic depths. According to the abundance of micrite matrix and the *Sporolithon-Polystrata* dominated red-algal association, a similar setting can also be inferred for the dolomitized coralgal buildups within Selandian-Thanetian platform margin to slope carbonates from the Galala mountains (Scheibner et al., 2003).

Meter-thick tabular buildups, made by coralline-red algae, corals and encrusting foraminifers within abundant micritic matrix, occur in the upper Thanetian (Th-2 sequence) deposits of the Tremp area (Einchenseer, 2003). The most distinct buildup occurs at the top of the Paleocene succession at Campo, below the subaerial exposure surface marking the Paleocene-Eocene boundary (Pujalte et al., 2014). According to Baceta et al. (2011), it resembles turbid-water coral banks developed in shallow sheltered positions of sub-littoral areas (Sanders and Baron-Szabo, 2005).

In Slovenia, some isolated build-ups of discrete size, low relief and low-diversity coralgal associations occur in the upper Thanetian ramp of the Trstelj Formation (Zamagni et al., 2009). There, microbial carbonates (leiolites, stromatolites and thrombolites) encrusting corals and filling inter-colony spaces were interpreted as mid-ramp buildups developed under stressful conditions. Zamagni et al. (2012) have suggested that the progressive expansion of coral communities that did not build reefs from the middle Paleocene to the early Eocene was likely related to perturbation of the ocean chemistry due to high atmospheric pCO_2 levels, combined with moderately high nutrient loads.

3.2. Eocene

During most of the Eocene coral buildups retreated, in both size and relative abundance, particularly during the Early Eocene Climatic Optimum (EECO) (Kiessling and Baron-Szabo, 2004) (**Fig. 7**). The reef retreat is more evident in areas with extensive platform development, such as the Pyrenees, the Syrte Basin and the margins of the Arabian plate. In Oman, near the paleo-equator, coral-rich facies and buildups are only documented from the early Ypresian and the Priabonian, at the beginning and end of the Eocene (Jones and Racey, 1994; Racey et al., 2001; Bernecker, 2011). Scheibner and Speijer (2007) postulated that the short-term climatic perturbation at the Paleocene-Eocene boundary, the PETM, marked the initiation of the stepwise demise of coral reefs through the early Eocene. Conversely, LBF spread during the PETM, becoming dominant carbonate producers in Eocene tropical platform systems, from the littoral to the deep oligophotic zones, along with increasingly diverse red corallines, bryozoans and mollusks (Aguirre et al., 2000; Beavington-Penney and Racey, 2004; Scheibner and Speijer, 2007; Pomar and Hallock, 2008).

3.2.1 - Lower Eocene (Ilerdian, before the EECO)

Lower Eocene coral buildups are relatively abundant in the Tremp area, in the south-central Pyrenees, within carbonate to mixed carbonate-siliciclastic successions of Ilerdian (early Ypresian) age (**Fig. 8**, Einchenseer and Luterbacher, 1992; Einchenseer, 2003). An early Eocene transgression resulted in deposition of two extensive LBF-dominated ramp sequences during the SBZ5 and SBZ6 biozones of Serra-Kiel et al. (1998). Differential uplift and subsidence due to the emplacement of thrust sheets (SBZ7 to 9) induced a progressive basin compartmentalization, with shallow marine siliciclastic and mixed sediments deposited along depressions, and foramol carbonate ramps and associated reefal facies across intervening depositional highs (**Fig.** 8). The most representative buildups occur in three zones: near Aren (Berganui), between Iscles and col del Vent and in the Merli high, where the largest, a 45–60 m thick compound, near-massive bioconstruction, developed.

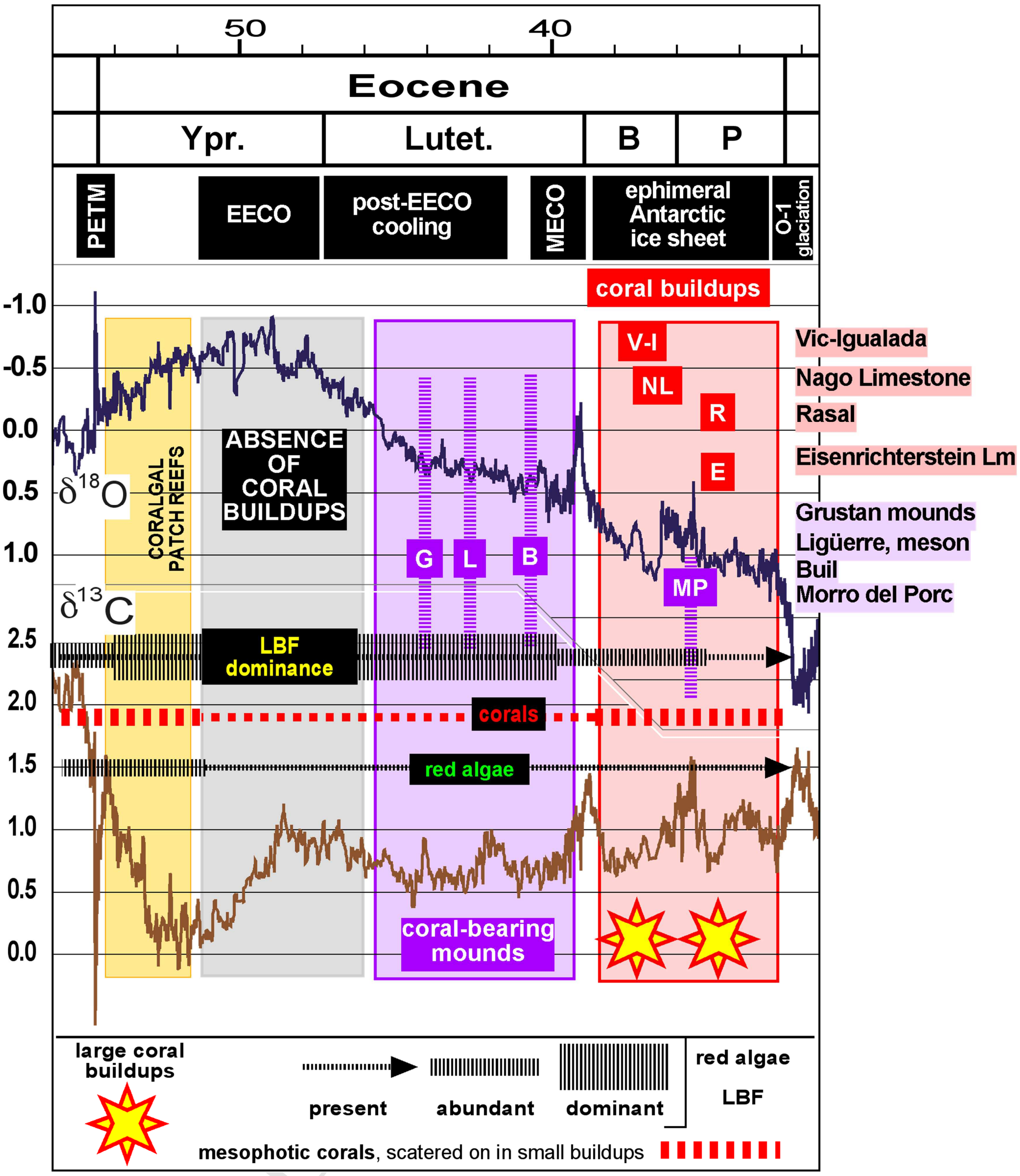

Fig. 7 – Eocene climatic events and buildup types. Oxygen and carbon isotopic curves are from Cramer et al. (2009) recalibrated to GTS201 in Vandenberghe et al. (2012).

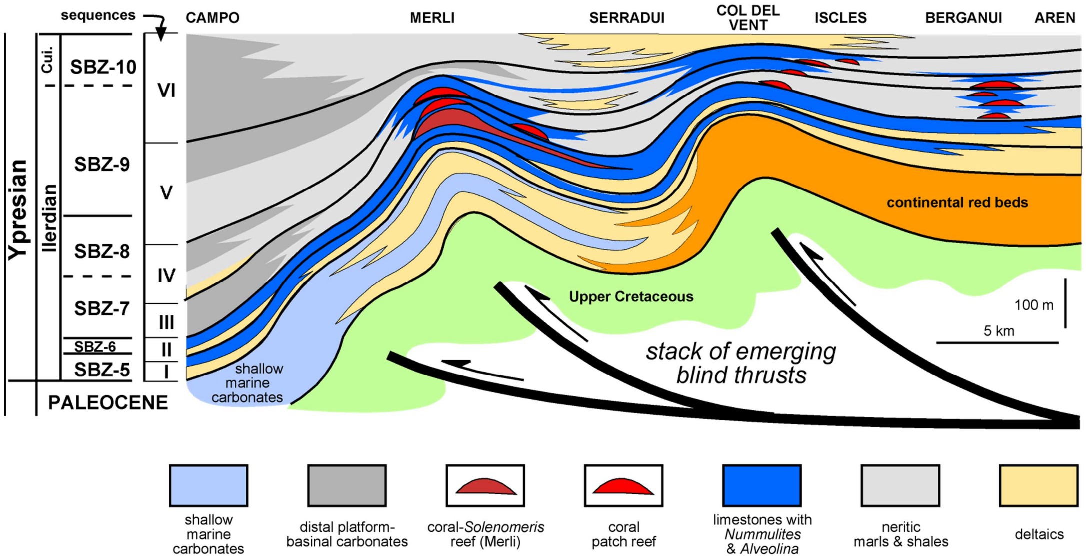

Fig 8 – Synthetic stratigraphic section of the northern margin of the Tremp area during Ilerdian times, with indication of main facies types, depositional sequences I to VI, and biostratigraphy based on LBF (adapted from Einchenseer, 2003).

In the Merli buildup, corals and the encrusting foraminifer *Solenomeris* are the main builders (Einchenseer, 2003). Corals, with moderate diversity, change shapes from laminar in the deeper parts, to platy-domal in the middle, and into massive-ramose-encrusting forms at the top. Matrix is abundant and ranges from marly to fine-grained bioclastic. *Solenomeris* forms discrete biostromes at the base, but it is also common in the middle-upper parts, either overgrowing corals or forming bindstones associated with crustose red algae. Capping the buildup, coralline-red-algal (geniculate and non-geniculate) floatstones and packstones, with *Solenomeris* debris and scattered alveolinids, miliolids and rotalids, often occur in cross-bedded bars indicative of tidal-current activity. The abundance of muddy matrix, the widespread presence of *Solenomeris* (which is a relatively deep-water foraminifer; Plaziat and Perrin, 1992), and the absence of green algae and other shallow-water components in the capping beds, more likely place coral development at deep euphotic to mesophotic depths, below wave base.

By contrast, the coral buildups between Iscles-Col del Vent and Aren-Berganui (**Fig. 8**), 2–10 m in thickness, appear as low-relief discrete bodies, encased between *Alveolina*-red-algal bioclastic limestones and *Nummulites* banks and sheets. They consist of low-diversity platy-domal corals, red-algal nodules and *Solenomeris,* within a muddy to fine-grained bioclastic matrix with bivalves, bryozoans and *Discocyclina*. Similar buildups and biostromes also occur locally along the eastern and southern margins of the basin, near Tremp and to the north of the Montsec ridge (Einchenseer and Luterbacher, 1992). The sheetstone-platestone to domestone coral growth fabrics and the absence of primary cavities characterize these buildups as cluster reefs sensu

Riding (2002), while the light dependent components, along with the muddy character of the matrix, place them in the mesophotic zone.

3.2.2. - Middle Eocene (Lutetian)

In the Pyrenees, the shallow marine sedimentation during the Early Eocene Climatic Optimum (EECO) [late Ypresian (Cuisian) to the early Lutetian] was, like other Tethyan basins, almost exclusively characterized by LBF-dominated ramps (Barnolas et al., 2004 and references therein).

Middle Eocene coral buildups occur in the Ainsa fold and thrust Oblique Zone, where a thick progradational deltaic to alluvial succession (Sobrarbe and Escanilla Fms) was deposited between the Mediano, Boltaña and Balces growing anticlines (Poblet et al., 1998; Dreyer et al., 1999; Barnolas et al., 2004; Arbués et al., 2011). Four regressive composite sequences build the Sobrarbe deltaic complex (Dreyer et al., 1999), which includes several thin *Nummulites*-rich horizons, often with glauconite, and locally with small coral-bearing mounds (Mateu-Vicens et al., 2012).

In the growing strata of the western flank of the Mediano anticline (**Fig.** 9), three successive carbonate ramp units (Grustan 1 to 3 of Arbués et al., 2011) developed during the middle Lutetian post-EECO cooling and before the MECO hyperthermal. They define a progressive unconformity and occur interbedded with siliciclastics, breccias-slumps and, distally, with the prodelta clays of the Sobrarbe system (Poblet et al., 1998). The unstable Grustan ramps consist of medium- to fine-grained bioclastic carbonates rich in LBF (*Nummulites, Alveolina, Orbitolites* and *Discocyclina*), mollusks, echinoderms, small benthic foraminifers and red algae (often as rhodoids) (Arbués et al., 2011). Branching and solitary corals are found in shallower lithofacies, and discrete mounds capped by irregular massive corals occur in deeper positions, commonly affected by early sliding and brecciation. A fine-grained, mud-dominated to clay-rich bioclastic matrix form the bulk of the mounds. Very similar coral mounds can be observed along the western flank of the Balces anticline in the time-equivalent Guara Fm. (Barnolas et al., 1991). They consist of massive corals dispersed in bryoalgal-foralgal matrix and occur interbedded in the nummulitid–alveolinid packstones to wackestones characteristic of the middle ramp.

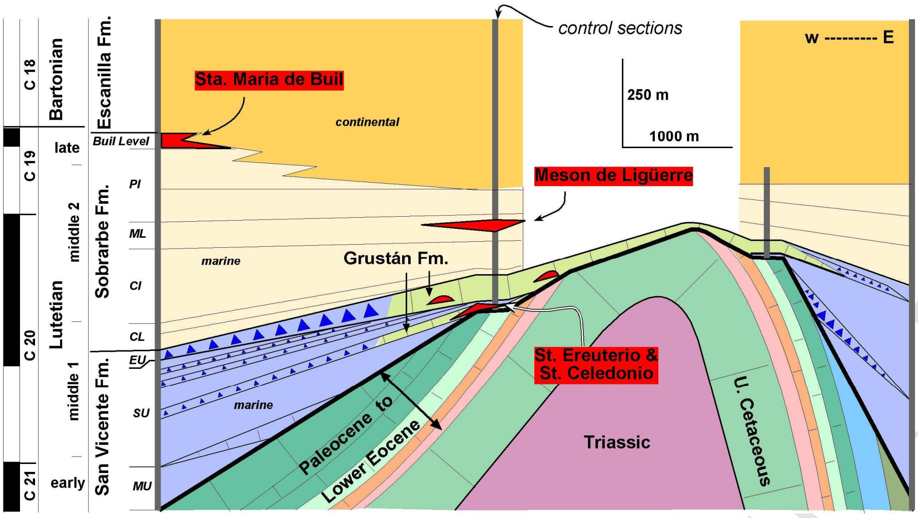

Fig. 9 - Stratigraphic section of the Mediano anticline, in the Ainsa fold and thrust Oblique Zone (Muñoz et al., 2013) in the eastern part of the South Pyrenean piggyback basin. Coral buildups are in red. Modified from Poblet et al. (1998)

<u>The Meson de Ligüerre level</u>. This is a discrete carbonate unit composed of calcarenites, small mounds with corals, and nummulitic beds interbedded with the laminated, pro-delta silt and clays of the Sobrarbe complex (**Fig. 9**). These pro-delta deposits occasionally include scattered and horizontally lying, flat-discoidal *Nummulites*. Nummulitic rudstone/floatstones with silty to fine-grained packstone matrix occur as 0.5–3.5 m thick beds with persistent nodular character due to discontinuous clay interbeds (**Fig.** 10). Among *Nummulites*, ellipsoidal tests predominate but are mixed with flat, discoidal shapes, all commonly imbricated.

Scattered mounds nucleate on the nummulitic beds. They consist of wackestones with sparse bioclasts, including crustose red algae, scarce green-algal fragments, serpulids, oysters and foraminifers. Corals occur as fragments or as in-situ colonies on top of the buildup; oysters mostly occur in-situ. Coralline-red algae occur overgrowing corals or as crustose forms within the muddy matrix. Large rotalid foraminifers, including *Rotalia* fragments and megalospheric A-forms of *Nummulites*, occur mixed with planktic taxa and the relatively deep-water *Lenticulina*. Encrusting forms (*Fabiania, Haddonia*) and seagrass-associated taxa (small miliolids, cibicidids) are scarce. Irregular patches of micrite are very common within the mounds, which amalgamate or are superposed through consecutive beds. The mound-flanking beds consist of *Nummulites*–coral floatstones interfingering with mudstone-wackestones. Their poorly sorted packstone matrix contains fragments of red-algal crusts, foraminifers, and very rare fragments of articulate red algae and decapods. Among foraminifers, *Nummulites* A-forms and *Rotalia* are frequent.

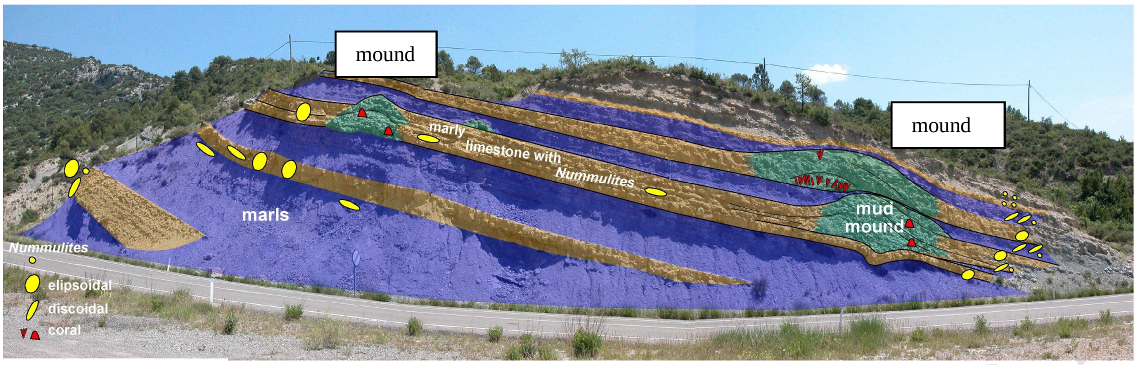

Fig. 10. The Meson de Ligüerre: mud-mounds nucleated on nummulitic banks.

Interpretation – In a clay-dominated, *Nummulites*-barren environment, a progressive and punctuated change to carbonate production is recorded in the thickening-upward succession of carbonate nodular beds. Flat discoidal *Nummulites* started to thrive on the clay substrate, in the lower part of the photic zone. Upsection ellipsoidal *Nummulites* become predominant associated with carbonate deposition and a shallowing trend. The laterally persistent calcarenite beds provided substrata for oyster and coral colonization, forming m-scale mounded features. Resedimented articulate red algae, epiphytic foraminifers (on seagrasses) and some green algae attest for a shallower production area updip, supplying these components.

The Buil Level. The upper Lutetian nummulitic banks and associated small coral biostromes and bioherms of this distinct interval (Fig. 9) occur within the uppermost composite sequence "Barranco El Solano" of Dreyer et al. (1999), overlying deltaic sandstones and clays, in turn overlain by the Bartonian alluvial Escanilla Formation. Coral biostromes, locally biohermal, occur interbedded with the nummulitic lithosomes (Mateu-Vicens et al., 2012). Coral colonies occur sparsely within a packstone matrix, lacking in-situ intergrowths and primary cavities (spaced cluster reef sensu Riding, 2002). The bulk matrix is unsorted, and components include abundant *Nummulites* (A-forms, 2–7 mm in diameter) and fragments of other LBF such as *Operculina*, and rare *Discocyclina, Asterocyclina*, and *Orbitolites*. Red algae are very scarce. The encrusting foraminifers *Victoriella, Fabiania*, *Acervulina, Solenomeris* and *Haddonia* occur attached to coral colonies. Small benthic foraminifers such as *Lobatula* (very abundant), *Sphaerogypsina*, *Planorbulina*, *Quinqueloculina* and very rare bolivinids and discorbids also occur.

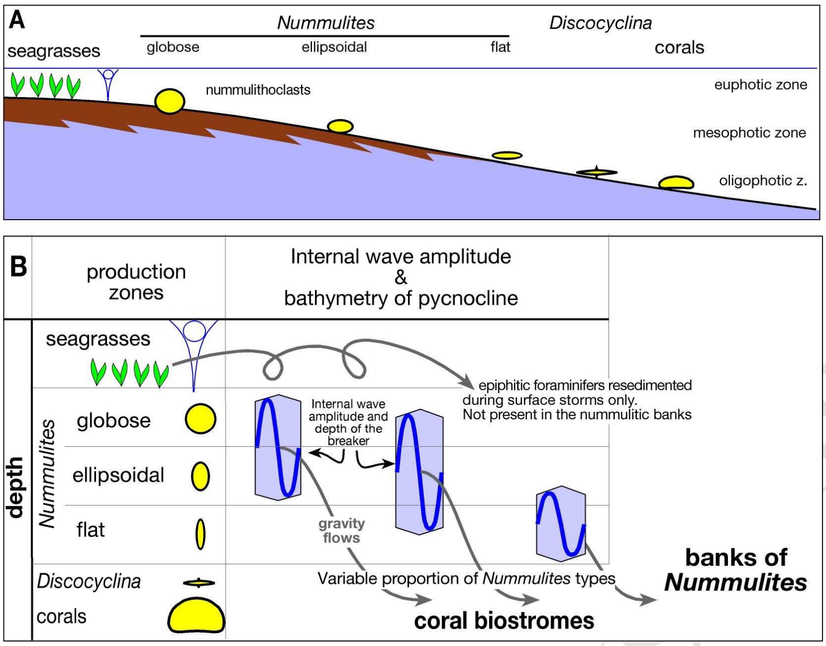

Fig. 11 - **A)** Along-dip distribution of the carbonate factories in the Buil Level. In the euphotic zone, epiphytic organisms thriving in seagrass meadows dominated carbonate production. The mesophotic zone was characterized by globose to ellipsoidal-flat *Nummulites* and, in the lower part, by coral biostromes. The oligophotic zone was dominated by large flat benthic rotalids (e.g., *Discocyclina*, *Nummulites millecaput*). **B)** Internal waves impinging the sea floor at the mesophotic zone (the zone where *Nummulites* thrived) explain the composition of the allochthonous nummulitic lithosomes. The compositional and textural differences among nummulitic lithosomes reflect the bathymetry of the pycnocline and the amplitude of the zone swept by breaking internal waves. Modified from Mateu-Vicens et al. (2012).

Interpretation – Mateu-Vicens et al. (2012) interpreted the Buil nummulitic banks to derive from gravity flows (**Fig.11**) triggered by internal waves propagating along the pycnocline (Pomar et al. 2012 b). The textural and compositional differences among banks were interpreted to reflect the characteristics of the *Nummulites* at the depths where the internal waves broke. Globose *Nummulites* thrived in shallow water with abundant nummulithoclasts (finely comminutted *Nummulites* debris), ellipsoidal tests predominated in intermediate water depths, and flat-discoidal *Nummulites* thrived in deeper, clay-dominated settings.

In this context, the coral biostromes and coral mounds, bearing *Operculina*, *Discocyclina* and *Asterocyclina*, clearly represent in-situ production and accumulation in meso-oligophotic conditions, below the zone inhabited by *Nummulites* (Mateu-Vicens et al., 2012). The abundance of mud in the matrix, along with the absence of sediment sorting, reflects accumulation below storm-wave base. Within the biostromes, only a few allochthonous components occur: slightly abraded small A-forms of *Nummulites* and some small seagrass epiphytic foraminifers (i.e., *Lobatula, Planorbulina, Quinqueloculina*) (Langer, 1993) that were shed down from the shallower zones during surface storms.

3.2.3 - Upper Eocene outcrops (post-MECO)

Bartonian-Priabonian coral buildups crop out extensively in the Igualada-Vic area (**Fig. 12),** in the eastern sector of the Ebro foreland basin (e.g., Busquets et al., 1985; Santisteban and Taberner, 1988; Alvarez et al., 1994; Hendry et al., 1999; Romero et al., 2002) and on the south margin of the Jaca foredeep (Morsilli et al., 2012). These buildups developed during the progressive cooling subsequent to the MECO interval. Besides scleractinian corals, red algae and LBF are conspicuous in these buildups, which developed downdip of prograding shallow-marine siliciclastic systems, prior to widespread accumulation of transitional to continental deposits.

In both the Igualada and Vic sectors, two marine Bartonian to lower Priabonian sedimentary cycles have been distinguished, sandwiched between continental deposits (Serra-Kiel and Travé, 1995; Serra-Kiel et al., 2003; Cascella and Dinares-Turell, 2009; Costa et al., 2013). Coral patch reefs occur in both sedimentary cycles, but particularly abound and attain larger size in the la Tossa Formation, the regressive part of the upper sedimentary cycle, which vertically consists of an alternation of progradational deltaic units, coral bioconstructions and marls containing *Nummulites* and *Operculina* (**Fig. 12**). Previous interpretation of the Igualada-Vic coralgal buildups were based on the modern-reef model and most rock descriptions were biased by the influence of modern Caribbean analogs (Busquets et al., 1985; Santisteban and Taberner, 1988; Alvarez et al., 1994; Hendry et al., 1999; Romero et al., 2002). Three Bartonian coral buildup examples are here reviewed: La Tossa, La Trona and Morro del Porc (see location on **Fig. 12**).

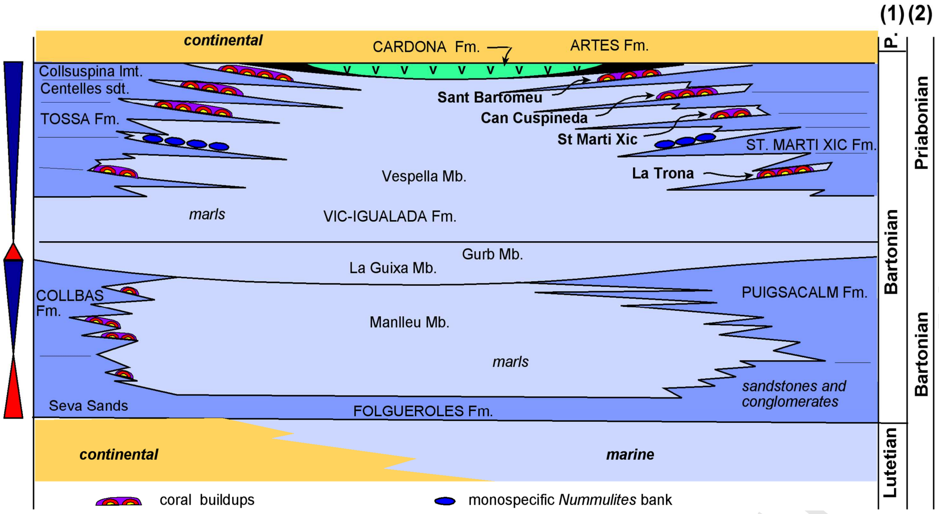

Fig. 12 – Stratigraphic position of coral buildups and nummulitic banks in the Igualada-Vic sub-basin (modified from Pisera and Busquets, 2002). Chronostratigraphy is from (1) Taberner et al. (1999) and (2) Cascella and Dinares-Turell (2009).

La Tossa (Bartonian), Igualada area. Coral colonies grew in a clay-dominated environment, overlaying and alternating with prograding deltaic lobes (Salas, 1995). The mixture of coral, bioclastic matrix and marl/clay results in a characteristic nodular stratification, and no evident zonation in lithology, coral communities or colonial shapes can be seen, other than some subtle differences. Corals are not densely stacked nor in contact, and lag the characteristics of a framework reef (**Fig. 13**). They better fit the “cluster” architectural type of Riding (2002). Wackestone to poorly sorted packstone is the dominant texture of the embedding carbonate matrix, which includes encrusting and agglutinated foraminifers, coralline-red algae, bryozoans, planktic foraminifers and, locally, some LBF.

Well-lithified limestone strata of poorly to well sorted packstones, with fragments of red algae, echinoids, molluscs, corals, *Nummulites*, miliolids and encrusting foraminifers, occur in discrete lithosomes. These have sharp bases and grade upwards into the nodular marly limestone. Overturned colonies and fragments are common near the base and, locally, fan-like sorted grainstone to packstone also occurs. These packstone strata only contain components derived from the buildup, thus recording the occurrence of high-energy episodes in a low-energy setting dominated by clay accumulation, below the base of wave action.

Locally, miliolid grainstones to well-sorted packstones, rich in fragments of coralline-red algae, mollusks, green algae and quartz sand also occur. Salas (1995) noted the paradox of having a mixture of miliolids and quartz in the highest-energy lithofacies of the reefal system. This lithofacies indicates a shallow-water setting of deposition, above wave base in the euphotic zone.

Interpretation – Although geometries are not clearly visible, distal and proximal talus, reef-wall, and back-reef facies within fringing- and barrier-reef systems were previously interpreted. A more realistic interpretation, based on the light-related components and on the textures (cluster type), indicates this buildup grew in a mud dominated setting, below the base of wave action and between the chlorocline and the rhodocline (absence of green algae and presence of red algae). The poorly to well-sorted packstone with components only sourced from the buildup, can be interpreted as flank deposits derived from breaking internal waves, as it was interpreted in similar deposits and in a similar context in Rasal (Morsilli et al., 2012; see below).

Fig. 13 - La Tossa. Coral colonies occur in a clay-dominated environment. The mixture of coral, bioclastic matrix and marl/clay results in a characteristic nodular stratification, without evident zonation in lithology.

<u>La Trona (Bartonian), Vic area.</u> La Trona buildup (San Marti Xic Fm.) developed on the top of a deltaic sandy lobe (**FIG. 12**). Five main reef facies are distinguished (Alvarez et al., 1994, 1995) from base to top: a) Lime mudstones/wackestones with in-situ lamellar corals, locally encrusted by red algae. b) Lime mudstones/wackestones with in-situ red algal crusts, branches and rhodoliths. c) Skeletal packstone/coral-fragment rudstone, with red algal crusts, rhodoliths and red algal fragments (this is the most conspicuous lithofacies in La Trona buildup), d) Nodular wackestones with in-situ corals; corals are highly diverse, close but not in contact and surrounded by the wackestone matrix ("cluster" architectural type, sensu Riding, 2002). e) Mixed carbonate-siliciclastic packstone with red algal crusts and rich in foraminifers, locally with some corals, occur on top of the buildup, at the transition to the overlaying siliciclastics.

The lithofacies distribution of La Trona buildup was interpreted accommodating the scheme of modern Caribbean-type of reefs: proximal reef slope (a lithofacies), distal reef slope (b lithofacies), reef talus (c lithofacies), reef framework and reef wall (d lithofacies), and reef crest (e lithofacies) (Alvarez et al., 1995). Although the depositional geometries are not visible, lithofacies "d" coral colonies are not in contact and lack the characteristics of a framework reef. Alvarez et al. (1995) however, already called attention to the symmetry in coral distribution, as low-light corals occur both at the base and at the top of the buildup.

Interpretation – The dominance of coralline algae along with lamellar corals at the base of la Trona buildup (lithofacies a and b) place this interval in the meso-oligophotic zone, below the base of wave action; lithofacies c, d and e possibly define more mesophotic conditions. Packstone/rudstone (lithofacies c) may also represent internal wave deposits, although clear diagnostic criteria are not seen, and the uppermost lithofacies (e) still lacks green algae characteristic of the shallow-water euphotic zone above the chlorocline. Predominantly muddy textures also place the environment of deposition below the influence of surface waves.

Morro del Porc mud-mound (Bartonian?), Vic area. Nodular wackestone/packstone lithosomes with corals, overlying deltaic sandstones, are common in the Bartonian deposits of the Vic area. These carbonate bodies accumulated synchronously to the deltaic siliciclastic sedimentation (Taberner and Bosence, 1995). The core of the Morro del Porc buildup consists of convex-up wackestone beds with abundant coral fragments and scattered branching corals, with vertical and seaward accretional stacking. Coral fragments are commonly bored by sponges and encrusted by red algae. On the landward side, scour surfaces cut the wackestone lithosome, and thin landward-dipping beds with fragments of branching corals abut the mounded lithosome, interbedded with nummulitic marls. Skeletal components in the wackestone matrix consist of foraminifers and fragments of corals, mollusks, bryozoan and red algae, along with detrital quartz. According to Taberner and Bosence (1995), lime mud was produced and accumulated in situ, with no evidence of early cementation. On top of the mud-mound, nodular coral boundstone occurs; corals are mostly domal, but broken coral branches also occur.

Interpretation – The characteristics of this coral-bearing mud mound resembles the Meson de Ligüerre and Buil Level biostromes and bioherms, in which the proximity of fluvial influence (nutrients, continental detrital organic matter, lower salinity) likely affected water transparency. Although the stratigraphic position is uncertain, the sequence fits well near the Bartonian-Priabonian boundary and it is tentatively correlated with the Late Eocene Warming, when temperature values may have been similar to the pre-MECO.

Rasal (Priabonian)**.** Lower Priabonian coral lithosomes on the southern margin of the Aínsa-Jaca basin, South Central Pyrenean Zone, Spain, occur either as isolated m-thick bioherms or amalgamated in larger, up to 50 m thick buildups (Morsilli et al., 2012).

The buildups grew interbedded with prodelta clays (**Fig. 14)**, with bases mainly defined by platy-coral colonies 'floating' in a fine-grained matrix rich in branches of red algae. Their cores consist of domal to massive corals, locally with colonies with branching and phaceloid shapes, but lacking organic framework (mixstones to sparse pillarstones forming ("Close Cluster Reefs" sensu Riding, 2002). Coral colonies are surrounded by wackestone to packstone matrix, locally floatstone, where laminar and branching red algae and coral fragments are conspicuous. Abutting the buildup margins, wedges of skeletal packstone and coral rudstone with wackestone to packstone matrix are common.

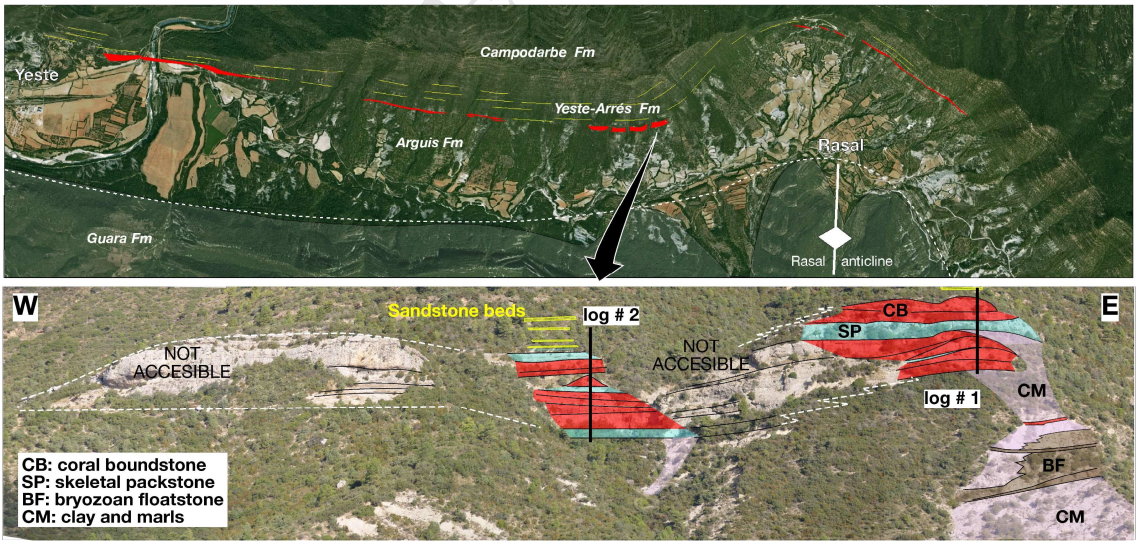

Fig. 14. Simplified geological map onto an orthophotograph between the Yeste and Rasal villages (red: coral buildups; yellow lines: prominent sandstone successions in the Yeste-Arrés Formation) Yeste-Rasal distance: about 9 km. (B) Architecture of a large, complex buildup near Rasal. Perspective deformation has been partially corrected and only the accessible parts have been mapped. Note the lateral

heterogeneities that prevent lateral correlation of log sections. Log #1: 55 m; log #2: 75 m.

Interpretation – Based on the integrative analysis of rock textures, skeletal components, buildup anatomy and detailed facies architecture, Morsilli et al. (2012) constrained the depositional bathymetry from two key observations: 1) the coral buildups developed below the effective storm-wave base (sensu Immenhauser, 2009), where clays brought by the hypopycnal riverine inflows settled out; and 2) the abundance of red algae and the presence of flat larger benthic foraminifers such as *Heterostegina*, *Operculina* and some discoidal *Nummulites* within the matrix, suggest mesophotic conditions. Additionally, Pomar et al. (2012 b) recognized that the episodic turbulent events that hit the buildups were not produced by surface storm waves but by internal waves moving along a pycnocline.

It is worth emphasizing that the Bartonian-Priabonian buildups of the Vic-Igualada area and those of the Jaca basin share a number of analogies: 1) similar biotic associations; 2) no interlocking framework made of closely packed coral colonies has been recognized; 3) low-hydrodynamic energy, individual corals are embedded either in clayey- or in well-lithified silty-packstone matrix; 4) the exclusive occurrence of red algae as in-situ autotrophs; green algae in some buildups locally occur in high-energy grainstones, indicating they are ex-situ. This suggests buildups in both areas grew in the meso-oligophotic zone, between the chlorocline and the rhodocline sensu Liebau (1984). 5) In both areas, buildups occur associated with deltaic systems, and, as such, the mesophotic zone could be as shallow as 10 m.

Morsilli et al. (2012) also emphasized the similarities of these deltaic-related buildups with the middle-late Eocene Nago Limestone in Italy and the Priabonian Eisenrichterstein limestone in Germany, both without siliciclastic influence: 1) coral bioherms are discrete, 2) there are associated packstone and rudstone-floatstone flanks, 3) red algae are abundant, and 4) the matrix is mud-rich to mud-dominated.

3.3. Oligocene

As culmination of the post-MECO cooling trend, a major temperature drop occurred at the Eocene-Oligocene transition (**Fig. 15**). This, referred to as Oi-1 glaciation, involved continental ice accumulation and high-latitude cooling (Liu et al., 2009), as well as a profound reorganization of the climate/ocean system, overall increase in ocean fertility, and a major drop in the calcium carbonate compensation depth, all associated with enhanced deep-ocean circulation (e.g., Viebahn et al., 2016 and references therein). The onset of strong thermohaline circulation probably affected environments at depths below the surface mixed layer. High-latitude cooling progressively restricted warm-water biota to lower latitudes, and both planktic and benthic foraminiferal diversities declined (Hallock et al., 1991a; Knoll and Lipps, 1993). Paradoxically, while other groups declined in diversity and prominence, scleractinian corals maintained the high diversities attained in the Eocene, while greatly expanding in their role as reef builders, particularly by the Late Oligocene (Budd, 2000; Perrin, 2002). After a transient platform crisis during the earliest Oligocene, coral reefs spread throughout the Tethys and proliferated with new lineages of larger benthic foraminifers (Höntzsch et al., 2013). During the Late Oligocene, coral reefs spread throughout the Tethys regions (Frost, 1977; Frost et al., 1983) and were also diverse in the Caribbean and the Indo-Pacific regions (Budd, 2000; Wilson, 2008). All these changes parallel the diversification of dinoflagellate *Symbiodinium* zooxanthellae (Pochon et al., 2006). Nevertheless, coralline-red algae and larger benthic foraminifers continued to dominate carbonate production during the Oligocene compared with the coral factory (Aguirre et al., 2000; Beavington-Penney and Racey, 2004; Pomar and Hallock, 2008), with the exception of some loci along the Tethys and Paratethys margins where coral buildups developed in pure carbonate systems or in mixed siliciclastic-carbonate settings (Bosellini and Perrin, 2008; Perrin and Bosellini, 2012).

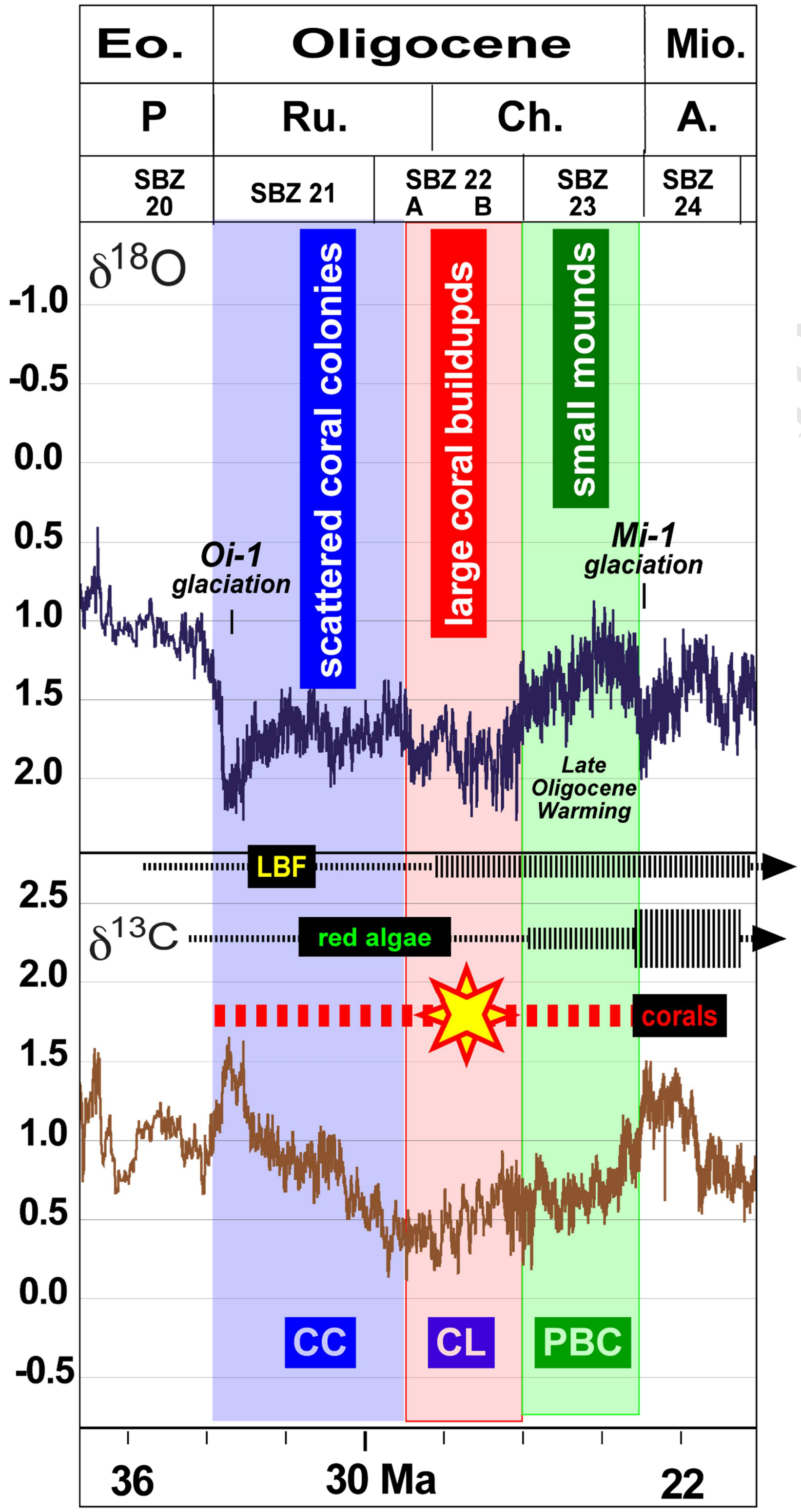

Fig. 15 – Oligocene climatic events and buildup types. Oxygen and carbon isotopic curves are from Cramer et al. (2009) recalibrated to GTS201 in Vandenberghe et al. (2012). CC: Castelbomberto Calcarenite; CL: Castro Limestone; PBC: Porto Badisco Calcarenite. Symbols as in Figs. 4 and 7.

3.3.1.- Lower Oligocene (Rupelian) coral buildups: the Vicentin area, northern Italy

The Vicentin area of northeastern Italy is one of these loci where Oligocene reef facies are well known because of the extensive collections of fossil reef corals made from them, and the influential paper published by Frost (1981). The paper on the Oligocene Calcarenite di Castelgomberto, in northern Italy, has long been a landmark for Oligocene reefs worldwide. Frost considered the Castelgomberto Limestone in the Colli Berici and in the eastern Monte Lessini Mountain as one of the largest and best-exposed barrier-reef/lagoon Cenozoic reef complexes. Frost interpreted that the barrier reef cropped out in the southeast face of the Colli Berici with a 150–200-m thick, 800–900-m wide and about 8-km long reef core, whereas he concluded that the Castelgomberto Limestone represented most of the lagoonal facies that extends for about 30 km northwestward, inboard of the barrier-reef. Most authors studying the area, before and after Frost (1981), also adopted the barrier-reef/lagoonal complex model (Rossi and Semenza, 1958; Bosellini and Trevisani, 1992, Bosellini and Stemann, 1996) and as such, this model is also considered in review analyses (e.g., Perrin, 2002; Perrin and Bosellini, 2012; Gatt and Gluyas, 2012). The only exceptions were, earlier, Geister and Ungaro (1977), who considered the Castelgomberto Calcarenite as a ramp system without any reef barrier, and more recently Bassi and Nebelsick (2010) and Nebelsick et al. (2013), who interpreted these limestones as a homoclinal ramp. Nebelsick et al. (2013) recognized four main carbonate lithofacies in the Colli Berici close to Lumignano: 1) coralline algae; 2) coralline algae-coral; 3) coralline algae-LBF and 4) coralline algal debris.

Near Castelgomberto, the locality classically reported as a lagoonal environment (e.g., Rossi and Semenza, 1958; Frost, 1981; Bosellini and Trevisani, 1992, Bosellini and Stemann, 1996; Perrin, 2002; Perrin and Bosellini, 2012), the facies succession is here considered to characterize a low angle ramp with alternating episodes of clay input (**Fig. 16**). Bathymetric changes are indicated by changes in the depth-dependent fossil associations, which reveal sea-level cyclicity. Corals occur as isolated colonies along the whole ramp profile in the meso- to oligophotic zone. In the middle ramp, however, large coral colonies occur stacked in small mounds with “cluster” internal structure (sensu Riding, 2002), but no corals have been identified in the shallow euphotic lithofacies, interpreted as seagrass meadow deposits.

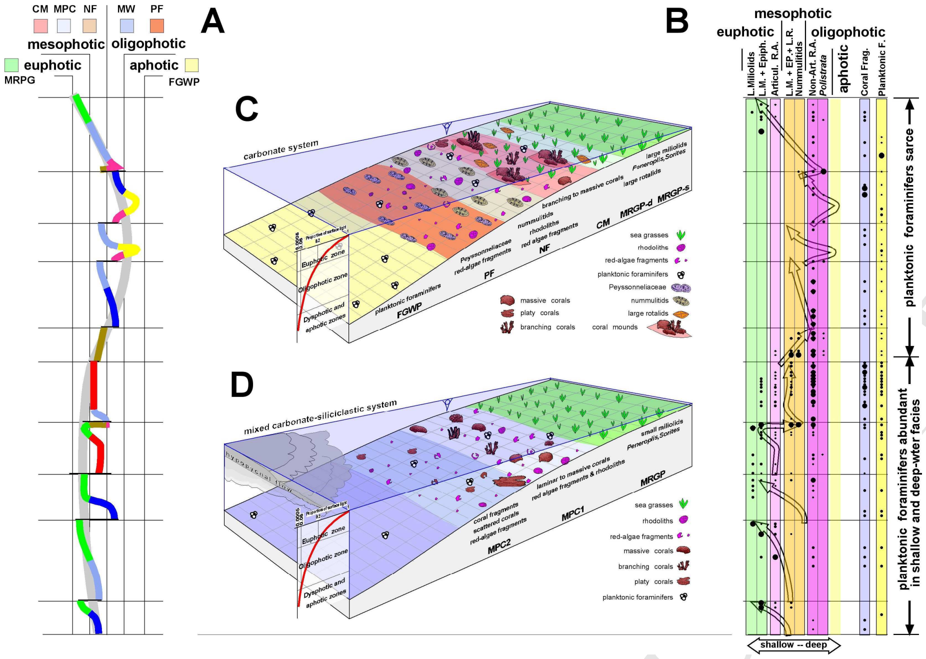

Fig. 16. Calcarenite di Castelgomberto. Application of Walter's Law to the facies succession (A) and bathymetry changes as recorded by foraminifers and other components (B) reveals the existence of two alternating depositional systems: a carbonate (C) and a mixed carbonate-clay models (D).

Near Lumignano, the locality in the southeastern end of the Colli Berici considered as representative of the Oligocene barrier rim (Frost, 1981), a ramp dominated by red algae rudstones with a packstone to wackestone matrix has been characterized recently (Nebelsik et al., 2013). Non-algal components include both large and small benthics, and planktic foraminifers associated with bryozoans, zooxanthellate corals, and echinoderms. In the dip-oriented cliff section, distinct prograding clinobeds are visible, made of dominantly oligophotic skeletal components characterizing a distally steepened ramp setting.

3.3.2- Upper Oligocene (Chattian) coral buildups: Salento, southern Italy

Upper Oligocene coral buildups are well exposed in the Salento Peninsula, southern Italy. There, two stratigraphic units are distinguished: the lower Chattian Castro Limestone and the upper Chattian Porto Badisco Calcarenite, respectively, comprising the SBZ 22B and the SBZ 23 of Cahuzac and Poignant (1997).

The lower Chattian *Castro Limestone* consists of coral-bearing limestones, with abundant and relatively diverse coral faunas and subordinate coralline algae. This unit has limited thickness and, with limited progradation, abuts against a Mesozoic carbonate paleo-escarpment on the margin of the Apulian block (Bosellini et al., 1999). This configuration confers a sigmoid-like shape to the Castro Limestone lithosome that, using the standard Modern Caribbean barrier-reef shelf-lagoon model, has been interpreted as a fringing reef with distinct back reef, reef flat, reef front and fore reef subenvironments (Bosellini and Russo, 1992; Bosellini and Perrin, 1994). The overlying upper Chattian *Porto Badisco Calcarenite* consists of poorly cemented bioclastic, horizontally bedded calcarenites, with abundant rhodoliths and LBF (Bosellini et al., 1999; Brandano et al., 2010). The LBF assemblages associated to the rhodolith facies and the dominance of melobesioids and sporolithaceans with respect to mastophoroids led Brandano et al. (2010) to conclude that the main carbonate production likely occurred at oligophotic depths.

Recently, however, Pomar et al. (2014) reinterpreted the depositional setting of both the *Castro Limestone* and the *Porto Badisco Calcarenite*. The former represents a distally steepened ramp with a distal talus induced by the basal paleo-escarpment (**Fig. 17**). Organisms thriving in seagrass meadows dominated the carbonate production in the shallow euphotic waters, whereas large rotalid foraminifers prevailed in the mesophotic zone. Near the edge of the paleo-escarpment, at mesophotic depths, luxurious growth of corals built discrete mounds with no evidence of wave-resistant growth fabrics (“cluster” structure, sensu Riding, 2002), grading to 25° to 30° dipping clinobeds made of resedimented coral rudstone-floatstones with bioclastic matrix. In the upper Chattian *Porto Badisco Calcarenite*, corals only occur forming discrete “cluster” mounds located seawards of the euphotic inner ramp, where autochthonous biota reveals the occurrence of extensive seagrass meadows. The small coral mounds clearly developed at mesophotic conditions, within facies with large rotalid foraminifers accumulated in a mud-dominated environment. Basinward, rhodolithic floatstone to rudstone and large lepidocyclinid packstones characterize the deeper oligophotic outer ramp. In contrast with modern zooxanthellate corals, which require shallow, high-light conditions for most rapid reef accretion (e.g., Hallock and Schlager, 1986, and references therein), in these two Chattian examples, corals did not build three-dimensional wave-resistant structures up to sea level, but rather lived in the middle part of the photic zone (mesophotic zone) below the base of wave action.

The differences observed in the abundance and building potential of corals in the two Chattian ramps from the Salento peninsula can be interpreted in terms of changing environmental conditions. The luxuriant coral growth in the early Chattian Castro Limestone, although influenced by the marginal position in the ACP promontory, coincided with low global temperature ($\delta^{18}O$ proxy) and low $\delta^{13}C$ (**Fig. 15**). By contrast, the upper Chattian Porto Badisco Calcarenite, with only small, sparse coral mounds, accumulated during the latest Oligocene through Early Miocene global warming ($\delta^{18}O$ decrease), coeval to an increase in $\delta^{13}C$, and characterized by prolific LBF production, as documented in Indo-Pacific carbonates (e.g., Chaproniere, 1984; Betzler, 1997; Hallock et al., 2006).

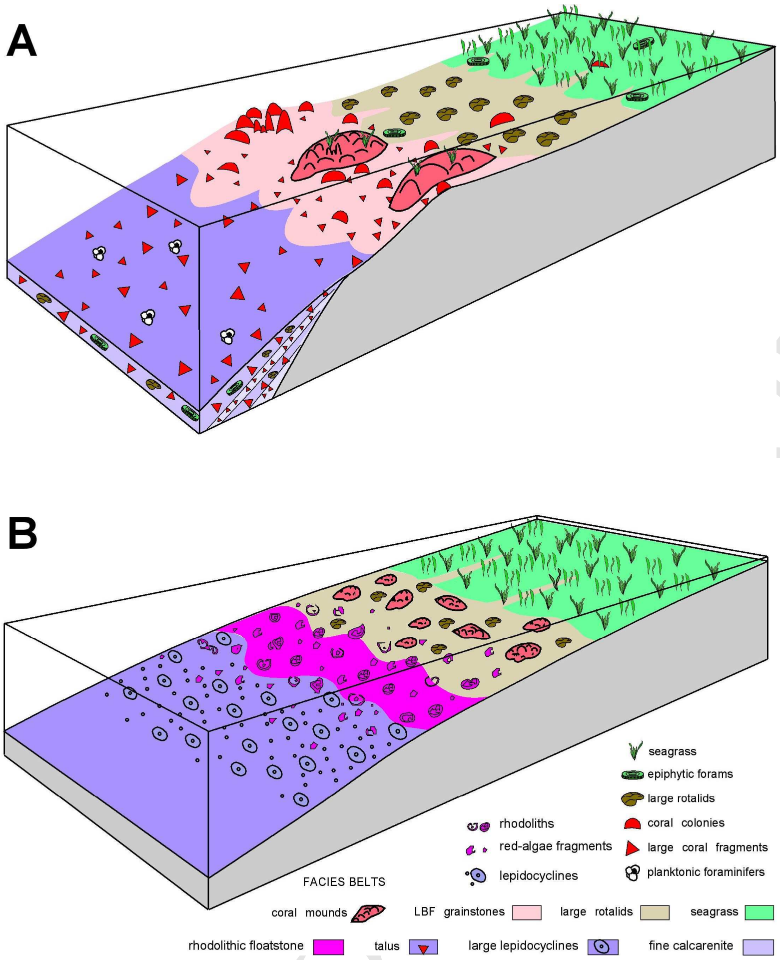

Fig. 17 – A) Depositional model for the lower Chattian Castro Limestone: a distally steepened ramp induced by a substrate paleo-escarpment. **B:** Depositional model for the Porto Badisco Calcarenite (from Pomar et al., 2014)

3.3.3.- The Oligo-Miocene Asmari Formation, Iran

The facies architecture and skeletal composition of the Oligo-Miocene Asmari Formation (southeastern Izeh Zone, Zagros Basin, Iran) have recently been documented with great detail by Van Buchem et al. (2010) and Shabafrooz et al. (2014), who differentiate four main platform-growth stages. An initial homoclinal ramp with seagrass facies in the shallow euphotic zone developed during the Rupelian, grading downdip into *Nummulites* rudstone/floatstone, packstones and grainstones with fine- to medium-grained silt to medium sand–sized nummulithoclasts, and distally into outer ramp laminated fine-grained dolo-wackestone-packstone rich in planktic and small benthic foraminifers.

During the Rupelian to Chattian, the euphotic inner ramp remained dominated by seagrasses and with high-diversity benthic foraminiferal assemblages, whereas the meso-oligophotic mid ramp recorded partial replacement of *Nummulites* by

Lepidocyclina, overproduction and basinward transport induced progradation. As a result, up to 90 m long, 15°-22° dipping clinoforms developed, showing progressive downdip change of components, from miliolid–rich packstone/grainstones (seagrass components) at the shallower parts to large *Lepidocyclina* and *Heterostegina*, to *Operculina* and *Spiroclypeus* (meso-oligophotic components) in the deeper facies. This change was induced by a decrease in accommodation that also caused the oligophotic production to shift down: large, flat lepidocyclinids (mainly *Eulepidina*) abundantly thrived along with nummulitids on the basin floor, where their shells mixed with those of planktic foraminifers.

By the Chattian, large coral buildups developed in a zone dominated by large rotalids, basinward of the seagrass-dominated zone and the previous clinoforms. Corals are encrusted by red algae and did not build a rigid framework; some are in contact, embedded in floatstone/packstone matrix, though no framework cavities exist. Mound structure fits in “cluster” reef type rather than a frame reef (sensu Riding 2002). On the flanks, coral debris admixes with coarse- to medium-grained packstones with very abundant large rotalids (such as *Neorotalia*, nummulitids, *Nephrolepidina*) and red algal fragments. Abundance of fine-grained, muddy matrix attests to a position below the wave-action zone. Inter-reef mound zones were later infilled by foraminiferal packstones, including debris of porcellaneous foraminifers, molluscs and green algae. This facies indicates a final shallowing of the platform that persisted during the early Miocene, when increasing isolation and salinity lead to extensive evaporite deposition.

3.4. Miocene

The late Oligocene to early Miocene warming trend reduced the extent of global ice volume, coevally to slightly higher bottom-water temperatures, with the exception of several brief glaciation pulses (Mi-events, Zachos et al., 2001). The warming trend peaked in the late Middle Miocene Climatic Optimum (17–15 Ma), characterized by the warmest temperatures of the past 20 million years (Kennett, 1985; Billups and Scheiderich, 2010). Thereafter, a gradual cooling led to reestablishment of a major ice sheet on Antarctica by 10 Ma. Mean δ^{18}O values then continued to rise gently through the Late Miocene until the Early Pliocene (6 Ma), indicating additional cooling and ice-sheet expansion on west-Antarctica and the Arctic Ocean (Zachos et al., 2001).

Most interpretations of Miocene coral buildups apply the traditional barrier-reef shelf-lagoon complex model, although outcrop studies are increasingly identifying facies associations and geometries remarkably different from the standard modern tropical carbonate mode, and stressing the importance of the meso-oligophotic carbonate production, mostly by LBF and red algae. The red algae increased in diversity during the Oligocene (e.g., Manker and Carter, 1987; Buxton and Pedley, 1989; Pedley, 1998;

Aguirre et al., 2000; Rasser and Piller, 2004) and globally became the dominant Miocene carbonate producers (Halfar and Mutti, 2005). Larger benthic foraminifers were still active carbonate producers during the Miocene, though not as prolific as during the Paleogene. *Heterostegina, Amphistegina, Cycloclypeus*, and *Lepidocyclina* are common in packstones and grainstones from the Late Oligocene through the Miocene, at least in the eastern Tethys (e.g., Chapronière, 1984; Betzler, 1997; Hallock et al., 2006). Through the Miocene, as thermal gradients strengthened and pycnoclines migrated upward, the more stenothermal LBF suffered extinctions that diminished their abundance, diversity, and contribution to carbonate sedimentation. This interpretation is consistent with Hottinger's (1983, 1997) reports of reduction of the bathymetric distributions of many LBF, particularly during the Miocene.

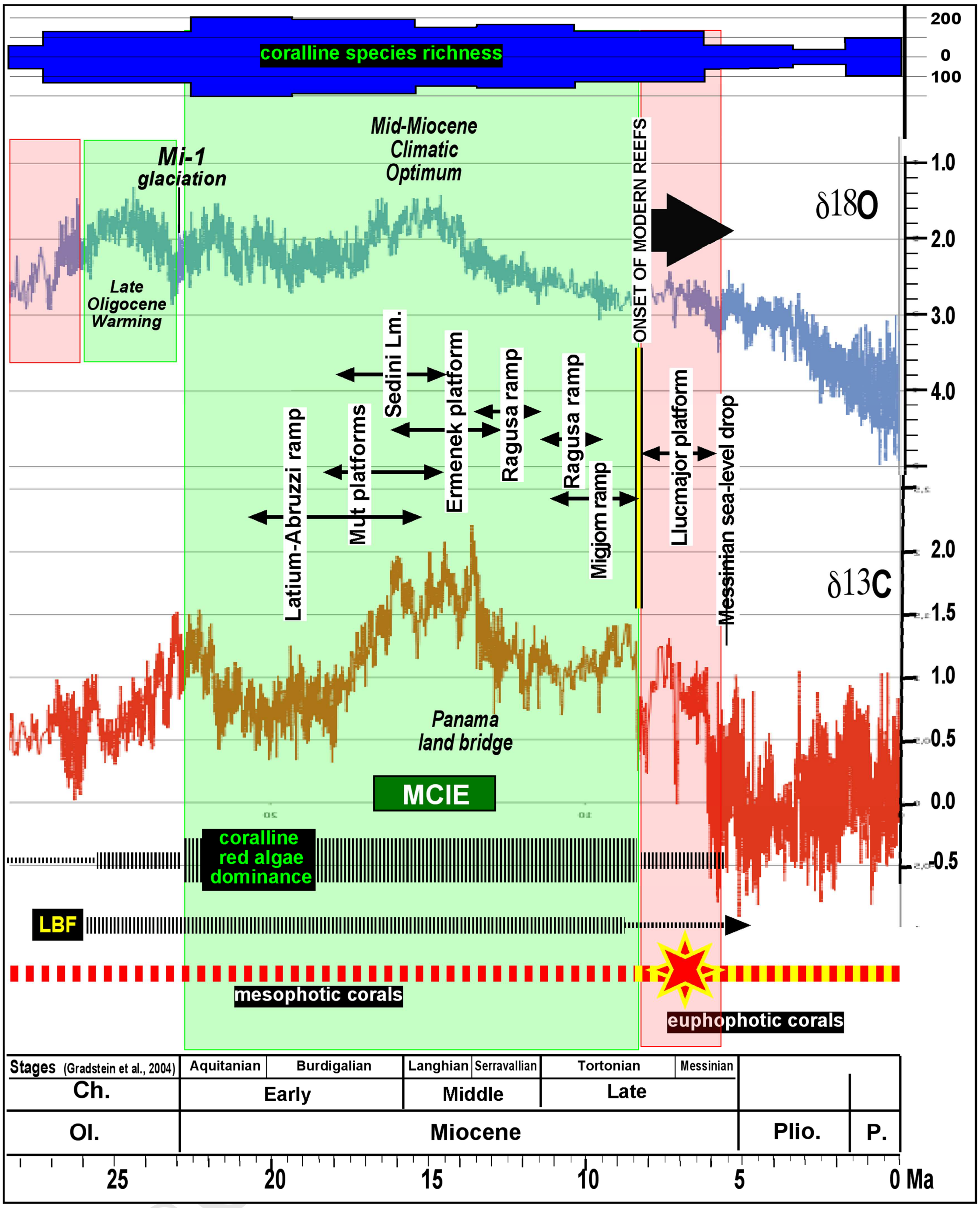

Fig. 18 – Miocene platforms, climatic events and red algal species richness. Oxygen and carbon isotopic curves are from Zachos et al. (2001); red algal species richness is from Aguirre et al. (2000). MCIE: Monterey Carbon Isotope Excursion.

A series of well-exposed Miocene platforms around the Mediterranean (**Fig. 18**) permits analyzing the relationship between the type of platform, the predominant skeletal composition and the loci of carbonate production (Pomar et al., 2012 a). During the Early Miocene, with a global climate warmer than at present (Zachos et al., 2001), a low-angle, heterozoan-dominated ramp formed in the Latium-Abruzzi region of Italy, though coeval platforms in Sardinia (Sedini) and South Turkey (Mut) were flat topped.

The *Latium-Abruzzi ramp* is mostly composed of bryomol and rhodalgal sediment associations, produced respectively in the aphotic and lower part of the photic zones, with very scarce coralgal bioherms. Enhanced trophic resources in the Latium-Abruzzi area have been proposed to explain the dominance of heterozoan carbonate producers (Brandano and Corda, 2002; Brandano, 2003; Pomar et al., 2004, 2012 a).

In the *Sedini platform* (Sardinia), mesophotic coralline-red algae and LBF (*Heterostegina, Amphistegina, Borelis*) dominated carbonate production in the oligophotic zone, whereas planar-bedded wackestones and packstones of the inner ramp can be interpreted as shallow-water seagrass deposits. Downdip, branching red algal packstones and floatstones define the outer ramp (Benisek et al., 2009, 2010). Hermatypic corals only built discrete bioherms from the platform top to the toe of slope.

In South-Central Turkey, the Burdigalian to early Serravallian was a time of high temperature and precipitation, associated with the Mid Miocene Climatic Optimum (MMCO). Enhanced precipitation likely increased terrestrial runoff but optimal temperatures allowed the rhodalgal carbonate factory to spread despite the elevated clastic input (Bassant, 1999; Bassant et al., 2004, 2005; Janson et al., 2007, 2010; Pomar et al., 2012 a). In the Mut and Ermenek regions, small, flat-topped platform banks started to aggrade and prograde with steep slopes, largely composed of red-algal pack-grainstone.

By the mid Langhian, the platform top and clinobeds, previously composed of coarse- to medium-grained red algal grainstone/packstone with LBF, changed in the topsets to foraminiferal packstone dominated by miliolids, alveolinids and peneroplids with rare green algae, revealing the inception of seagrass-related carbonate production. Coral buildups, largely made of branching and spherical forms encrusted by red algae, are abundant in both the platform top and margins. Bathymetric estimates for the platform top settings range from 5 – 20 m.

Small reef buildups, biostromes and coral carpets of relatively diverse assemblages of faviid and poritid corals developed extensively along the rifted margins of the Red Sea during the Langhian to early Serravallian (e.g., the Gebel Abu Shaar platform: Perrin et al., 1998; Perrin, 2000). Coral buildups preferentially developed on the footwall edges of basement rotated blocks, laterally associated with fan delta siliciclastics and/or bioclastic deposits with rhodoliths, mollusks and oolite. Corals did not form frameworks, rather they occurred as cluster-segment reefs with abundant biodetrital and/or muddy skeletal matrix.

During the late Serravallian, when global average temperature was decreasing from the MMCO to the cooler Late Miocene, and sea level was falling, the foramol association accumulated in the euphotic zone (seagrass meadows) and rhodalgal in the meso-oligophotic zone of the *Ragusa platform* (Ruchonnet, 2006). Consistent with the global cooling trend, this interval is characterized by relatively low faunal diversity around the Mediterranean shelves (Rögl et al., 1978; Demarcq, 1984, 1987). Demarcq attributed this low diversity to significant tectonic activity causing paleo-biogeographic disruptions and to the global cooling trend. Nutrient delivery from terrestrial runoff (Chamley et al., 1986; Vissier, 1991; Ruchonnet, 2006) increased trophic resources and reduced water transparency, which also influenced the carbonate-producing communities.

During the early Tortonian, sediment production in the euphotic zone of the *Ragusa ramp* changed to chlorozoan, although foramol sediments were still present (Ruchonnet, 2006). The sudden onset of the chlorozoan factory at the Serravallian/Tortonian boundary might reflect an abrupt change in the physical parameters of the Mediterranean waters; particularly the narrowing of marine gateways (Riffean and Bethic Straits) during the early Tortonian likely reduced the entry of cool Atlantic waters, favoring the warming and increasing salinity of the paleo-Mediterranean sea (Ruchonnet, 2006).

The lower Tortonian foramol-rhodalgal *Migjorn ramp* of Menorca, however, located in the Western Mediterranean, only 2º to the North but about 1000 km to the West from Sicily, contains very scarce aragonitic hermatypic corals (*Porites*) and *Halimeda*. The major biotic change to the aragonitic chlorozoan carbonate factory took place at the early to late Tortonian transition, when reefal platforms spread across the Mediterranean (Pomar, 2001 b; Pomar et al., 2002).

3.4.1. – *The upper Tortonian – lower Messinian reefal platforms: the inception of modern reefs*

Numerous upper Tortonian–lower Messinian coral-reef platforms occur across the Mediterranean (i.e., Brachert et al., 1996, 2001; Martín and Braga, 1994; Martín et al., 1996; 1999; Betzler et al., 1997, 2000; Franseen et al., 1997; Braga and Aguirre, 2001; Braga et al., 2001). Among these platforms, we choose as case study the Llucmajor platform on Mallorca as it is a well-preserved and well-exposed example of reef-rimmed shelf, which fully exhibits the facies architecture (Pomar, 1991, 1993; Pomar and Ward, 1994, 1995, 1999; Pomar et al., 1996). Although diversity was very low (1–3 coral genera), coral reefs actively prograded about 20 km during a period of tectonic quiescence. In this carbonate buildup, two distinct sediment associations occur: (1) chlorozoan sediment association compose the back-reef lagoon, the reef wall and the fore-reef slopes, with (2) a rhodalgal sediment association on the slope and at the base of the slope, in off-reef, shallow-basinal settings (Pomar, 1991; Pomar and Ward, 1994, 1999; Pomar et al., 1996, 2012 a).

Within the reef system, the reef wall consists of corals in living position interfingered with coral rudstone. In the reef wall, well-developed coral zonation is related to bathymetry: platy corals at the base are intermixed with poorly sorted wackestones and packstones. Branching corals forming "bush-like" thickets occur at mid-reef wall, and head-like corals, growing on top of each other, make up several meters-wide spurs separated by coral rudstone (breccia) and skeletal grainstone that represent the infill of the grooves on the wall, similar to modern reefs. Encrusting red algae and corals produced a rigid wave resistant framework in the shallowest euphotic zone, up to sea level, similarly to modern reefs.

Fig. **19**. Primary framework pore in the reef core of the Llucmajor Platform. A framework of branching corals makes up the walls of the pore, and there are abundant cones of coarse skeletal grainstones that sieved down through the corals interspaces.

Primary pores are large and abundant: interparticle porosity predominates in the rudstones, but framework pores occur abundantly within the coral framestone. Some of these primary pores can be up to 6 m across and 2 m high (**Fig. 19**). Evidence that the reef crest reached sea level can be seen in: 1) the existence of shallow-water lagoonal beds in backreef position, 2) an erosional surface associated with a sea-level fall, locally with thin caliche crusts, and the associated downward shift of the coral-morphology zones within the reef-core (Pomar, 1991; 1993; Pomar and Ward, 1994; 1995; 1999).

Facies architecture within this platform clearly indicates vertical up and down shifts of the reef-core facies along progradation, revealing sea-level cyclicity. Transgressions induced aggradation in all the sub-environments, whereas regressions induced downward migration of these sub-environments and subaerial exposure of the previous back-reef lagoon and upper part of the reef core.

The shift from foramol/rhodalgal-dominated to chlorozoan/rhodalgal-dominated production systems that occurred in the Tortonian might have resulted from a climatic change from cool-temperate to warm water, but there is no evidence of such climatic change in the global temperature trend (Zachos et al, 2001). Contrarily, Nikolaev et al. (1998) noted that maximum gradient variations occurred at the depth of 100 m resulting from thermocline onset and evolution, and suggest a first sharp increase of gradient by 4–6°C to have occurred between 10 and 5 Ma (the period of deposition of the LRP), and a second one also 4–5°C during the Middle– Late Pliocene.

This change from foramol to chlorozoan production in shallow water euphotic zones is coeval to a) the increase of thermal gradient (Nikolaev et al., 1998), b) the diversification of *Symbiodinium* dinoflagellates (Pochon et al., 2006), c) a sharp negative carbon isotope excursion (Zachos et al., 2001), d) a climate switch from humid to arid in the Western Mediterranean (Calvo et al., 1993), and a sharp climate change at 8.8–8.5 Ma with the establishment of a truly dry season in central Iberia around 8.5 Ma (Van Dam, 1997, 2006; Van Dam and Weltje, 1999). Pomar and Hallock (2007) suggested a coevolution of corals and zooxanthellae to be behind this sudden onset and expansion of the modern type of coral reefs. The convergence of all these factors contradicts the common view of the sediment associations as being related to temperature only (e.g.; foramol and rhodalgal: cool/temperate; chlorozoan: subtropical/tropical)

4. Discussion

4.1 – Carbonate buildups through the Cenozoic: a synopsis

Critical analysis of the type, shape and size of Cenozoic coral buildups in the Western Mediterranean region, complemented with observations of the predominant- and complementary biotas, internal-facies architecture and position within the depositional profile, has revealed several characteristics:

1. Rimmed platforms with a bio-constructed margin up to sea level do not occur before the late Tortonian; the modern Caribbean reef model biased previous interpretations.

2. Pre-late-Tortonian reef-rimmed platform margins and buildups developed in the mesophotic zone, where corals and red algae were the main constructors.

3. Green algae, indicative of the euphotic zone, are scarce in most of the analyzed buildups, but are abundant in reef-crest and back-reef facies of the Danian rimmed shelf, and in the reef and lagoonal facies of the upper Tortonian–lower Messinian barrier reefs.

4. Clinoforms on buildups prior to the late Tortonian do not correspond to fore-reef slopes of modern barrier reefs but to flank facies abutting the buildups. The Oligocene Castro Limestone is an exception, where the structural escarpment on the margin of the Apulian Block controlled the talus deposits.

5. Shallow-water facies in pre-late Tortonian ramps were colonized by seagrasses, particularly after the Priabonian-Rupelian cooling.

6. Through the Cenozoic, corals were able to build extensive, thick reefal structures in the central Tethyan region only during four time intervals: Danian, Bartonian–Priabonian, early Chattian, and late Tortonian–early Messinian (**Fig.20**). The size of these buildups was unrelated to coral diversity, in agreement with evidence from the tropical western Atlantic (e.g., Johnson et al., 2008).

7. The waxing, waning and changes in coral-buildup attributes, and the production modes through the Cenozoic, follow a trend that is marked by the changes in both deep-sea $\delta^{13}C$ and $\delta^{18}O$ stable isotopes.

The $\delta^{18}O$ is a proxy for a combination of surface temperature of deep-water source regions (high latitudes) and global ice volume. The $\delta^{13}C$, although influenced by biological oceanic productivity, is an indicator of perturbations of the global carbon cycle, changes in deep-ocean circulation patterns, carbon burial, and carbon release including methane accumulation and release, oxidation or erosion of organic carbon when sea level falls, and increased sequestration below upwelling zones (Bijl et al., 2009; Cramer et al., 2009, 2011; Zachos et al., 2011; Vandenberghe et al., 2012).

8. Red algae became dominant platform builders during the positive excursions of the δ^{13}C.

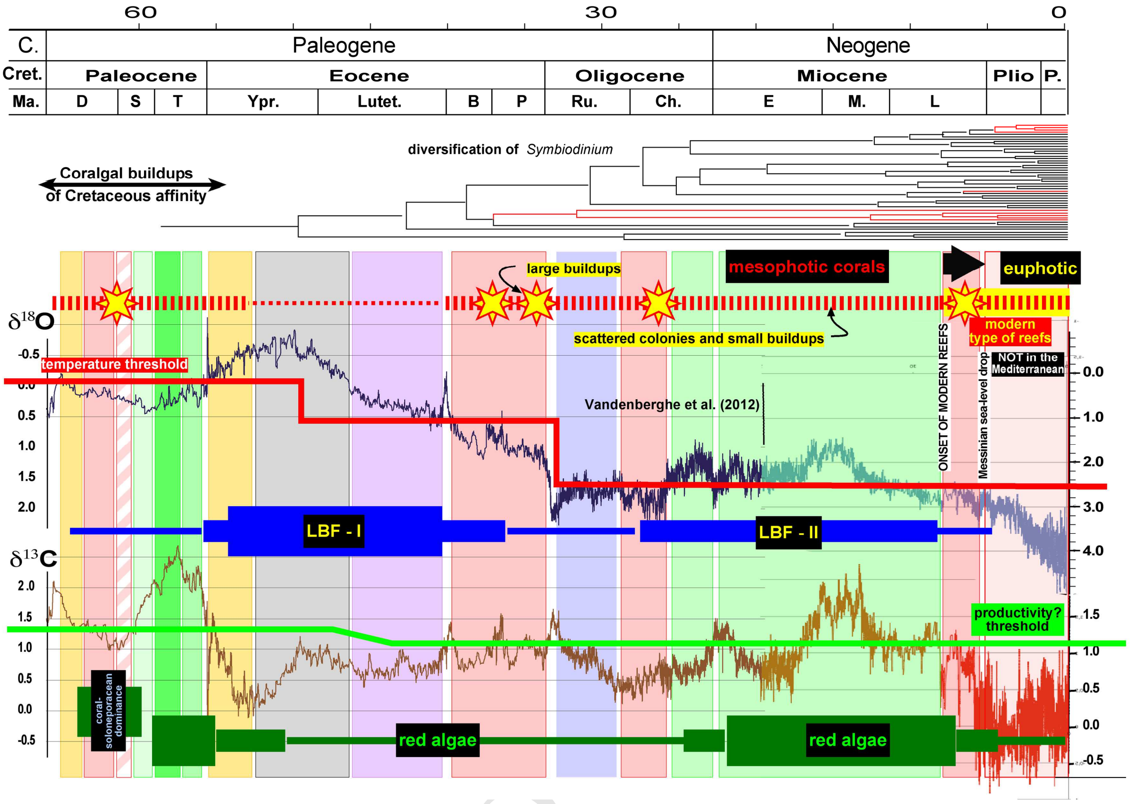

Fig. 20. Top: Phylogenetic tree of *Symbiodinium* zooxanthellae, with divergence times of all extant lineages (from Pochon et al., 2006). Oxygen and carbon isotopic curves superimposed to the platform-type stages. Periods of predominance of red algae follow positive excursions of deep-sea δ^{13}C, whereas larger benthic foraminifers follow the Eocene and Miocene warming phases. Large coral buildups developed when both oxygen and carbon isotope curves were below the two lines marking the temperature and productivity thresholds (stars). Oxygen and carbon isotopic curves are from Cramer et al. (2009) recalibrated to GTS201 in Vandenberghe et al. (2012) for the Paleogene, and from Zachos et al. (2001) for the Neogene.

9. Eocene and Miocene LBF assemblages parallel temperature records in both diversity and abundance.

10. Corals became effective builders during times when high-latitude temperatures were declining and deep-ocean δ^{13}C had low values.

The four episodes of development of large coral buildups can be framed by two arbitrary threshold lines, drawn in the way that the large-buildups developed when both the temperature (δ^{18}O) and δ^{13}C curves simultaneously occur below both threshold lines. In the temperature-threshold line however, two steps of temperature decrease are noted. These steps coincide with the main steps in zooxanthellae evolution. In the first interval, from the Cretaceous into the Lutetian, coral buildups retain Cretaceous affinities. The first step at the Bartonian-Priabonian coincides with the first diversification of *Symbiodinium* zooxanthellae (Pochon et al., 2006). A second step, by the Oligocene, coincides with a second episode of *Symbiodinium* diversification and coral reorganization. Pochon et al. (2006) suggested that *Symbiodinium* zooxanthellae harbored by corals originated in Early Eocene and divergence took place during periods of global cooling. Coral diversity was probably the highest for the whole Cenozoic by the Late Oligocene (Veron, 1995), and large coral buildups occurred worldwide. At other times, corals were either isolated or grouped, forming small mounds with cluster-fabric architecture in the mesophotic zone.

4.2. – Mixotrophy

Zooxanthellate corals, larger benthic foraminifers, and a few bivalve taxa (notably Tridacninae) host algal endosymbionts in a relationship that allows the holobiont (the host-symbiont association) to acquire trophic resources by both feeding and photosynthesizing. This relationship can provide the holobiont with tens to hundreds of times more energy than either pure autotrophy or heterotrophy in euphotic, nutrient-limited environments (Hallock, 1981, 2001), such as conditions for present-day tropical reefs. Moreover, because chemical reactions, and therefore metabolic rates, double with a 10ºC rise in temperature (e.g., between 20º and 30ºC), mixotrophy is even more advantageous in warm, tropical seas. Because of the energetic advantages, mixotrophic organisms tend to show rapid rates of diversification and specialization during times in the geologic record when such environments are consistently present over millions of years. However, as Hallock (1985, 1987) pointed out, such habitats are very sensitive to global changes and their inhabitants suffer higher rates of extinctions than less specialized taxa.

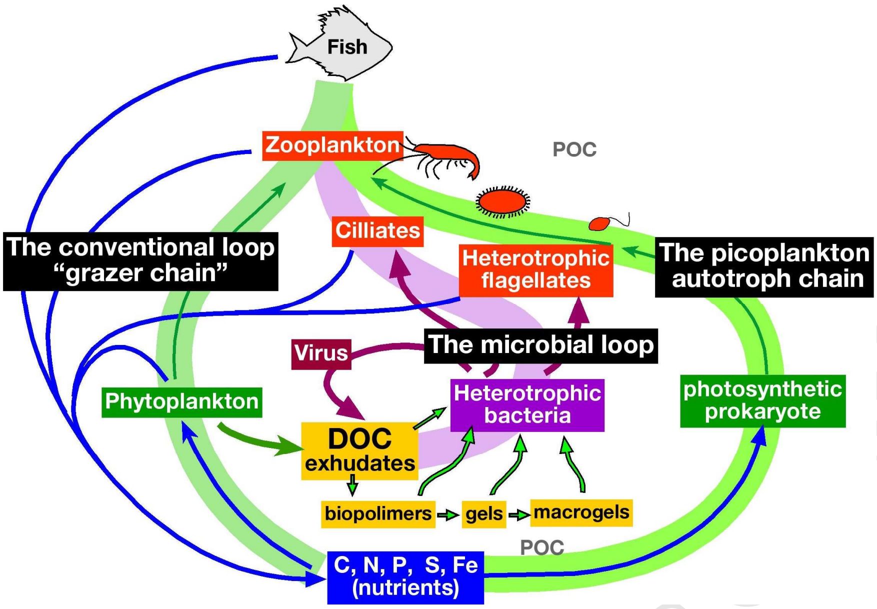

Fig. 21 – The three marine food-web loops. To the conventional loop, for which phytoplankton is the basis of primary production, the heterotrophic microbial loop and the photosynthetic picoplankton have to be considered. High rates of photosynthesis, partially decoupled from nutrient supply, produce photosynthetically derived dissolved organic carbon (DOC) that can polymerize in gels and macrogels, providing substrate for heterotrophic bacterial growth. Heterotrophic flagellates graze on the heterotrophic bacteria and are grazed, in turn, by ciliates and metazoans. CO_2 concentration fuels photosynthesis, temperature controls metabolic rates, and irradiance depends on water transparency, depth and latitude. Photosynthetic picoplankton (prokaryotes and picoeucaryotes) may account for more than half of the photosynthetic biomass in oligotrophic oceans. POC: particulate organic carbon; DOC: dissolved organic carbon. Based on Azam (1998), Verdugo et al. (2004) and Johnson et al. (2006).

Recognition of the advantages of mixotrophy in low nutrient environments further emerged with understanding that when phytoplankton cells become nutrient limited, photosynthesis decouples from cell growth. Where nutrients flux into shallow water systems, they promote cell growth and reproduction (e.g., Yang and Gao, 2003). High-irradiance, temperature and CO_2 levels increase photosynthetic rates that, if not matched by availability of nutrients, produce nutrient-poor organic matter, mostly polysaccharides (e.g., Riebesell et al., 1993; Hein and Sand-Jansen, 1997; Dubinsky and Berman-Frank, 2001; Riebesell, 2004). These photosynthates can be stored, diverted to various cellular functions, or excreted as DOC (dissolved organic carbon).

DOC includes polysaccharides and mucus that contain little or no nitrogen (**Fig. 21**). In open waters, DOC released from photoautotrophs can energetically support heterotrophic bacteria (Azam et al., 1983; Peduzzi and Herndl, 1992; Maurin et al., 1997; Azam, 1998), on which heterotrophic flagellates can graze, and those, in turn are grazed by ciliates and metazoans **(Fig. 21)**. This trophic path, known as the ***microbial loop***, operates in parallel with, and in some instances instead of, the ***"conventional loop"*** where phytoplankton is directly grazed by zooplankton. Azam et al. (1983) and Azam (1998) estimated that one-half of modern oceanic primary production might be channeled via bacteria into the microbial loop. More recently, the "**picoplankton autotroph chain**" (picoeukaryotic algae and photosynthetic prokaryotes) has been identified. Estimated primary production of the picoplankton chain may account for about 70% of total in tropical and subtropical oceans (Vaulot et al., 1995; Partensky et al., 1999; Charpy, 2005; Johnson et al., 2006). As nutrient concentrations are reduced, the competitive growth advantage shifts to smaller phytoplankton cells. Bacteria are a major biomass component of marine food webs, and, with marine viruses, play key roles in marine system energetics (Meyers, 2000); both can benefit from the products of excess photosynthesis.

The decoupling of photosynthesis and growth, when nutrients are growth limiting, supports not only the microbial loop but also a vast array of algal symbioses. Mixotrophic holobionts exploit this decoupling of photosynthesis and growth by "encapsulating" the photosynthesis within the host and creating a double external farming (see Hallock 2001, and references therein). In zooxanthellate corals and many larger benthic foraminifers, ingested particulate food (POC) provides nutrients to the host while respiratory energy comes principally from carbohydrates or lipids (DOC) translocated from the algal partner to the host. The respiratory CO_2 of the host is added to the photosynthetic circuit, increasing the production of DOC, polysaccharides and mucus (**Fig. 22**). Excess photosynthates, beyond the holobiont's needs, are excreted, providing DOC substrates upon which bacteria can thrive. This provides additional advantages in periods when ambient CO_2 was decreasing, such as during the Paleogene (nummulitids) and during the Permo-Carboniferous (fusulinids). While a correlation is clear between the abundance and diversification of these protist-protist holobionts with decreasing ambient CO_2, a relationship between decreasing CO_2 and corals (metazoan-protist holobiont) is not so evident. There appears to be plasticity by corals in changing and regulating the type and proportion of their zooxanthellae (Rowan, 2004; Baker et al., 2004; Chen et al., 2005; Stanley Jr, 2006).

While warm temperatures and high water transparency are prime factors favoring mixotrophy, atmospheric CO_2 also may be a key element for the effectiveness of the symbiotic partnership. Declining ambient pCO_2 likely favored co-evolution, as increased supply of CO_2 from host respiration and calcification could increase the production of photosynthates by the algal symbionts, while the increase of organic-carbon translocation (photosynthate) from the algae energetically benefitted their hosts (Pomar and Hallock, 2008; Hallock 2011).

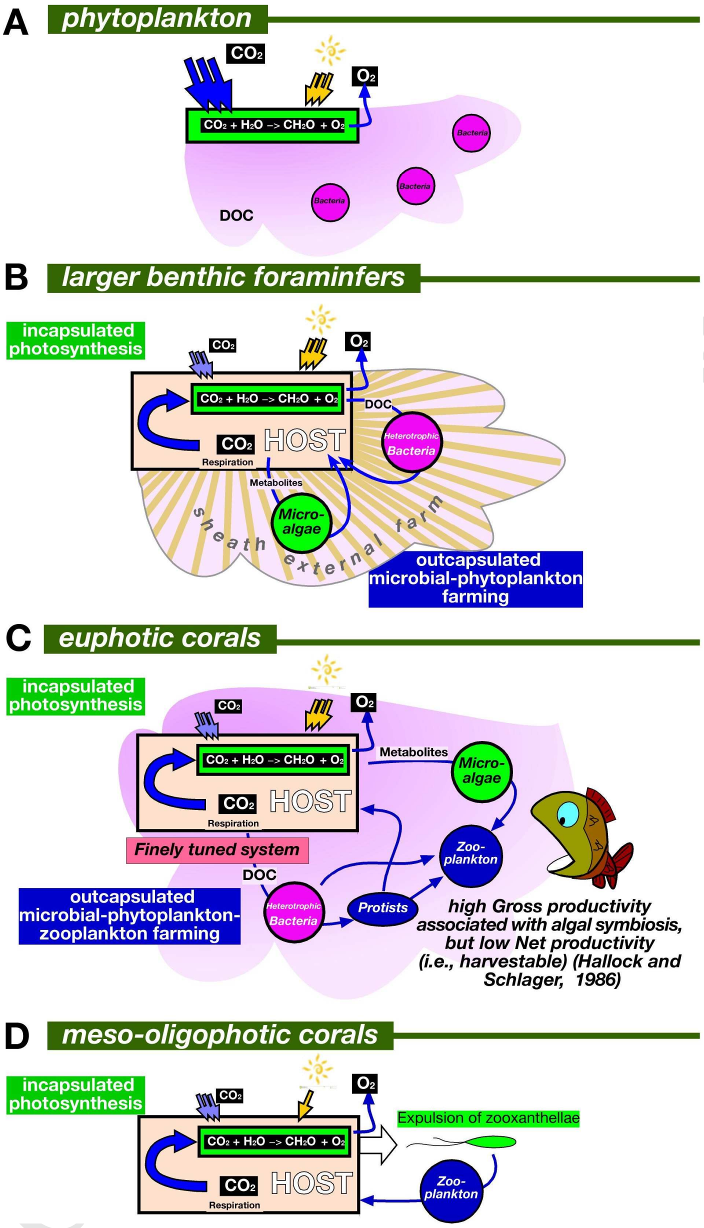

Fig. 22 – The decoupling of photosynthesis and growth, when nutrients are growth limiting, supports not only the microbial loop (**A**) but also a vast array of symbioses (**B, C & D**). Mixotrophic holobionts exploit this decoupling of photosynthesis and growth by “encapsulating” photosynthesis within the host and creating a double external farming, phytoplankton from the metabolites and the heterotrophic bacteria from the excess photosynthates. Mixotrophic nutrition provides orders of magnitude energetic advantage over purely autotrophic or purely heterotrophic nutrition for individual organisms and communities where light is plentiful but dissolved nutrients (DIN, DIP) are scarce (Hallock, 1981, 2001). D) Under limited light conditions in the meso-oligophotic zones, advantages of the symbiosis are subtle and possibly more episodic, and the recycling of nutrients, as modeled by Hallock (1981), rather than the

production of excess photosynthate (e.g., Hallock, 2001), may be the major advantage of algal symbiosis

4.2.1 - Corals

Cenozoic coral taxa that produce substantial buildups are primarily members of the Order Scleractinia. Although with significant taxonomic and systematic uncertainties, most compilations reveal that the Cenozoic evolution of scleractinians consisted in a progressive increase in diversity during the establishment of a marked provincialism (i.e., Coates and Jackson, 1987; Veron, 1995; Rosen, 2000; Budd, 2000; Kiessling and Baron-Szabo, 2004). However, the pattern of global diversification did not seem to have influenced the waxing and waning of coral buildups observed through the Paleogene and Neogene, which most likely were controlled by processes and patterns associated with changing environmental conditions.

Scleractinian corals can be solitary or colonial, but most reef-building taxa are colonial. They precipitate aragonite skeletons and are inherently heterotrophic, in the sense that they feed upon plankton. However, many scleractinian taxa are mixotrophic, hosting dinoflagellate symbionts that can provide up to 95% of the coral’s energy needs, as well as carbohydrates and lipids essential to skeletal accretion and reproduction respectively, though feeding is still required to access the very scarce nutrients (N, P, trace nutrients) essential for growth (Houlbrèque and Ferrier-Pagès, 2009).

As much as half the photosynthate produced by the symbiont is excreted as mucus by the holobiont. These exudates disperse in the water and stimulate microbial growth, establishing a recycling loop that supports grazing protists and zooplankton that, while reducing loss of energy and nutrients from the reef ecosystem, supplements coral feeding requirements (**Fig. 22 C)**. The symbiosis between dinoflagellates and corals is a finely tuned system. Under high-irradiance conditions (euphotic zone) in nutrient-depleted tropical waters, carbon fixation rates by the zooxanthellae are maximal, as is the excretion of photosynthates (DOC) that are “translocated” to the host or “exuded” as mucus (**Fig. 22 C**). The fine-tuning of this system includes changes of symbiont clades (Baker, 2003; Putnam et al., 2012) and the resulting efficiency explains the high gross primary productivity of modern reefs in oligotrophic conditions.

In the meso- and oligophotic zones, where irradiance levels are lower, photosynthesis rates and carbon assimilation are much slower (**Fig. 22 D)**, and nutrients are sufficient to support algal growth (Dubinsky and Berman-Frank, 2001). Under such limited light conditions, advantages of the symbiosis are subtle and possibly more episodic, and the recycling of nutrients, as modeled by Hallock (1981), rather than the production of excess photosynthate (e.g., Hallock, 2001), may be the major advantage of algal symbiosis. This explains why corals living under mesophotic conditions throughout the Cenozoic could not accrete at the rates comparable to modern reefs in the euphotic zone.

Pre-late Tortonian corals were neither able to form large, wave-resistant structures in shallow-water areas nor rims up to sea level. Rather, corals mostly thrived, along with red algae, in meso-oligophotic conditions, either in mid-ramp settings, or in the shallower inner ramps, associated with seagrass. The onset of the modern type of coral reefs occurred by the Late Miocene (Pomar and Hallock, 2008). Quite rapidly, at the early to late Tortonian transition, corals became the main reef builders all over the Mediterranean area, even though coral diversity was very low (e.g., Esteban, 1996).

The increase in light intensity associated with the upward migration into shallow water induces an increased production of photosynthates (DOC) by the symbiont and, consequently, an increase of oxygen. Protection against damaging solar radiation is provided by biochemical sunscreens, including amino acids that, produced by the symbiont, are translocated to the host (Furla et al., 2005). Moreover, to protect itself against oxygen produced during algal photosynthesis, the cnidarian host has developed antioxidant defenses that are unique among animals. Finally, living in nutrient-poor waters, the animal partner has developed several mechanisms for nitrogen assimilation and conservation such as the ability to absorb inorganic nitrogen, highly unusual for a metazoan. Consequently, the upward migration of corals to zones with higher light intensity required the co-evolution of host and zooxanthellae (Furla et al., 2005). In modern corals, shuffling of symbionts permits corals to adapt to changing temperature to some degree (Baker et al., 2004; Rowan, 2004; Chen et al., 2005; Stanley Jr., 2006). The advent of deeper diving technology has revealed mesophotic coral ecosystems, found in tropical and subtropical regions at depths ranging from 30 m to more than 100 m depths (Kahng et al., 2014; http://www.mesophotic.org/; http://oceanservice.noaa.gov/facts/mesophotic.html). The dominant communities providing structural habitat in the mesophotic zone are corals, sponges, and coraline algae.

4.2.1.1.- Functionality of the buildup accretion (how to catch the food)

Distinguishing different types of buildups necessitates understanding the functionality of the relief. Current classifications of buildup types (e.g., James, 1984; Kiessling et al., 1999; Riding, 2002) are basically descriptive and compositional, but do not capture functionality.

From a functional point of view, buildup accretion may result from colonization of pre-existing topography above the sea floor or from a simple residual piling of skeletons. For metazoans, the advantages of accretion increase the efficiency in getting food. Being sessile, suspension catchers (e.g., corals) and pumpers (e.g., sponges) require that particulate food be carried to them. Topographic relief enhances turbulent flow (Bilger and Atkinson, 1992; Hearn et al., 2001; Ribes et al., 2003). Elevation above the sea floor increases the feeding competence for suspension feeders as turbulence increases the impinging efficiency of currents carrying plankton (**Fig. 23**). Larvae fixed in a higher position, or on the upcurrent side, have better chance to catch food, so will grow more efficiently than the larvae fixed on the leeward side. Hydrodynamic requirements can also be distinguished among metazoans: pumpers (filter feeders) can thrive in relatively limited current if the plankton is sufficiently abundant, whereas higher turbulence will benefit catchers (suspension feeders) by bringing the plankton to the radius of tentacle activity.

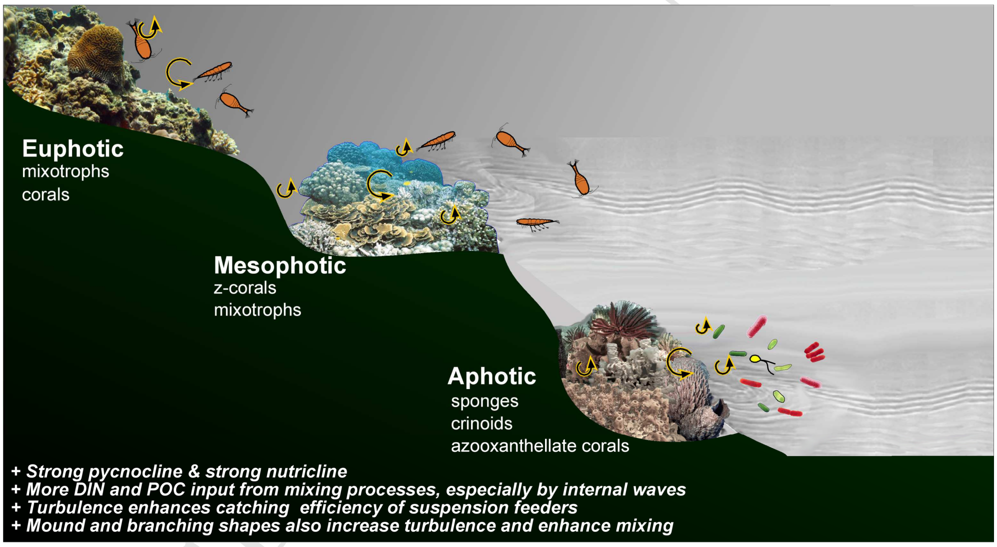

Fig. 23. Occurrence of bioherms requires advantageous functionality. Skeletons of sessile metazoans, single or colonial, will produce mounded accumulations when there is 1) enough food availability (particulate organic carbon: POC) to promote growth and reproduction, and 2) water turbulence both to carry the plankton and to increase the impinging efficiency upon the feeding structures (e.g., tentacles, pumping pores). These two conditions are most commonly met at the pycnoclines. Pycnoclines in the aphotic zone will promote heterotrophs only to form the mound, whereas in the photic zone, heterozoans and mixotrophs coexist, along with autotrophs, depending on the availability of dissolved inorganic nutrients (DIN).

Mixotrophs however, have an additional requirement: in addition to POC (particulate organic carbon) supply, they need light for photosynthesis. Thus, upward accretion may also be influenced by the competition for light, and vertical zonation of mixotrophs is controlled by light penetration. In shallow waters, where light is plentiful and scattered, branching morphologies are most advantageous if water motion is sufficient but not extreme. At intermediate light intensities (<60% of surface light) and water motion, mounded morphologies are advantageous. At lower light levels (<10% of surface intensities), light is unidirectional from above and plate-like morphologies allow maximum light capture. However, because energy for photosynthesis is very limited and plate-like morphologies are not advantageous for food capture, accretion potential is minimal, resulting in biostromes.

4.2.1.2. – Where were the buildups located (where the food is)

Carbonate buildups produced by azooxanthellate corals, bryozoans, bivalves, or other heterotrophic calcifiers, are thus controlled by two basic requirements for accretion: food source and delivery system, i.e., water motion, in addition to suitable water chemistry (i.e., aragonite saturation). From this perspective, buildups will preferentially be where there is a concentration of food. For example, aphotic coral buildups in modern environments lie beneath relatively productive surface waters in areas of subsurface currents, whether thermohaline, tidal, or internal-wave driven (Bruntse and Tendal, 2001; Davies et al., 2009). Bryozoan buildups are found off the south coast of Australia, where the extreme turbulence of the Southern Ocean waves reaches depths of 50 m or more (James et al., 1992, 1994).

Carbonate buildups produced by autotrophic and mixotrophic organisms represent a delicate balance between “trophic resources” and water transparency. Abundant trophic resources limit water transparency; extremely clear waters mean very scarce trophic resources but abundant sunlight for photosynthesis. In modern low latitude environments, the balance occurs in shallow waters with adequate water motion or turbidity (from CDOM, plankton, or small amounts of fine sediments) to limit the most damaging intensities of shorter wavelength solar radiation. As noted by Hallock (2001) and references therein, the highest accretion rates of modern carbonate buildups occur in wave or current-swept waters verging upon mesotrophic, because the plankton-feeding corals and the coralline and calcareous algae are at their maximum production potential. However, they are also approaching conditions that turn off reef accretion because of community change (phase shift) to predominance of non-accreting benthic organisms.

Modern mesophotic carbonate buildups are found in places where the surface waters are extremely clear and oligotrophic, allowing adequate light to penetrate to depths of 30–50 m or more, and where topographic features or internal waves bring uppermost pycnocline waters to those depths, providing exceptional supplies of trophic resources. For example, on the deep shelf between Puerto Rico and the US Virgin Islands, mesophotic corals are abundant, though their accretion rates are not fully known. Better known in terms of production rates are the *Halimeda* bioherms, often in association with abundant LBF, that have been described from the western Caribbean (Nicaraguan Rise), Sunda Straights, and lagoon behind the narrow channels through the Ribbon Reefs of the Australian Great Barrier Reef.

In mid- to low-latitude oceans, the surface mixed layer is separated from the much colder, deep ocean water masses by the thermocline, which mostly coincides with the pycnocline because density changes in modern oceans are primarily driven by temperature. A uppermost pycnocline is typically a zone of high plankton concentration (food availability) and of internal-wave propagation (turbulence) (e.g., Dickson and McCave, 1986; White and Dorschel, 2010; Hernández-Molina et al., 2011). Internal waves are fundamental mechanisms in carrying nutrients and in influencing distributions of plankton and larvae, although they may also cause ecological stresses (Lennert-Cody and Franks, 1999; Inall et al., 2001; Apel, 2002; Scotti and Pineda, 2004; Wolanski et al., 2004). Under thermohaline circulation as in modern oceans, the thermocline is primarily responsible for the pycnocline, but in a “greenhouse” world, ocean circulation and the origin and locations of the pycnocline were probably dominated by halothermal (primarily salinity-driven) conditions (e.g., Kennett and Stott, 1991; Pak and Miller, 1992; Nunes and Norris, 2006).

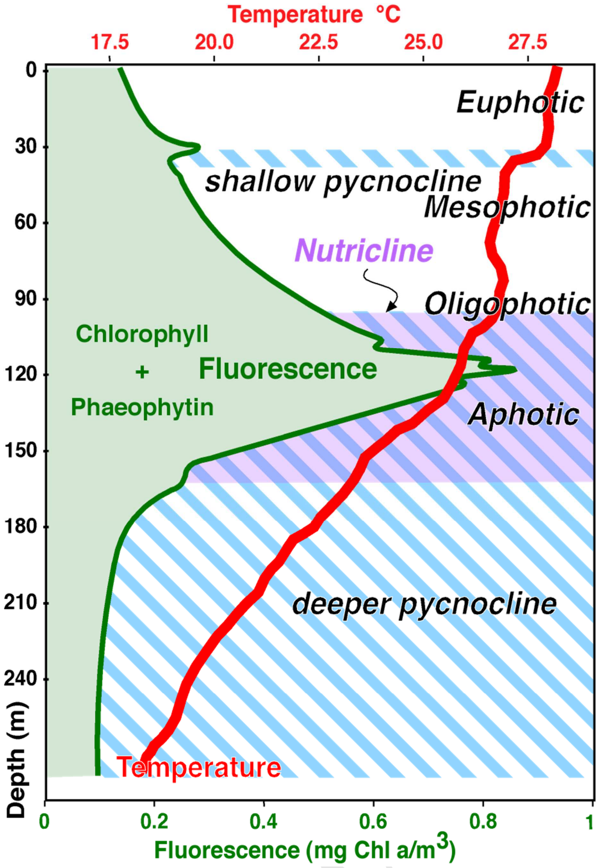

Fig. 24 –A peak in chlorophyll and phaeophytin (degrading chlorophyll) typically occurs at the nutricline, which coincides also with the top of pycnocline (Hallock et al., 1991a). The nutricline generally begins in the lower part of the photic zone, where nutrient-rich (deeper) water can mix upward via upwelling or internal waves, and where available light energy, not nutrients, limits primary production (modified from Hallock and Pomar, 2008).

Chlorophyll maximum layers are typically associated with pycnoclines in the ocean, whether seasonal or permanent (**Fig. 24**), and the concentrations of phytoplankton attract aggregations of mobile zooplankton (Sandstrom and Elliott, 1984; Pingree et al., 1986; Nielsen et al., 1993; Richardson et al., 2000; Leichter et al., 2003; Ryan et al., 2005; Mann and Lazier, 2006). A maximum in fluorescence, representing a peak in chlorophyll and phaeophytin (degrading chlorophyll) concentrations, typically occurs at the nutricline, which also coincides with the top of pycnocline (Hallock et al., 1991a). The nutricline generally begins in the lower part of the photic zone, where nutrient-rich (deeper) water can mix upward via upwelling or internal waves, and where available light energy, not nutrients, limits primary production. Thus, both the seasonal pycnocline and the upper part of the permanent pycnocline in lower latitude regions represent zones of likely internal-wave propagation and enhanced plankton concentrations.

In modern systems, internal waves increase the supply of inorganic nutrients as well as POC when they impinge upon a shelf margin or upper slope In the Florida Keys, internal waves increase by one order of magnitude the fluxes of inorganic nutrients (Leichter et al., 2003, 2008), and also induce high frequency variations in the concentration of chlorophyll-*a* when breaking, associated with changes in temperature, salinity, and turbulence (Leichter et al., 1996). The arrival of internal waves is associated with large increases in phytoplankton and zooplankton concentrations (Leichter et al., 1998). Eventually, if the induced fluid velocities exceed the wave speed, trapped cores may form and, at this stage, the solitary waves become highly turbulent, leading to strong vertical mixing that has been postulated to contribute to biological productivity (Alford et al., 2015).

Azooxanthellate scleractinian corals, thriving in cold, deep, dark waters, form abundant banks along continental margins and seamounts, at mid-depths from the high latitudes to the low latitudes of both hemispheres (e.g., Freiwald, 2003; Roberts et al., 2006; White and Dorschel, 2010). These mounds coincide with pycnoclines where food particles accumulate and can form nepheloid layers (e.g., Mienis et al., 2006; Roberts et al., 2006; Wheeler et al., 2007; Eisele et al., 2011; Henriet et al., 2014). Consequently, the pycnoclines are the preferential locations for suspension-feeding metazoans to grow and where they preferentially produce buildups.

Where the formation of subsurface chlorophyll maximum layers is associated with the pycnocline, and subsurface concentrations of phytoplankton attract aggregations of mobile zooplankton, then the pycnocline represents a zone of both likely internal-wave propagation and high plankton concentrations, so that suspension-feeder metazoans should produce buildups preferentially at the bathymetry of the pycnocline. This explains why most Phanerozoic metazoan buildups tend to be placed at mid- to outer ramp settings (e.g., Tucker and Wright, 1990; Burchette and Wright, 1992), the bathymetry where the pycnocline is located (Pomar et al., 2012 b).

4.2.2.- Larger Benthic Foraminifers

The LBF have been major contributors to tropical carbonate platforms worldwide since the late Paleocene. The LBF are a diverse, informal group that includes several porcelaneous-imperforate and hyaline-perforate lineages. They are mixotrophs and their adaptation to variable light conditions has been achieved through two different strategies. One strategy has involved specialization with different symbiont types under different light conditions. This is the strategy of the porcelaneous lineages, in which symbiotic relationships have been established with only one type of alga, and the alga's preference for a given light-wavelength allows the colonization of different environments. Many large porcelaneous taxa live in seagrass meadows (see seagrass section below), occupying leaves or rhizomes according to the type of symbiont.

Large rotalids exclusively host diatoms as symbionts, allowing photosynthesis under a broad light spectrum and, consequently, a substantial depth range. Living at different depths requires adaptation to different light intensities and diverse hydrodynamic conditions (Hallock and Hansen, 1979; Ter Kuile and Erez, 1984; Hallock and Glenn, 1986; Hallock, 1999; Mateu-Vicens et al., 2009). Thus a second strategy, adopted by large rotalids, involves changing the test shape to adapt to different light and energy conditions. Flat, thin tests are relatively delicate and well adapted to low light intensities in low-energy environments. Modern flat, large rotalids live at depths below the wave base or occupy sheltered areas within reef rubble or below the blades in seagrass meadows. Although larger foraminifers are predominantly free-living, some can temporarily or permanently anchor using organic sheaths or “glues”. Thicker lenticular to round shapes are better adapted to well-illuminated and stronger hydrodynamic regimes. Robust stellate morphologies that anchor using organic sheaths are well adapted to even stronger hydrodynamic regimes (Hallock, 1999). Nevertheless, intense water turbulence is detrimental for most large foraminifers in comparison to encrusting coralline algae and encrusting corals.

These strategies have allowed the different taxa of LBF to adapt to diverse environments, ranging from full-sunlight reef crests to the deep oligophotic zone. The organic sheaths, in which the sugars (glycosaminoglycans) act as natural glue, are also used as a source of energy for bacteria, fungi and algae. Thus, the foraminifers can supplement feeding by consuming microrganisms growing upon the sheaths.

4.2.2.1- The saga of LBF during the Cenozoic

Cenozoic LBF appeared after the K-P event, when old lineages (e.g., *Miscellanea*) became extinct and families such as the nummulitids, discocyclinids, alveolinids, and orthophragminids rose to prominence and diversified at the generic level during warming in the late Paleocene (**Fig. 25)**. During the Early Eocene, differences in thermal conditions between the deep sea and the thermocline were minimal (Bralower et al., 1995; Dutton et al., 2005; Tripati and Elderfield, 2005; Bijl et al., 2009) as likely was the density contrast at the pycnocline. The smaller density gradients likely resulted in reduced hydrodynamism in both subsurface current velocities and internal waves. The smaller the density contrast, the lower the wave frequency and slower the propagation speed of internal waves (Apel, 1987).

Under reduced hydrodynamic conditions, large rotalid taxa such as *Nummulites* reached large sizes with very flat shapes, and were prolific in meso-oligophotic conditions. This unique foraminiferal factory ended when thermal gradients between the mixed layer and the deep ocean strengthened and turbulence hit the shelf at depths typical of the meso-oligophotic zone.

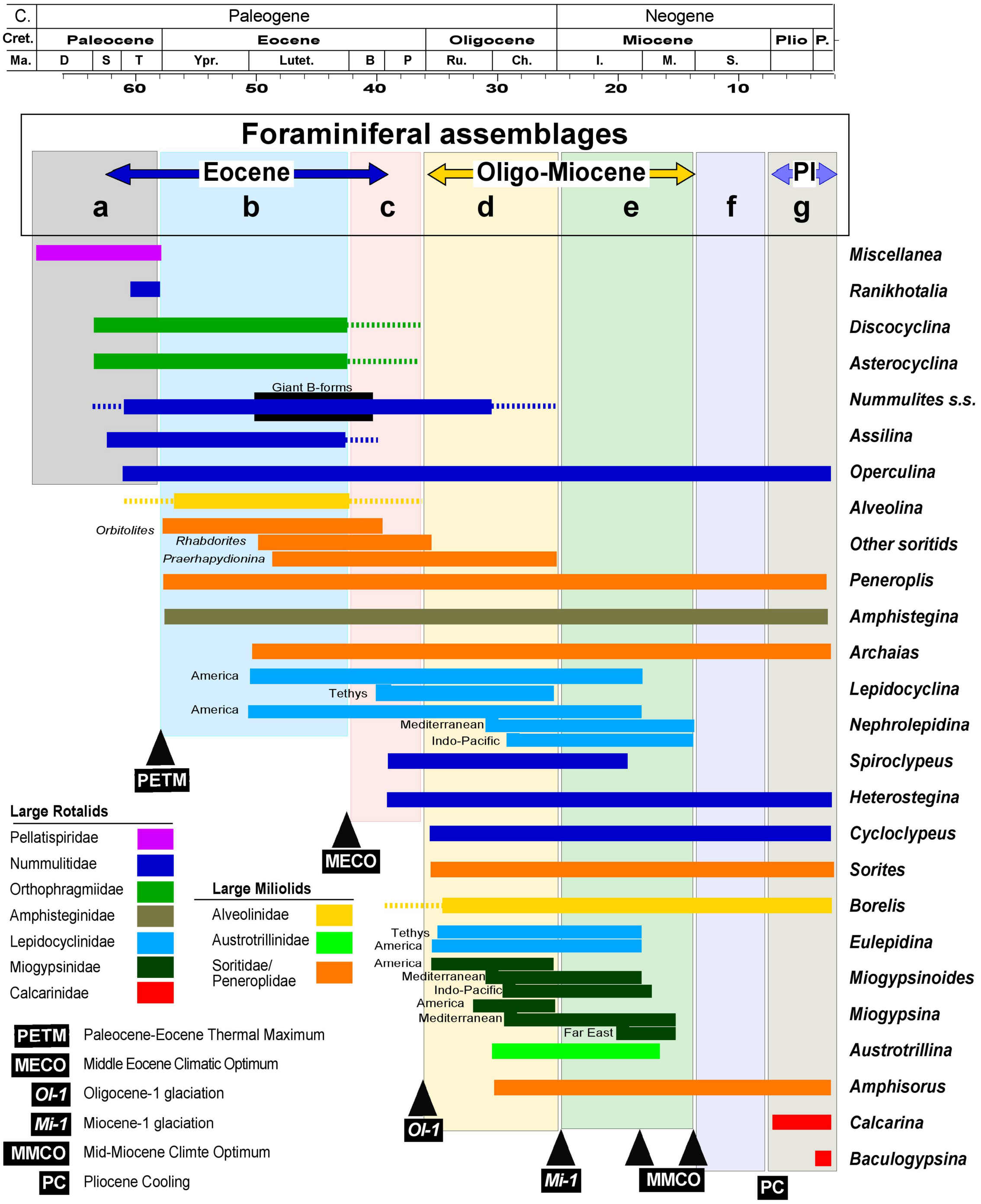

Fig. 25. Chronostratigraphic distribution of the main Cenozoic LBF genera and foraminiferal assemblages.

The taxa responsible for the prolific nummulitic factory, unique in terms of the gigantic size of the holobionts and the volume of accumulated tests, became extinct along with other taxa characteristics of the Eocene, when high latitude temperatures began to decline in the late Eocene and deep-ocean circulation accelerated, especially with the onset of the Oligocene. The gigantism in the protist-protist holobiont reappeared with the late Oligocene warming, when forms of *Eulepidina* (*E. elephantina*) reached comparable dimensions to those of the largest *Nummulites* species (*N. millecaput*). Both giant species are interpreted to have occupied equivalent, low-energy, oligophotic environments, when higher latitudes were warmer and bathymetric thermal gradients were weaker.

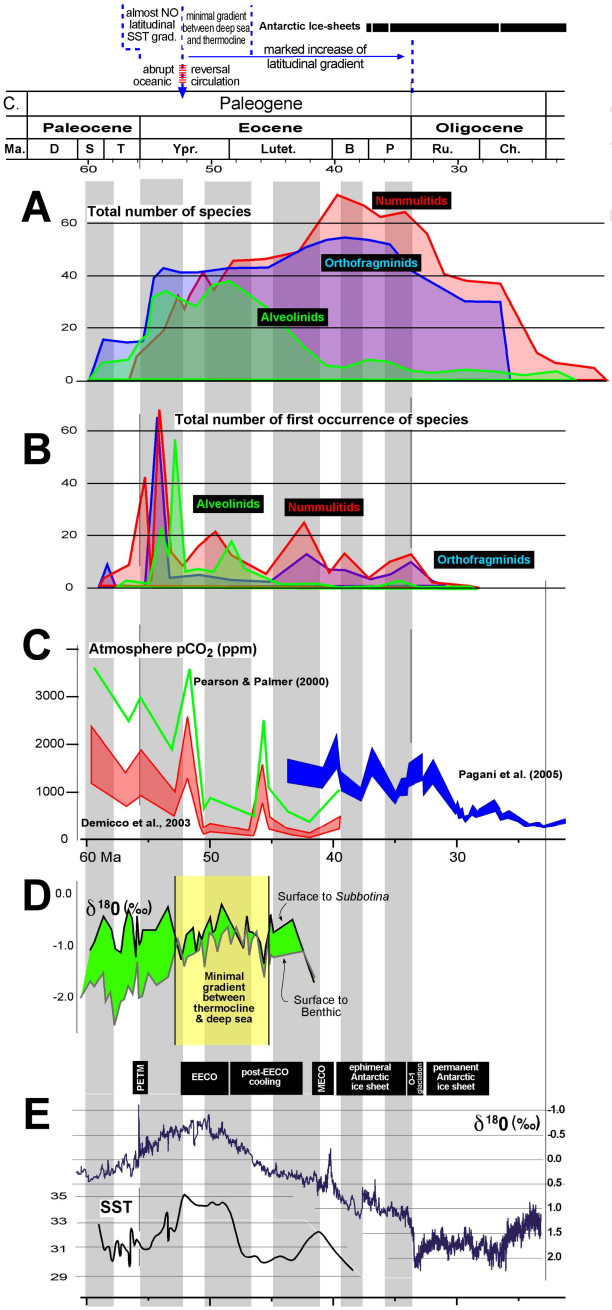

Fig. 26 – Paleocene and Eocene larger benthic foraminifers (gray shaded rectangles are for visual correlation only). A: Total number of species of nummulitids, orthophragminids and alveolinids. B: Total number of first occurrence of species of

nummulitids, orthophragminids and alveolinids. C: Estimations of atmospheric CO_2 concentration, based on: boron-isotope ratios of ancient planktic foraminifers to estimate the pH of surface-layer seawater (Pearson and Palmer, 2000); stable carbon isotopic values of di-unsaturated alkenones extracted from deep-sea cores (Pagani et al., 2005); secular changes in the major ion composition of seawater (particularly Ca and Mg) and in the oscillations in the mineralogy of primary oceanic carbonate sediments (Demicco et al., 2003). D: Surface-to thermocline versus surface-to-bottom temperature gradients at the Shatsky Rise, subtropical North Pacific, during the Paleocene and Eocene, as recorded by the $\delta^{18}O$ gradients. The apex time for Eocene *Nummulites* and other LBF (according to Hottinger, 1998) coincides with the time when the thermal gradients were minimal (from Dutton et al., 2005). E: Global deep-sea oxygen isotope record based on data compiled from more than 40 DSDP and ODP sites; it provides constraints on the evolution of deep-sea temperature and continental ice volume (Zachos et al., 2001)

But what is really intriguing is the correspondence between the diversification of the Eocene LBF and atmospheric CO_2 lows (**Fig. 26 A, B and C**). This correspondence suggests that atmospheric CO_2 was a prime factor in the evolution of the LBF. When ambient CO_2 declined, the symbiotic partnership benefited from the supply of CO_2 from host respiration to the algal symbiont, thus increasing the translocation of organic carbon from the algae to the host. Similar to the Eocene, the large and diverse fusulinids during the Carboniferous and the Permian radiated following a significant drop in CO_2. The efficiency of the protist-protist symbiotic relationship appears to promote extreme specialization (Hallock, 1987), thus subtle changes in the temperature and, also probably CO_2, can induce rapid turnovers and species replacement.

The Oligo-Miocene is characterized by the diversification and expansion of a different LBF assemblage (lepidocyclinids, miogypsinids, amphisteginids, heterosteginids) and by the gigantism of the Oligo-Miocene *Eulepidina*, although without the massive accumulation of monospecific tests characteristic of Eocene facies. The inception of this Oligo-Miocene LBF assemblage parallels the late Oligocene warming, but by the warmest Mid Miocene Climatic Optimum, some of these taxa disappeared (miogypsinids, lepidocyclinids) and others reduced production (amphisteginids, heterostegınds), coinciding with high values in $\delta^{13}C$ and the dominance of more eurythermal coralline red algae (**Fig. 25)**.

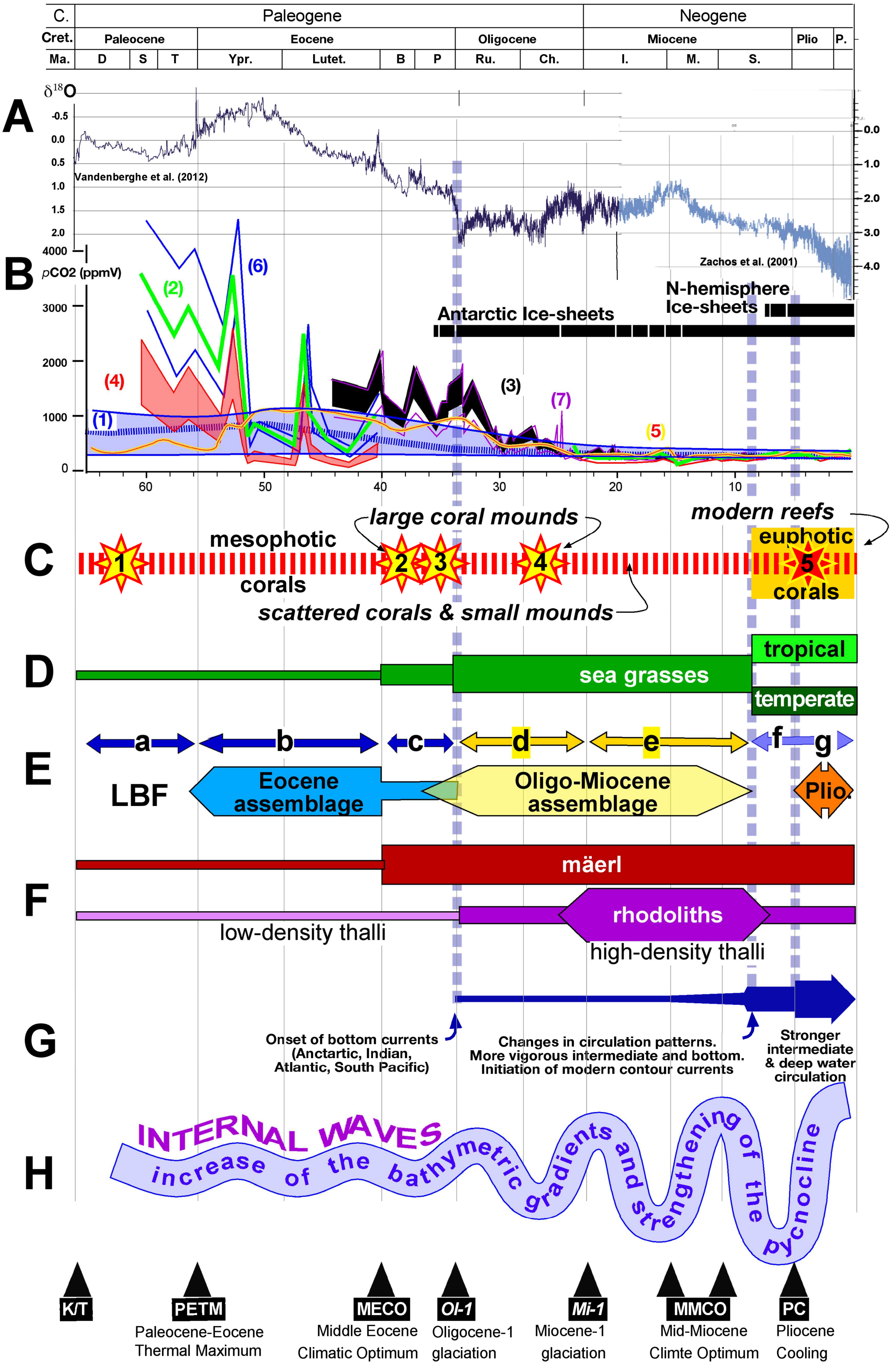

Fig.27.- Relationships between: **A)** global temperature (as in Fig. 20), **B)** CO$_2$ concentration in the atmosphere ((1) Berner & Kothavala, 2001; (2) Boron: Pearson &

Palmer, 2000; (3) Pagani et al., 2005; (4) Demicco et al., 2003; (5) Beerling & Royer, 2011; (6) Boron, Zachos et al. (2008); (7) Alkenones, Zachos et al. (2008)), **C)** main stages of large coral buildups (as in Fig. 20), **D)** expansion of seagrasses, **E)** foraminiferal assemblages (as in Fig. 25), **F)** changes in coralline red algae, **G)** onset and strengthening patterns of intermediate- and bottom-currents circulation (Hinz et al., 1999; Nisancioglu et al., 2003; Hernandez-Molina et al., 2009; 2010); H: estimation of the increasing turbulence due to the progressive ocean stratification.

The onset of the deep-water flow around Antarctica by the Early Miocene affected the global atmospheric and oceanic circulation patterns and reduced the north–south surface circulation flows, reducing the mixing of warm tropical ocean water and cooler polar water. Temperature gradients between high and low latitudes continued to increase by the Middle Miocene, when the Antarctic ice sheet had fully formed and temperatures at high and low latitudes were largely decoupled (Sclater et al., 1985). This strengthened bathymetric gradients and the pycnocline, and consequently the impact of internal waves in the mesophotic habitats (**Figs. 27** and **28**). Halfar and Mutti (2005) suggested that increased extinction rates of planktic foraminifers, radiolarians, corals and larger foraminifers in the mid Miocene paralleled enhanced upwelling resulting from strengthening thermal gradients and thermohaline circulation.

Concomitant with these global-scale changes, other major changes in benthic habitats affected mesophotic and euphotic environments, supporting proliferation of seagrasses (see below, and **Fig. 27**).

4.3. - Autotrophy

4.3.1.- Seagrasses

Seagrasses are flowering plants with true leaves, stems and roots. Having appeared by the Late Cretaceous (Brasier, 1975; Eva, 1980; Ivany et al., 1990), their expansion started by the late Ypresian, paralleling the global cooling trend. Seagrasses increased during the Late Eocene and were widespread in shallow, euphotic inner ramps by the Oligocene (Brasier, 1975; Ivany et al., 1990; Côsovic et al., 2004; Mateu-Vicens et al., 2008; Zamagni et al., 2008; Brandano et al., 2009 a, b; Riordan et al., 2011).

The late Miocene inception of modern reefs, with the reef framework growing up to sea level, introduced a change in the euphotic habitats of the tropical and subtropical regions. The wide, high-energy inner-ramp habitats became greatly reduced while shallow-water, protected backreef lagoons became dominant. Behind the hydrodynamic barrier, green algae proliferated and seagrass could form large patches with limited vertical growth, but with a more reduced distribution than the Oligocene and Early to Middle Miocene meadows. In contrast, in temperate areas (e.g., Mediterranean, southern Australia, northeastern Gulf of Mexico) where coral reefs do not occur, seagrasses still colonize the open inner ramps forming extensive meadows with very long life spans and considerable vertical growth, whose bathymetric distribution is similar to what it was in the ancient meadows.

Since their first occurrence, seagrasses have played a major role in carbonate production and sedimentation. These flowering plants sustain a prolific carbonate factory, as many of their epibionts possess a calcareous skeleton (e.g., coralline algae, bryozoans, mollusks, serpulid polychaetes, and foraminifers; Brasier, 1975; Eva, 1980; Fornós and Ahr, 1997, 2006; Mateu-Vicens et al., 2012). Only exceptionally, seagrasses may directly precipitate aragonite (Enríquez and Schubert, 2014). Additionally, the plant structure contributes to the accumulation of sediments. Thus, the extensive canopy of leaves dissipates water motion, promoting particle settling, while their root and rhizome systems trap and hold sediments in place (Pomar et al., 2002, and references therein). Due to the wide size range of the skeletal components produced within seagrass meadows and to the capacity of trapping and retaining sediments, including the finest fraction, the dominant textures are heterometric, poorly-sorted packstones with variable but significant amounts of mud.

During their expansion, seagrasses progressively became a dominant ecosystem in shallow, soft bottoms. Occupying a relatively wide bathymetric range within the euphotic zone and providing a plethora of ecological niches favored the emergence of new taxa and the migration of already existing ones into the seagrass meadows. The adaptive radiation of seagrass-related biota was rapid, as it is evidenced for example by both small and large benthic foraminifers.

Benthic foraminiferal taxa with epiphytic living mode split into several morphotypes according to their motility, life span and feeding modes (Langer, 1993; Mateu-Vicens et al., 2014), which, in turn, reflect their adaptation to the plant life cycle. Sessile, encrusting forms (e.g., *Planorbulina, Miniacina, Nubecularia*) and taxa with reduced motility (e.g., *Lobatula, Cibicides, Rosalina*) have life spans synchronized with the leaf-turnover rates. In contrast, more opportunistic, less specialized taxa (e.g., miliolids and textularids) that are also common in other substrates, have much shorter life cycles.

Most small rotalid families with epiphytic representatives appeared during the emergence and early expansion of the seagrasses, by the Late Cretaceous or the Paleogene. Nevertheless, the genera of these families with significant preference for phytal substrates appeared later. For the small porcelaneous forms (miliolids s.l.), families with epiphytic taxa date back to Middle Jurassic, but the genera characteristic of vegetated environments appeared much later, often coinciding with seagrass expansion periods.

Among the symbiont-bearing foraminifers, empty niches were occupied by taxa of both rotalid and miliolid groups. In contrast to the small benthic taxa where epiphytic rotaliids diversified, the porcellaneous LBF adapted very effectively to seagrass environments (Reich et al., 2015). Discoid morphologies (extinct meandropsinids, peneroplids, soritids) have recurrently appeared since Late Cretaceous and along the Cenozoic, coinciding with the appearance and expansion of seagrasses. The disc-shaped taxa, when attached to a leaf surface, maximize nutrient absorption from below and offer maximal exposure surfaces to light (Hallock et al., 1991b), which is indicative of an evolutive adaptation.

Other symbiont-bearing miliolids, less adapted than the flat forms, also have occurred in seagrass meadows since the end of the Oligocene. Among these taxa, *Austrotrillina* and some alveolinids that colonized the vegetated bottoms during the Eocene-Oligocene transition, evolved from elongate (e.g., *Alveolina*) to subspherical forms of the genus *Borelis* (Boudagher-Fadel, 2008) and became abundant as seagrass-dwelling species (**Fig. 28**).

For the large rotalids, not all taxa occurring in seagrass meadows are exclusive of these environments, although various families and genera (i.e., nummulitids: small *Nummulites, Operculina, Heterostegina, Planostegina*; amphisteginids: *Amphistegina*) have adapted their ecological requirements to vegetated niches since the Paleogene. Some of these foraminifers (e.g., flat nummulitids) dwelled preferentially in the oligophotic zone under low hydraulic energy. Expansion of seagrass meadows, however, provided similar low light and low energy regimes at much shallower depths, below the leaf canopy, which facilitated the colonization of these niches by flat nummulitid forms.

Among large rotalids, only few have developed epiphytic behaviors, as it is the case of *Amphistegina,* some forms of the extinct genus *Miogypsina*, and the stellate calcarinids. The miogypsinid lineage, which appeared in the Western Tethys during the early Oligocene and migrated eastwards until the middle Miocene, was partly related to the seagrass expansion as some forms evolved morphologically to become epiphytic (BouDagher-Fadel, 2008). Thus, irregularly shaped *Miogypsina* is thought to have thrived attached, adopting the shape of the substrate. For attached forms, the effects of hydraulic energy are less important than in free-living forms. Forms encrusting phytal substrates, including small taxa, grow with one side strongly attached to the plant, offering less exposed surface and hindering the test entrainment.

The small and large forms of the rotalid and porcelaneous taxa living in seagrass meadows have inverse adaptive trends. These differences in adaptation to the seagrass meadows might be related to the algal symbionts hosted by each group. Large miliolid taxa host a variety of unicellular algae (red algae, green algae, dinoflagellates, diatoms) that have established univocal symbiotic relationships. On the contrary, large rotalids host diatoms exclusively. The array of algal symbionts of the epiphytic porcelaneous taxa can perform photosynthesis over a fairly broad light range, despite the inherent opacity of the porcelaneous test (Hallock, 1988a,b). Thus, soritids hosting green algae or dinoflagellates (Hallock, 1999) are better adapted to well-illuminated settings such as the foliar stratum of the seagrasses. In contrast, peneroplids, with red-algal symbionts, live preferentially attached to the rhizome, under lower light conditions. Consequently, flat disc-shaped large miliolids exploited very effectively the ecological niches in the seagrass meadows. Large rotalids and alveolinids host diatoms that can use a wide light-spectrum and therefore are less specialized to particular photic environments. Thus, diatom-bearing taxa (i.e., *Amphistegina*) are often reported as seagrass-dwellers, beneath the leaf canopy, but also in deeper environments with equivalent, poor-light conditions.

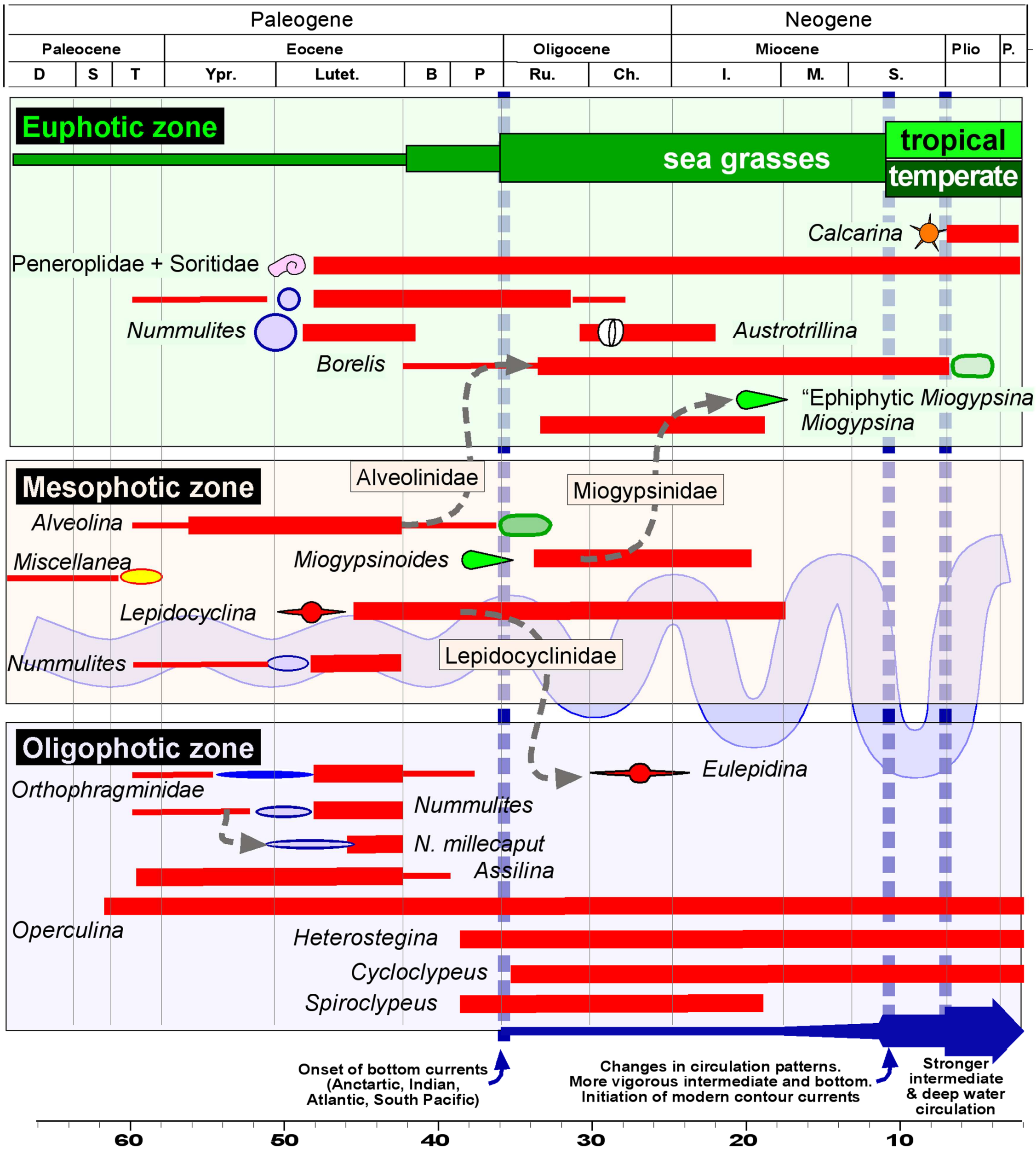

Fig. 28.- Appearance, desapearance and changes in habitat of the main groups of larger benthic foraminifers and the expansion of seagrasses, according to changes in global temperature, associated and to dee p-water circulation patterns (as in Fig. 27) and turbulence induced by the strenghthening of the thermal gradients turbulence.

4.3.2.- Green algae

In the coral buildup examples here reported, green algae are scarce through the Cenozoic, except during the Danian and Miocene, times when dasyclads and/or Halimedales became abundant. Calcareous green algae tend to thrive under low to moderate nutrient flux, in moderate water energy environments, even under low water motion in shallow waters. Heavily calcified *Halimeda* species are abundant in reefs and lagoons, showing higher growth with nutrient enrichment in shallow depths

(Kooistra et al., 2002*;* Teichberg et al., 2013). *Halimeda*, however, may also grow in deeper conditions, even producing bioherms (Roberts et al., 1987; Marshall and Davies, 1988; Braga et al., 1996; Granier, 2012). In modern tropical settings, such bioherms commonly occur where surface waters are very clear and abundant light penetrates to 30 m or more, and where subsurface currents bring uppermost pycnocline waters onto the *Halimeda* meadows, providing a habitat with both abundant light, adequate nutrients, and suitable carbonate saturation for prolific calcification by the *Halimeda* (see Hallock, 2001 and references therein).

By the Danian, the vigorous coral growth in the mesophotic zone created broad areas appropriate for green algae to thrive in back-reef settings. For most of the Danian, solenoporaceans, dasyclads and small benthic foraminifers characterized the shallow euphotic zones, whereas scleractinian corals, along with coralline red algae and bryozoans dominated the mesophotic to oligophotic seaward fronts (see **Fig. 5)**.

Similarly, the onset of the modern type euphotic reef by the late Tortonian created broad areas within the reef and mostly in the backreef lagoons suitable for the green algae, and this is when the chlorozoan sediment association fully developed. The abundance of green algae does not follow their biodiversity, which was maximum during the Paleocene and progressively decreased paralleling global temperatures (Aguirre et al., 2000; Barattolo, 2002; Aguirre and Riding, 2005; Dragastan et al., 2012).

For the rest of the Cenozoic, coral buildups developed in the mesophotic zone, thriving along with red algae below the chlorocline. The shallow-water euphotic settings were occupied by the seagrasses, where Halimedales and dasyclads could thrive and produce sediments. Although a dense seagrass canopy reduces the hydrodynamic energy within the meadow, it also reduces light intensity and, through photosynthesis and respiration, induces diurnal fluctuations in the environmental CO_2 concentrations. When corals along with encrusting coralline red algae developed rigid framework up to sea level by the Late Miocene, new shallow water and well-lit areas became abundant in the reef and in the backreef lagoons. In these settings green algae, even despite their low biodiversity, again became prolific producers.

4.3.3.- Coraliine red algae

Among the major eukaryotic, autotrophic producers of carbonate through the Cenozoic are the coralline red algae, which primarily precipitate Mg-calcite, and to a lesser extent the peyssonnelids, which precipitate aragonite (Basso, 2012). Solenoporaceans, an intriguing calcareous algae group originated in the Paleozoic, are also relatively abundant in Paleocene shallow carbonates. Because calcite and aragonite represent different crystal polymorphs of $CaCO_3$, they have quite different environmental constraints with respect to temperature and carbonate saturation, and also very different preservation potential. Moreover, differences in the photosynthetic pigments, thallus structure, efficiency in floridean starch storage and exploitation, intercellular connections and reproductive strategies, allow the different algal groups to occupy different marine habitats. Both coralline red and calcareous green algae can be found in warm, shallow water in full sunlight, while some coralline taxa can calcify at extremely low light levels, and even thrive under the extreme light seasonality of the cold polar oceans.

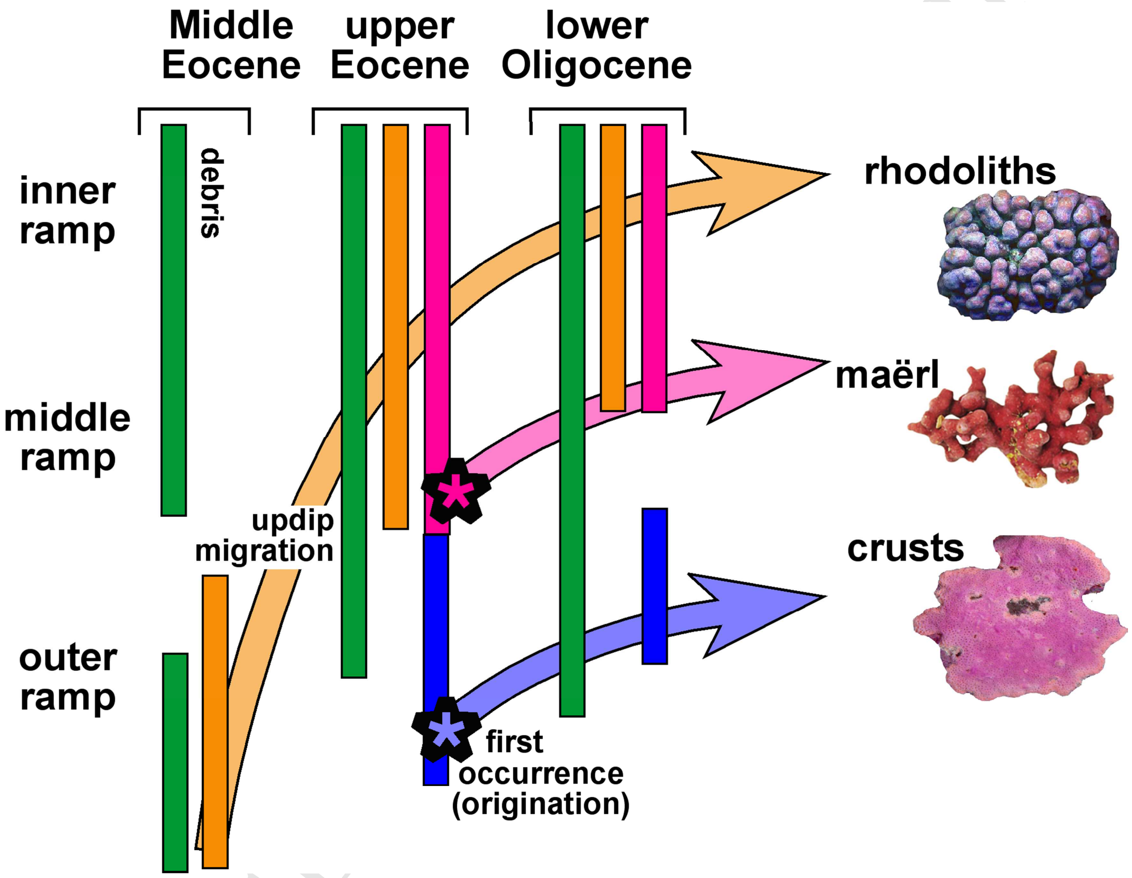

Fig. 29 – First occurrence (*) and dynamics (->) of sedimentary facies dominated by red algae during mid Eocene to early Oligocene times. Facies are shallowing through time. From Nebelsick et al. (2005).

In the Central Tethys area, red algae were prolific carbonate producers before the K/T extinction event and during the whole Cenozoic. Moreover, during the Paleocene and Miocene, both green and red algae were abundant and diverse. This trend parallels the positive values of the $\delta^{13}C$, suggesting the positive excursions of $\delta^{13}C$ to reflect marine productivity. In the Mediterranean regions, phosphate-rich sediments are abundant and have been linked to changes in climate and concurrent changes in paleoceanographic conditions, notably during periods of climate warming near the onset of the Miocene, the Middle Miocene climate optimum, and the latest Miocene phase of Indian monsoon intensification (Compton et al., 1990; Filippelli, 2008; Föllmi et al., 2015).

For most of the Cenozoic (pre-late Tortonian), coralline red algae occur along with corals in the meso-oligophotic zone whereas green algae and corals only coexist after the late Tortonian when wide backreef lagoons developed. In terms of sediment component associations, the chlorozoan association is very infrequent for most of the pre-late Tortonian, and only occurs in shallow-water inner ramps where corals were shaded under seagrass canopy.

The evolution of coralline red algae through the Cenozoic indicates changes in the algal assemblages reflecting major environmental changes. In the Danian, the coralline flora is still of Cretaceous affinity, with dominant Sporolithales. This anatomically and phylogenetically primitive group, well diversified in the late Cretaceous, survived the K/P crisis in warm, deep-water settings, although with reduced species diversity, accompanied by a poorly diversified group of deep-water melobesioids (Aguirre et al., 2007). During the Paleocene the slow increase and diversification of the mesophotic coralline association was able to promote the development of coralline-dominated buildups, corresponding to times of positive values of the $\delta^{13}C$. The coralline groups that presently dominate the shallow-water tropical settings, the Neogoniolithoideae and Lithophylloideae, were more severely affected by the K/P extinction event, and did not start their new radiation and occupation of the corresponding shallow paleoenvironments until the Late Paleocene (Aguirre et al., 2000; 2007). Paleocene corallines mostly occur as crustose thalli, loose fragments, open-structure and loosely packed rhodoliths with a nucleus infilled by carbonate mud and, when with corals, as encrusters (Adey, 1986; Bosence, 1991; Aguirre et al., 2000).

Rhodoliths, mono- or multispecific nodules formed by unattached coralline red algae, are known since the Cretaceous (Sanders, 1998). In the middle Eocene, rhodoliths occupy the middle to outer shelf. By the Late Eocene, when ephemeral Antarctic ice sheets developed after the MECO, neogoniolithoids and lithophylloids diversified and expanded in shallower water, accompanying the scleractinian-coral diversification. Peyssonneliaceans became locally important carbonate producers, and the accumulation of twig-like, unattached coralline algal branches and nodules (maërl; Basso et al., 2009) also appeared in the Late Eocene inner ramp facies. A crustose coralline algal facies producing a solid, porous substrate composed of superposed crustose thalli, appears for the first time in the Late Eocene middle shelf (Rasser, 2000; Rasser and Piller, 2004; Nebelsick et al., 2005; Jaramillo-Vogel et al., 2013).

With the Oligocene stepwise cooling, the Antarctic ice sheet became permanent, and the rhodolith/maërl facies profusely developed. The shallowing trend of all the coralline-dominated facies continued, although red algae were still often an important additional component of the coral reefal and peri-reefal facies, even under turbidity caused by active fluvial systems (Vannucci et al., 2003). According with the ramp depositional model of the Oligocene Mediterranean (Buxton and Pedley, 1989; Brandano, 2017), the mid-ramp association is dominated by mollusk and foraminifera packstone to wackestone, and by coralline algal rhodolith facies (rhodolith rudstone to floatstone) interfingering with coralgal patch-reefs. The outer ramp association is characterized by the gradual passage from coralline algal to large benthic foraminifer facies (LBF wackestone to packstone) and distal pelagic marl facies (plankton-rich wackestone).

With increasing latitudinal and bathymetric temperature gradients, Sporolithales species diversity sharply declined. This loss was largely compensated by the rapid increase in diversity of other coralline taxa, reaching their maximum in the earliest Miocene, again corresponding to a positive excursion of δ13C (Halfar & Mutti, 2005). Miocene carbonate platforms are dominated by red algae, particularly in the Langhian and late Tortonian-early Messinian intervals. They occur more frequently as packed large rhodoliths, with evidence of development within a mesophotic, mesotrophic, inner- and middle ramp environments (Coletti et al., 2015; Braga, 2017). Rhodolith-rich carbonates become scarce in the Mediterranean Pliocene, probably following an increase in siliciclastic sedimentation combined with climate cooling. These changes in coralline algal diversity and rhodolith-facies distribution and dominance appear to be related to the inception of the permanent thermocline, and the associated increased turbulence and nutrient availability in the meso-oligophotic zone by spread of internal waves.

The oscillation of atmospheric concentrations of CO_2 also appears to be an important constraint on the radiation or decline of particular groups of coralline algae. Sporolithales were dominant during high-pCO_2, early Cretaceous times, reaching their highest species diversity in the Late Cretaceous, and progressively declining during the Cenozoic (Aguirre et al., 2000). Within this general trend, however, the highest pCO_2 reached in the mid-Cretaceous apparently fostered an explosion of biodiversity in this group. The same pattern is observed just after the PETM, in contrast to the trend of all other corallines (Ghosh and Sarkar, 2013). This apparent paradox for a calcifier is explained by the physiological adaptation of *Sporolithon* to cope with variable and low pH (Raven and Hurd, 2012), resulting as a competitive advantage after ecological disasters during high CO_2 peaks of the Earth history.

Although considerations about changes of species diversity through time and facies dynamics can be biased by a confused nomenclature, incomplete fossil record, or lack of recognition (Nebelsick et al., 2005), it appears that total species diversity at any time slice is decoupled from the importance of the corresponding coralline-dominated carbonate deposition.

5. – Corollary: solving two apparent paradoxes.

For most of the Eocene to Oligocene, larger benthic foraminifers were the major contributors to tropical carbonate platforms around the Tethys. Paleogene families such as the nummulitids, discocyclinids, alveolinids, and orthophragminids rose to prominence, diversified, and increased in size and internal complexity during the late Paleocene warming, right up into the apex by the interval 52–45 Ma. Hallock and Pomar (2008) noted that this apex of *Nummulites* and other LBF (sensu Hottinger, 1998) coincided with the highest temperatures of the EECO and a minimal bathymetric gradient between the thermocline and deep sea (see **Fig 28, D**), as shown by Dutton et al. (2005). Subsequently, these LBF declined by the late Eocene and Oligocene as the climate cooled in the higher latitudes and thermohaline circulation intensified (Hottinger, 1998; Zachos et al., 2001; Pearson et al., 2008).

Eocene LBF reached the apex when the absence of a thermocline with significant water stratification impeded the generalized occurrence of internal waves. In modern oceans, diapycnal mixing (vertical mixing across constant-density surfaces) is an essential part of the ocean circulation, and it provides the main way to warm the cold deep waters that sink at high latitudes, allowing them to rise through the thermocline. The processes leading to mixing in the main thermocline involve random internal-wave breaking (Gregg, 1989; Polzin et al., 1995), and to some degree also double-diffusive mixing. Recent observations in the deep ocean have, however, found that turbulence is greatly enhanced in regions of rough bottom topography (Polzin et al., 1997), and the most likely cause is internal waves generated by tidal flows over bathymetric irregularities (Wall et al., 2015; DeCarlo et al., 2015). Diapycnal mixing and turbulence (Gregg, 1989; Taylor, 1992) is highly dependent on internal waves, which act as nutrient pumps, bringing plankton and cool, nutrient-rich water up to the photic zone (Leichert et al., 1996, 1998; Alford et al., 2015). Internal waves induce strong vertical and horizontal currents and the turbulent mixing caused by their breaking affects a panoply of ocean processes, such as the supply of nutrients and the transport of plankton (Alford et al., 2015).

Consequently, during the warm Eocene, although eutrophication likely occurred near river mouths and where deep waters did upwell (Hallock et al., 1991a), oligotrophic conditions predominated due to the slow deep ocean circulation (**Fig. 30 A**). The minimal vertical density gradient had expression in a very weak pycnocline, through which the DIN and POC input was very limited. The smaller the density contrast at the pycnocline, the lower the wave frequency and the slower the propagation speed of the internal waves are (Apel, 1987). These calm conditions were apparently advantageous for larger foraminifers. Their retractable rhizopodia (thread-like extensions of the ectoplasm) play an indispensable role for anchoring in turbulent conditions, locomotion, for catching prey and creation of their calcareous skeleton. In oligotrophic, low energy environments at the sea floor in mesophotic to oligophotic conditions, thin, flat, discoid shells of symbiont-bearing foraminifers maximize nutrient absorption from the sediments upon which they sit, while providing maximum exposure of the upward-facing surface to light penetration (Hallock et al., 1991b). Moreover, the production of external organic sheaths from excess photosynthate likely promotes farming of bacteria and other microbes that provide a major source of nutrition.

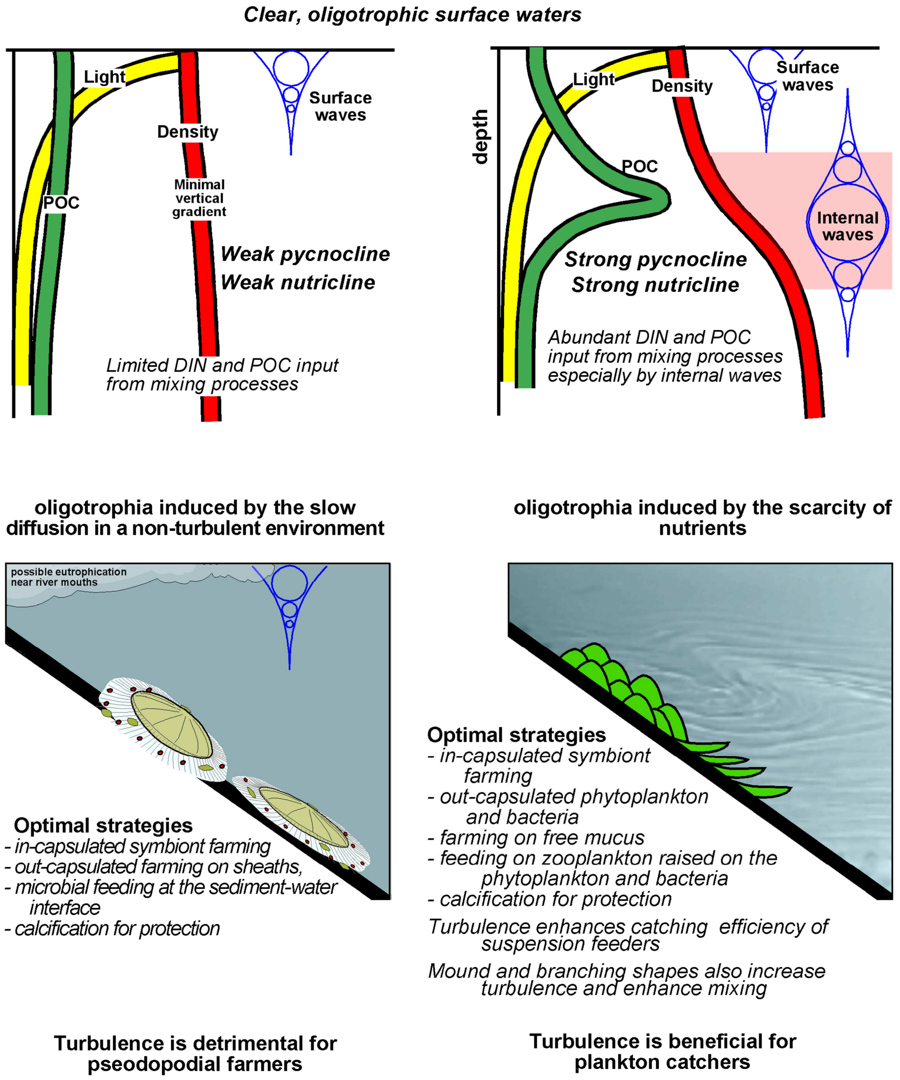

Fig. 30.- The waxing and waning of the nutritional conditionings during the Cenozoic have determined the boom and bust pattern of two mixotrophic groups, corals and larger benthic foraminifers, as dominant carbonate producers. First-order conditions have been the absence/existence of thermal gradients and the strength of the pycnoclines in controlling turbulence and diffusion of nutrients and particulate organic carbon (POC). Second-order conditions rely on the effectiveness of the double farming (encapsulated and out-capsulated), and the third-order condition in the efficiency of the mixotrophic system; e.g., the fine-tuning of modern reef system includes changes of symbiont clades and the resulting efficiency explains the high gross primary productivity in oligotrophic conditions.

Lutetian nummulitic banks in the northern Tethys (e.g., Buil, southern Pyrenees) exemplify the detrimental impact of turbulence on the LBF. These banks have been interpreted as gravity flow deposits induced by breaking internal waves (Mateu-Vicens et al., 2012). The large *Nummulites* tests were easily entrained and brought in suspension due to their low bulk density resulting from the high intraskeletal porosity (Aigner, 1982; Jorry et al., 2006; Yordanova and Hohenegger, 2007).

In contrast, corals rely on suspension feeding on zooplankton. Some water motion is essential to corals and turbulence is beneficial as it increases the impinging efficiency of the plankton with coral tentacles. Mound and branching morphologies also enhance catching efficiency. Consequently, the existence of strong pycnoclines and their associated turbulence (internal waves) favor suspension-feeders (**Fig.30 B**).

These differences solve two apparent paradoxes: (1) if both corals and LBF require tropical conditions and both have similar nutritional strategies (mixotrophy), why do they seem to be inversely correlated in the Cenozoic record? and (2) Why do coral buildups preferentially develop during cooling periods?

Both LBF and corals are primarily heterotrophic, the former feeding on detritus in the sediment, the latter as catcher/suspension feeders relying upon plankton in surrounding waters. Both benefit metabolically from algal symbiosis, especially in warm, oligotrophic, sunlit environments. But their different heterotrophic behaviors and physiologies have allowed them respond differently to predominant environmental conditions through Cenozoic. When global temperatures are high, latitudinal and bathymetric gradients are reduced so that pycnoclines are weak and deep-ocean circulation is diminished. The results include reduced density contrast, lower wave frequencies and slower propagation speeds of internal waves (Apel, 1987). Higher temperatures mean higher metabolic rates, requiring greater reliance on photosynthetic production by the algal symbionts as return of essential nutrients from aphotic waters would have been reduced (**Fig. 30 A**). Such extreme, low turbulence, oligotrophic conditions would have favored the LBF. As individual organisms with low metabolic rates, organic sheaths, and rhizopodial networks, they were able to thrive on scarce dissolved inorganic nutrients, while ingesting bacteria and other organic matter gathered from the surrounding sediments or growing on their organic sheaths, as long as energy from sunlight was sufficient to support photosynthesis by their algal symbionts. Moreover, by precipitating calcite rather than aragonite, construction and maintenance of their shells was less dependent upon local carbonate saturation.

In contrast, on a cooling Earth, accelerating thermohaline circulation strengthened bathymetric and latitudinal gradients that resulted in stronger high latitude storms that generated faster and more energetic surface waves and stronger pycnoclines that supported faster and more energetic internal waves (**Fig. 30B**). This enhanced turbulence favored plankton delivery to the catchers and pumpers, which favored coral buildups and platform-margin accretion. DeCarlo et al. (2015) emphasized the beneficial effects of internal waves on modern reefs: 1) internal waves elevate plankton flux and increase coral heterotrophy, 2) heterotrophy enhances coral growth rates, and 3) calcification is also enhanced by water motion. Wall et al. (2012) have also shown that diapycnal mixing not only affects the lower reaches (below 50 m) of the reef slope, but they highlight its importance for reef development in shallow water as well.

This inverse correlation between coral-buildup development and global temperature (**Fig. 31**) was noted long ago by Frost (1977). Perrin and Kiessling (2012) also noted, at a global scale, a correlation of the global cooling trend from the Eocene to the Miocene with an increase of reef carbonate production and a latitudinal expansion of the reef belt. For the Eocene and Early Oligocene, Höntzsch et al. (2013) also noted coral reefs spread throughout the Tethys during cooling events that corresponded with the demise of many symbiont-bearing larger foraminifers, whereas warming stages favored proliferation of larger benthic foraminifers.

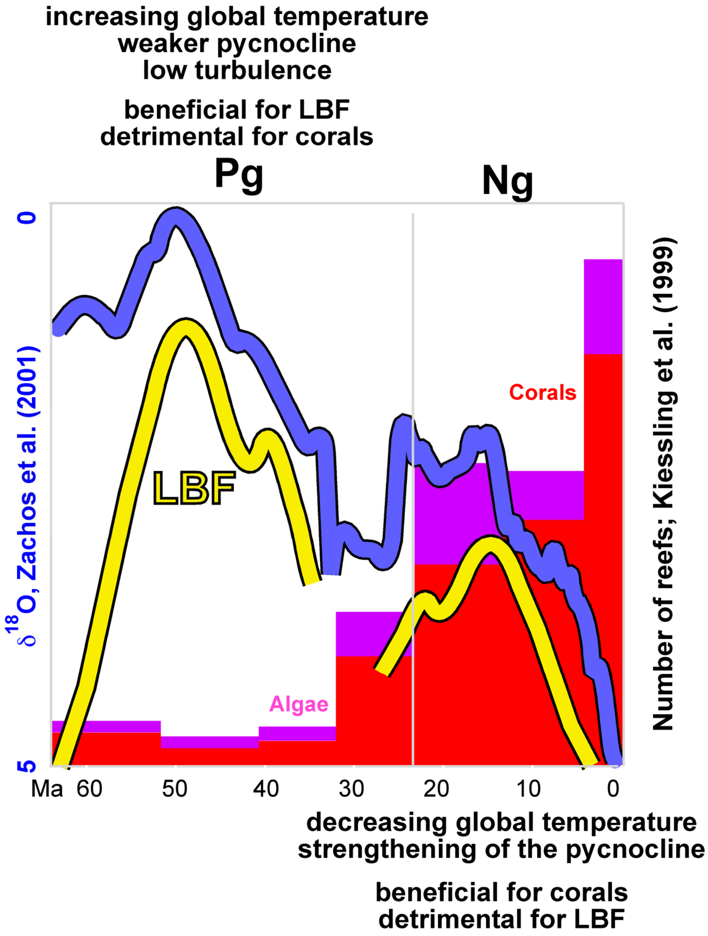

Fig. 31.- Apparent inverse correlation between coral-buildup development and larger benthic foraminifers during the Cenozoic. Although both LBF and corals require tropical conditions and both are mixotrophs, their differences in habitat, physiological requirements, feeding strategies and biomineralization result in different responses to changes in ocean circulation. High global temperatures and reduced thermal gradients favored individual life styles of calcitic LBF in calm, extremely clear and oligotrophic, poorly stratified oceans. On a cooling Earth, strengthening thermal gradients induce ocean stratification, promoting increased turbulence in both surface waters and internal waves along pycnoclines. As a result, even in relatively oligotrophic surface waters, higher dissolved nutrients and plankton abundances at the pycnocline support the nutritional needs of plankton-feeding, sessile, colonial, aragonite-producing corals.

6 – Regional vs. global control

Our analysis and interpretation is based on examples from the Mediterranean, a semi-enclosed basin with a complex geologic history. The sill-controlled structure and small size of the basin, compared to the global ocean, makes it very sensitive to oscillations in climatic and oceanographic conditions. The Mediterranean region provides a unique opportunity for analyses of coral buildups due to the quality and accessibility of exposures and the degree to which they have been studied in recent decades.

The uncertainty in extrapolating the observed patterns to the global scale is inherent to this field-based approach. Nevertheless, the Mediterranean region has long been considered an extraordinary natural laboratory to study the complex interactions between the geosphere and biosphere (Stanley, 1972). Although there are many papers reporting pre-late Tortonian reefs that reached sea level and exhibit zonation similar to that of modern euphotic reefs, all the examples analyzed in this paper have shown that previous interpretations were biased from application of the modern Caribbean model. Examples include buildups from the Middle Miocene (e.g., Egypt: Perrin, 2000; Turkey: Vescogni et al. 2016), Oligocene (e.g., Frost, 1981; Bosellini and Trevisani, 1992; Bosellini and Russo, 1992; Bosellini and Perrin, 1994) and Eocene (e.g., Alvarez et al., 1995). All the pre-late-Tortonian coral buildups here reviewed are cluster-reef types, developed in mesophotic conditions along with coralline red algae and were not able to build a rigid framework up to sea level.

The patterns of change in the coral buildups in the Mediterranean areas (central Tethys) follow changes in environmental trends that are not regional, but global: temperature from $\delta^{18}O$ proxy, $\delta^{13}C$ with more difficult interpretation signal but with global circulation and oceanic productivity components, atmospheric CO_2, and biological evolution of holobionts. Moreover, in the Miocene the cosmopolitan Tethyan reef province was only split into the three major reef provinces: Mediterranean, Caribbean and Indo-Pacific.

For the Miocene coral buildups in the Indo-Pacific region, Santodomingo et al. (2016) have recently shown that coral buildups show a similar temporal evolution to that of the Miocene Mediterranean: common low-relief patch reefs of platy corals dominated the environments up to the Serravallian, coral carpets were common pre- to late Tortonian, and the first appearance of a large framework reefs date from the Messinian, although the latter did not grow to sea level.

7 – Conclusions

The complexity of geologic facies is never to be fully understood, and the analyses presented here are no exception. From the case-studies presented, it appears that biological evolution, extinctions, replacement and turnovers of the main carbonate producers in the central Tethys area correlate with changes in global climatic and oceanographic conditions during the Cenozoic.

Corals were either isolated or able to build small patches and mounds during most of the Cenozoic, except for the late Danian, the Bartonian-Priabonian, early Chattian and Late Miocene. These four intervals coincide with periods of major zooxanthellae diversification and also when both temperature (indicated by higher $\delta^{18}O$) and $\delta^{13}C$ curves dropped below certain values. This suggests that coevolution of corals and zooxanthellae was associated with an increase in turbulence associated with the strengthening of latitudinal gradients and pycnoclines that increased water motion and concentrated particulate organic carbon, thereby favoring zooplankton catchers.

For most of the Cenozoic, corals and coral buildups developed under reduced light conditions (i.e., under mesophotic conditions). By the Late Miocene, the adaptation of corals and their zooxanthellae to high light environments, along with reinforcement of framework by encrusting red algae, allowed corals to construct steep reef walls up to sea level all over the Mediterranean region. This sudden onset and expansion of the modern type of coral reefs coincides with a major drop in the global $\delta^{13}C$ and with a sharp increase in latitudinal thermal gradients.

The multi-causal variability in $\delta^{13}C$ (global carbon-cycle perturbations, first-order changes in deep-sea circulation patterns and changes in biological productivity) broadly reflects such changes. The eurythermal coralline red algae became preponderant producers in the mesophotic zone during times when the $\delta^{13}C$ was relatively high.

For larger benthic foraminifers, diversifications and predominance in carbonate production were associated with warm temperatures locally and globally, and also coincided with times of lower $p\mathrm{CO}_2$. At high temperatures and consequent high metabolic activity, the benefit of respiratory CO_2 to enhance photosynthesis would be greater under lower $p\mathrm{CO}_2$. Higher global temperatures and weakened pycnoclines, with limited turbulence and extensive regions of oligotrophy with very deep and consistent light penetration, also favored diverse assemblages of LBF. These protists were able to survive using symbiont-produced photosynthate and also were able to uptake dissolved inorganic nutrients and organic matter from surrounding sediments or growing on their organic sheaths. The emergence of species with large embryonic and adult sizes with enhanced morphologic complexity represent adaptations that allowed longevity of many months to years in relatively predictable, very resource-limited environments, but such extreme specialization made them especially susceptible to extinctions when environmental changes eliminated those niches.

Reef-building corals truly are very special organisms. Widespread bleaching events in recent decades have revealed that these corals thrive very near their temperature thresholds, especially thresholds of temperature. Warm temperatures increase calcification rates, as do high rates of photosynthesis by their zooxanthellae. But small increases in temperature under high light can induce photo-oxidative stress, resulting in bleaching and often death. Water motion, whether induced by surface or internal waves or by currents, plays a critical role in promoting coral growth and carbonate production: water motion delivers food (plankton) while enhancing exchange that reduces both photo-oxidative stress in daytime and oxygen depletion at night. Some plankton feeding is essential for corals, though if plankton are too abundant, they reduce light penetration and promote growth of non-calcifying benthic organisms, including bioeroders. Very high waves and currents, such as those generated by hurricanes or typhoons, induce short-term structural damage to reefs, but also bring cooler, deeper water to the surface that reduce photo-oxidative stress.

Through the Cenozoic, water motion was strengthened by the strengthening of thermal gradients, both with depth and with latitude, and thus increased as high-latitude temperatures were falling. Active water motion is essential for plankton catchers such as corals, but less so for many LBF. This explains two apparent paradoxes: why tropical corals thrive in a cooling Earth, and why the occurrence of corals and LBF as dominant carbonate producers appears to be inverse, despite both requiring warm photic conditions and having similar nutritional strategies (mixotrophy).

Acknowledgments

Funding from Ministerio de Economía y Competitividad Projects CGL2014-52096-P and and CGL2011-23770 are acknowledged. Also funding from the Basque Government to the Research Group of the Basque University System IT-930-16 has contributed to this research. This paper represents a long process of evolution of ideas, to which many colleagues have contributed; in the last stages, M. Morsilli and M. Brandano have brought live discussions and confronted developing ideas. Review comments by R. Riding and associate editor N. Preto are acknowledged.

REFERENCES

Adey, W.H., 1986. Coralline algae as indicators of sea-level. In: van de Plassche, O. (ed.), Sea-Level Research: a manual for the collection and evaluation of data. Springer Netherlands, Dordrecht, pp. 229–280.

Aguirre, J., Baceta, J.I., Braga, J.C., 2007. Recovery of marine primary producers after the Cretaceous–Tertiary mass extinction: Paleocene calcareous red algae from the Iberian Peninsula. Palaeogeogr., Palaeoclimatol., Palaeoecol., 249: 393–

411.

Aguirre, J., Riding, R., 2005. Dasycladalean Algal Biodiversity Compared with Global Variations in Temperature and Sea Level over the Past 350 Myr. Palaios, 20, 581–588. doi:10.2110/palo.2004.p04-33

Aguirre, J., Riding, R., Braga, J.C., 2000. Diversity of coralline red algae: origination and extinction patterns from the Early Cretaceous to the Pleistocene. Paleobiology, 26, 651–667.

Aigner, T., 1982. Event-stratification in nummulite accumulations and in shell beds from the Eocene of Egypt. In: Einsele, G., Seilacher, A. (eds), Cyclic and Event Stratification. Springer-Verlag, New York, pp. 248–262.

Alford, M.H., Peacock, T., MacKinnon, J.A., Nash, J.D., Buijsman, M.C., Centuroni, L.R., Chao, S.-Y., Chang, M.-H., Farmer, D.M., Fringer, O.B., Fu, K.-H., Gallacher, P.C., Graber, H.C., Helfrich, K.R., Jachec, S.M., Jackson, C.R., Klymak, J.M., Ko, D.S., Jan, S., Johnston, T.M.S., Legg, S., Lee, I.H., Lien, R.-C., Mercier, M.J., Moum, J.N., Musgrave, R., Park, J.-H., Pickering, A.I., Pinkel, R., Rainville, L., Ramp, S.R., Rudnick, D.L., Sarkar, S., Scotti, A., Simmons, H.L., St Laurent, L.C., Venayagamoorthy, S.K., Wang, Y.-H., Wang, J., Yang, Y.J., Paluszkiewicz, T., and Tang, T.-Y., 2015. The formation and fate of internal waves in the South China Sea. Nature, 521, 65–69, doi: 10.1038/nature14399.

Alvarez, G., Busquets, P., Franqués, J., Reguant, S., Serra-Kiel, J., Taberner, C., 1995. Eocene deposits in the Vic area. In: Perejón, A., Busquets, P. (eds), Bioconstructions of the Eocene South Pyrenean Foreland Basin (Vic and Igualada areas) and of the Upper Cretaceous South Central Pyrenees (Tremp area). VII International Symposium on Fossil Cnidaria and Porifera, Field Trip C Guidebook, pp. 15–29.

Alvarez, G., Busquets, P., Taberner, C., 1994. Facies architecture and coral distribution in a mid-Eocene barrier reef track, South Pyrenean foreland basin (NE Spain). Courier-Forschungsinstitut Senckenberg, 172, 249–260.

Apel, J.R., 1987. Principles of Ocean Physics. Academic Press, Ltd., London, 634 pp.

Apel, J.R., 2002. Oceanic Internal Waves and Solitons. In: Jackson, C.R. (ed.), An atlas of internal solitary-like waves and their properties. Global Ocean Associates. Prepared for Office of Naval Research – Code 322 PO, Alexandria, VA., pp. 1–40. http://www.internalwaveatlas.com/Atlas42_PDF/IWAtlas_Pg001_Background&Theory.pdf.

Arbués, P., Butillé, M., López Blanco, M., Marzo, M., Monleón, O., Muñoz, J.A., Serra-Kiel, J., 2011. Exploring the relationships between deepwater and shallow-marine deposits in the Ainsa piggy back basin fill. (Eocene South-Pyrenean Foreland Basin). In: C. Arenas, L. Pomar and F. Colombo (eds), Pre-Meeting Field trips Guidebook, 28th IAS Meeting. Zaragoza. Sociedad Geológica de

España, Geo-Guías, 7, 200–239.

Azam, F., 1998. Microbial Control of Oceanic Carbon Flux: The Plot Thickens. Science, 280, 694–696.

Azam, F., Fenchel, T., Field, J.G., Gray, J.S., Meyer-Reil, L.A., Thingstand, F., 1983. The ecological role of water-column microbes in the sea. Mar. Ecol. Prog. Ser., 10, 257–263.

Baceta, J.I., Pujalte, V., Bernaola, G., 2005. Paleocene coralgal reefs of the western Pyrenean basin, northern Spain: new evidence supporting an earliest Paleogene recovery of reefal ecosystems. Palaeogeogr., Palaeoclimatol., Palaeoecol., 224, 117– 143.

Baceta, J.I., Pujalte, V., Serra-Kiel, J., Robador, A., Orue-Etxebarria, X., 2004. El Maastrichtiense final, Paleoceno e Ilerdiense inferior de la Cordillera Pirenaica. In: Vera, J.A. (ed.), Geología de España. Sociedad Geológica de España-Instituto Geológico y Minero de España, Madrid, pp. 308–313.

Baceta, J.I., Pujalte, V., Wright, V.P., Schmitz, B., 2011. Carbonate platform models, sea-level changes and extreme climatic events during the Paleocene-early Eocene greenhouse interval: a basin-platform-coastal plain transect across the southern Pyrenean basin. In: C. Arenas, L. Pomar and F. Colombo (eds), Pre-Meeting Field trips Guidebook, 28th IAS Meeting. Zaragoza. Sociedad Geológica de España, Geo-Guías, 7, 151–198.

Baker, A.C., 2003. Flexibility and specificity in coral-algal symbiosis: diversity, ecology and biogeography of *Symbiodinium*. Annu. Rev. Ecol. Evol. S., 34, 661–689.

Baker, A.C., Starger, C.J., McClanahan, T.R., Glynn, P.W., 2004. Corals' adaptive response to climate change. Nature, 430, 741.

Barattolo, F., 2002. Late Cretaceous-Paleogene dasycladaleans and the K/T boundary problem. In: Bucur, I.I., Filipescu, S. (eds), Research advances in calcareous algae and microbial carbonates. Cluj University Press, pp. 17–40.

Barnolas, A., Payros, A., Samso, J.M., Serra-Kiel, J., Tosquella, J., 2004. La Cuenca surpirenaica desde el Ilerdiense medio al Priaboniense. In: Vera J.A. (ed.), Geología de España. Sociedad Geológica de España-Instituto Geológico y Minero de España, Madrid, pp. 313-320.

Barnolas, A., Samsó, J. M., Teixell, A., Tosquella, J., Zamorano, M., 1991. Evolución sedimentaria entre la cuenca de Graus – Tremp y la cuenca de Jaca – Pamplona. I Congreso del Grupo Español del Terciario. Vic. Libro-guía de la excursión nº. 1, 123 pp.

Baron-Szabo, R.C., 2006. Corals of the K/T-boundary: Scleractinian corals of the suborders Astrocoeniina, Faviina, Rhipidogyrina and Amphiastraeina. J. Syst. Palaeontol., 4, 1–108. doi:10.1017/S1477201905001689

Baron-Szabo, R.C., 2008. Corals of the K/T-boundary: Scleractinian corals of the suborders Dendrophylliina, Caryophylliina, Fungiina, Microsolenina, and Stylinina. Zootaxa, 1952, 1–244.

Bassant, P., 1999. The high-resolution stratigraphic architecture and evolution of the Burdigalian carbonate-siliciclastic sedimentary systems of the Mut Basin, Turkey. GeoFocus. Institut de Géologie et Paléontologie de l'Université de Fribourg (Suisse), 277 pp.

Bassant, P., Van Buchem, F.S.P., Strasser, A., Lomando, T., 2004. A comparison of two early Miocene carbonate margins: the Zhujiang carbonate platform (subsurface, South China) and the Pirinç platform (outcrop, Southern Turkey). In: Grammer, M., Harris, P.M. (eds), Integration of Outcrop and Modern Analogs in Reservoir Modeling. AAPG Mem, 80, 153–170.

Bassant, P., Van Buchem, F.S.P., Strasser, A., Gorur, N., 2005. The stratigraphic architecture and evolution of the Burdigalian carbonate-siliciclastic sedimentary systems of the Mut Basin, Turkey. Sediment. Geol., 173, 187–232, doi: http://dx.doi.org/10.1016/j.sedgeo.2004.01.017.

Bassi, D., Nebelsick, J.H., 2010. Components, facies and ramps: Redefining Upper Oligocene shallow water carbonates using coralline red algae and larger foraminifera (Venetian area, northeast Italy). Palaeogeogr., Palaeoclimatol., Palaeoecol., 295, 258–280, doi: /10.1016/j.palaeo.2010.06.003.

Basso, D., 2012. Carbonate production by calcareous red algae and global change. In: Basso D. & Granier B. (eds), Calcareous algae and global change: from identification to quantification. Geodiversitas, 34, 13–33.

Basso, D., Nalin, R., Nelson, C.S., 2009. Shallow-water *Sporolithon* rhodoliths from North Island (New Zealand). Palaios, 24, 92–103.

Beavington-Penney, S.J., Racey, S., 2004. Ecology of extant nummulitids and other larger benthic foraminifera: applications in palaeoenvironmental analysis. Earth-Science Reviews, 67, 219–265.

Bebout, D.G., Pendexter, C., 1975. Secondary carbonate porosity as related to early Tertiary depositional facies, Zelten field, Libya. A.A.P.G. Bull., 59, 665– 693.

Beerling, D.J., Royer, D.L., 2011. Convergent Cenozoic CO_2 history. Nature Geosci., 4, 418–420. doi:10.1038/ngeo1186

Benisek, M.F., Betzler, C., Marcano, G., Mutti, M., 2009. Coralline-algal assemblages of a Burdigalian platform slope: implications for carbonate platform reconstruction (northern Sardinia, western Mediterranean Sea). Facies, 55, 375–386. doi:10.1007/BF02536947

Benisek, M.-F., Marcano, G., Betzler, C., Mutti, M., 2010. Facies and Stratigraphic Architecture of a Miocene Warm-Temperate to Tropical Fault-Block Carbonate

Platform, Sardinia (Central Mediterranean Sea). In: Mutti, M., Piller, W., Betzler, C. (eds), Carbonate Systems during the Oligocene–Miocene Climatic Transition. Wiley-Blackwell, pp. 129–148.

Bernecker, M., 2011. Distribution of Palaeogene Corals on the Arabian Shelf. Kölner Forum Geol. Paläont., 19, M. Aretz, S. Delculée, J. Denayer, E. Poty (eds), Abstracts, 11th Symposium on Fossil Cnidaria and Sponges, Liège, pp. 18–19.

Berner, R.A., Kothavala, Z., 2001. GEOCARB III; a revised model of atmospheric CO_2 over Phanerozoic time. Am. J. Sci., 294, 56-91; doi:10.2475/ajs.294.1.56

Bernoulli, D., Hottinger, L., Spezzaferri, S., Stille, P., 2007. Miocene shallow-water limestones from São Nicolau (Cabo Verde): Caribbean-type benthic fauna and time constraints for volcanism. Swiss J. Geosci., 100, 215-225.

Betzler, C., 1997. Ecological controls on geometries of carbonate platforms: Miocene/Pliocene shallow-water microfaunas and carbonate biofacies from the Queensland Plateau (NE Australia). Facies, 37, 147–166, doi: 10.1007/bf02537376.

Betzler, C., Brachet, T.C., Braga, J.C., Martin, J.M., 1997. Nearshore, temperate, carbonate depositional systems (lower Tortonian, Agua Amarga basin, southern Spain): implications for carbonate sequence stratigraphy. Sediment. Geol., 113, 27-53. doi: 10.1016/S0037-0738(97)00054-7

Betzler, C., Martin, J.M., Braga, J.C., 2000. Non-Tropical Carbonates Related to Rocky Submarine Cliffs (Miocene, Almería, Southern Spain). Sediment. Geol., 131, 51–65.

Bijl, P.K., Schouten, S., Sluijs, A., Reichart, J.-J., Zachos, J.C., Brinkhuis, H., 2009. Early Palaeogene temperature evolution of the southwest Pacific Ocean. Nature Geosci., 461, 776–779, doi: 10.1038/nature08399.

Bilger, R.W., Atkinson, M.J., 1992. Anomalous mass transfer of phosphate on coral reef flats. Limnol. Oceanogr., 37, 261–272.

Billups, K., Scheiderich, K., 2010. A synthesis of Late Oligocene through Miocene deep sea temperatures as inferred from foraminiferal Mg/Ca ratios. IAS Special Publication, 42, 1–16.

Bosellini, A., Bosellini, F.R., Colalongo, M.L., Parente, M., Russo, A., Vescogni, A., 1999. Stratigraphic architecture of the Salento coast from Capo d'Otranto to S. Maria di Leuca (Apulia, Southern Italy). Riv. It. Paleont. Strat., 105, 397–416

Bosellini, F., Perrin, C., 1994. The coral fauna of Vitigliano: qualitative and quantitative analysis in a back reef environment (Castro Limestone, Late Oligocene, Salento Peninsula, southern Italy). B. Soc. Paleontol. Ital., 33, 171–181.

Bosellini, F., Perrin, C., 2008. Estimating Mediterranean Oligocene-Miocene sea-surface temperatures: An approach based on coral taxonomic richness. Palaeogeogr., Palaeoclimatol., Palaeoecol., 258, 71–88. doi:10.1016/j.palaeo.2007.10.028

Bosellini, F., Russo, A., 1992. Stratigraphy and facies of an Oligocene fringing reef (Castro Limestone, Salento Peninsula, southern Italy). Facies, 26, 146–166, doi: 10.1007/BF02539798.

Bosellini, F., Stemann, T.A., 1996. Autoecological significance ofgrowth form in the scleractinian Actinacis rollei Reuss (Oligocene, Lessini Mountains, Northern Italy). In: Cherchi, A. (ed.), Autoecology of Selected Fossil Organisms. Achievements and Problems. B. Soc. Paleontol. Ital., 3, 31–43.

Bosellini, F., Trevisani, E., 1992. Coral facies and cyclicity in the Castelgomberto Limestone (Early Oligocene, Eastern Lessini Mountains, Northern Italy). Riv. It. Paleont. Strat., 98, 339–352.

Bosence, D.W.J., 1991. Coralline Algae: Mineralization, Taxonomy, and Palaeoecology. In: Calcareous Algae and Stromatolites, Springer Berlin Heidelberg, Berlin, Heidelberg, pp. 98–113. doi:10.1007/978-3-642-52335-9_5

Boudagher-Fadel, M.K., 2008. Evolution and geological significance of larger benthic foraminifera. Dev. in Palaeontol. Stratigraphy, 21, 1–544.

Brachert, T.C., Betzler, C., Braga, J.C., Martin, J.M., 1996. Record of climatic change in neritic carbonates: turnover in biogenic associations and depositional modes (Late Miocene, southern Spain). Geol. Rundschau 85, 327–337. doi:10.1007/BF02422238

Brachert, T.C., Hultzsch, N., Knoerich, A.C., Krautworst, U.M.R., Stückrad, O.M., 2001. Climatic signatures in shallow-water carbonates: High-resolution stratigraphic markers in structurally controlled carbonate buildups (Late Miocene, southern Spain). Palaeogeogr. Palaeoclimatol. Palaeoecol. 175, 211–237. doi:10.1016/S0031-0182(01)00373-X

Braga, J.-C., 2017. Neogene Rhodoliths in the Mediterranean Basins. In: Riosmena-Rodríguez R. et al. (eds.), Rhodolith/Maërl Beds: A Global Perspective. Coastal Research Library 15, Springer, DOI 10.1007/978-3-319-29315-8_7, pp. 169-193.

Braga, J.C., Aguirre, J., 2001. Coralline algal assemblages in upper Neogene reef and temperate carbonates in Southern Spain. Palaeogeogr. Palaeoclimatol. Palaeoecol. 175, 27–41. doi:10.1016/S0031-0182(01)00384-4

Braga, J.C., Martin, J.M., Riding, R., 1996. Internal structure of segment reefs. Halimeda algal mounds in the Mediterranean Miocene. Geology, 24, 35-38

Braga, J.C., Martin, J.M., Wood, J.L., 2001. Submarine lobes and feeder channels of redeposited, temperate carbonate and mixed siliciclastic-carbonate platform deposits (Vera Basin, Almeria, southern Spain). Sedimentology 48, 99–116.

doi:10.1046/j.1365-3091.2001.00353.x

Bralower, T.J., Zachos, J.C., Thomas, E., Parrow, M., Paull, C.K., Kelly, D.C., Silva, I.P., Sliter, W.V., Lohmann, K.C., 1995. Late Paleocene to Eocene paleoceanography of the equatorial Pacific Ocean: Stable isotopes recorded at Ocean Drilling Program Site 865, Allison Guyot. Paleoceanography, 10, 841–865, doi: 10.1029/95PA01143.

Brandano, M., 2003. Tropical/Subtropical Inner Ramp Facies in Lower Miocene “Calcari a Briozoi e Litotamni” of the Monte Lungo Area (Cassino Plain, Central Apennines, Italy). Boll. Soc. Geol. It., 122, 85–98.

Brandano, M., 2017. Oligocene Rhodolith Beds in the Central Mediterranean Area. In: Riosmena-Rodríguez R. et al. (eds.), Rhodolith/Maërl Beds: A Global Perspective. Coastal Research Library 15, DOI 10.1007/978-3-319-29315-8_8, pp. 195-219.

Brandano, M., Corda, L., 2002. Nutrients, sea level and tectonics: constrains for the facies architecture of a Miocene carbonate ramp in central Italy. Terra Nova, 14, 257–262.

Brandano, M., Frezza, V., Tomassetti, L., Cuffaro, M., 2009 a. Heterozoan carbonates in oligotrophic tropical waters: The Attard member of the lower coralline limestone formation (Upper Oligocene, Malta). Palaeogeogr., Palaeoclimatol., Palaeoecol., 274, 54–63, doi: http://dx.doi.org/10.1016/j.palaeo.2008.12.018.

Brandano, M., Frezza, V., Tomassetti, L., Pedley, M., Matteucci, R., 2009 b. Facies analysis and palaeoenvironmental interpretation of the Late Oligocene Attard Member (Lower Coralline Limestone Formation), Malta. Sedimentology, 56, 1138–1158, doi: 10.1111/j.1365-3091.2008.01023.x.

Brandano, M., Morsilli, M., Parente, M., Vannucci, G., Bosellini, F.R., Mateu-Vicens, G. 2010. Rhodolith-rich lithofacies of the Porto Badisco Calcarenite (Upper Chattian, Salento, Apulia, southern Italy). Ital. J. Geosci. (Boll.Soc.Geol.It.), 129, 119–131, doi: 10.3301/IJG.2009.10.

Brasier, M.D., 1975. An Outline History of Seagrass Communities. Paleontology 18, 681–702.

Bruntse, G., Tendal, O.S., 2001. *Lophelia pertusa* and other cold water corals in the Faroe area. In: Bruntse, G., O.S. Tendal (eds), Marine biological investigations and assemblages of benthic invertebrates from the Faroe Islands. Kaldbak Marine Biological Laboratory, the Faroe Islands, pp. 22-32.

Budd, A.F., 2000. Diversity and extinction in the Cenozoic history of Caribbean reefs. Coral Reefs, 19, 25–35.

Burchette, T.P., Wright, V.P., 1992. Carbonate ramp depositional systems. Sediment. Geol., 79, 3–57, doi: 10.1016/0037-0738(92)90003-A.

Busquets, P., Ortí, F., Pueyo, J.J., Riba, O., Rosel-Ortiz, L., Saez, A., R., S., Taberner, C., 1985. Evaporite deposition and diagenesis in the Saline (potash) Catalan Basin, Upper Eocene. In: Mila, M.D., Rosell, J. (eds), IAS 6th European Regional Meeting Excursion Guidebook, Excursion n° 1, Lleida, pp. 13-59.

Buxton, M., Pedley, H.M., 1989. A standardised model for Tethyan Tertiary carbonate ramps. J. Geol. Soc., 146, 746–748, doi: 10.1144/gsjgs.146.5.0746.

Cahuzac, B., Poignant, A., 1997. Essai de biozonation de l'Oligo-Miocène dans les bassins européens à l'aide des grands foraminifères néritiques. Bull. Soc. Géol. France, 168, 155–169.

Calvo, J.P., Daams, R., Morales, J., Lopez-Martinez, N., Agusti, J., Anadon, P., Armenteros, I., Cabrera, L., Civis, J., Corrochano, A., Diaz-Molina, M., Eliaga, E., Hoyos, M., Martin-Suarez, E., Martinez, J., Moissenet, E., Muñoz, A., Perez-Garcia, A., Perez-Gonzalez, A., Portero, J.M., Robles, F., Santisteban, C., Torres, T., Van der Muelen, A.J., Vera, A., Mein, P., 1993. Up-to-date Spanish continental Neogene synthesis of the paleoclimatic interpretation. Rev. Soc. Geol. España, 6, 29–40.

Cascella, A., Dinarès-Turell, J., 2009. Integrated calcareous nannofossil biostratigraphy and magnetostratigraphy from the uppermost marine Eocene deposits of the southeastern Pyrenean foreland basin: evidences for marine Priabonian deposition. Geologica Acta, 17, 281–296, doi: 10.1344/105.000000282.

Chamley, H., Coulon, H., Debrabant, P., Holtzapffel, T., 1986. Cretaceous Interactions between Volcanism and Sedimentation in the East Mariana Basin, from Mineralogical, Micromorphological, and Geochemical Investigations, Deep Sea Drilling Project Site 585. In: Initial Rep. DSDP, 89. U.S. Government Printing Office. doi:10.2973/dsdp.proc.89.113.1986

Chapronière, G.C.H., 1984. Oligocene and Miocene larger foraminiferida from Australia and New Zealand. Bull. Bur. Miner. Resour., Geol. Geophys., 188, 1–98.

Charpy, L., 2005. Importance of photosynthetic picoplankton in coral reef ecosystems. Vie et Milieu, 55, 217–223.

Chen, C.A., Wang, J.T., Fang, L.S., Yang, Y.W., 2005. Fluctuating algal symbiont communities in Acropora palifera (Scleractinia: Acroporidae) from Taiwan. Mar. Ecol. Prog. Ser., 295, 113–121.

Coates A.G., Jackson, J.B.C., 1987. Clonal growth, algal symbiosis, and reef formation by corals. Paleobiology, 13-4, 363-378.

Coletti, G., Basso, D., Frixa, A., Corselli, G., 2015. Transported rhodoliths witness the lost carbonate factory: a case history from the Miocene Pietra da Cantoni limestone (NW Italy). Riv. It. Paleont. Strat., 121(3), 345–368

Compton, J.S., Snyder, S.W., Hodell, D.A., 1990. Phosphogenesis and weathering of shelf sediments from the southeastern United States: Implications for Miocene δ^{13}C excursions and global cooling. Geology, 18, 1227–1230.

Côsovic, V., Drobne, K., Moro, A., 2004. Paleoenvironmental model for Eocene foraminiferal limestones of the Adriatic carbonate platform (Istrian Peninsula). Facies, 50:61–75.

Costa, E., Garcés, M., López-Blanco, M., Serra-Kiel, J., Bernaola, G., Cabrera, L., Beamud, E., 2013. The Bartonian–Priabonian marine record of the eastern South Pyrenean foreland basin (NE Spain): a new calibration of the larger foraminifers and calcareous nannofossil biozonation. Geologica Acta, 11, 177–193.

Cramer, B.S., Miller, K.G., Barrett, P.J., Wright, J.D., 2011. Late Cretaceous–Neogene trends in deep ocean temperature and continental ice volume: Reconciling records of benthic foraminiferal geochemistry (δ^{18}O and Mg/Ca) with sea level history. J. Geophys. Res.-Oceans, 116, C12023, doi: 10.1029/2011jc007255.

Cramer, B.S., Toggweiler, J.R., Wright, J.D., Katz, M.E., Miller, K.G., 2009. Ocean overturning since the Late Cretaceous: Inferences from a new benthic foraminiferal isotope compilation. Paleoceanography, 24, PA4216, doi: 10.1029/2008pa001683.

Davies, A.J., Duineveld, G., Lavaleye, M., Bergman, M., van Haren, H., Roberts, J.M., 2009. Downwelling and deep-water bottom currents as food supply mechanisms to the cold-water coral *Lophelia pertusa* (Scleractinia) at the Mingulay Reef Complex. Limnol. Oceanogr., 54, 620–629.

DeCarlo, T.M., Karnauskas, K.B., Davis, K.A., Wong, G.T.F., 2015. Climate modulates internal wave activity in the Northern South China Sea. Geophys. Res. Lett., 42, 831–838, doi: 10.1002/2014GL062522.

Demarcq, G., 1984. Bioprovinces et migrations au cours du Neogene en Mediterranean dapres les mégafaunaes marines benthiques. Ann. Geo!. Pays Hell. 32, 271 – 280.

Demarcq, G., 1987. Paleothermic Evolution During the Neogene in Mediterranea through the Marine Megafauna. *Budapest Regional Committee on Mediterranean Stratigraphy, 7e Congrès Néogène Méditerranéen. Budapest. Abstract*, 176–178.

Demicco, R.V., Lowenstein, T.K., Hardie, L.A., 2003. Atmospheric pCO_2 since 60 Ma from records of seawater pH, calcium, and primary carbonate mineralogy. Geology, 31, 793–796.

Dickson, R.R., McCave, I.N., 1986. Nepheloid layers on the continental slope west of Porcupine Bank. Deep–Sea Research, 33, 91–818.

Dragastan, O., Herbig, H.G., 2007. *Halimeda* (green siphonous algae) from the

Paleogene south of the central High Atlas (Morocco)–Taxonomy, phylogeny and paleoenvironment. Micropaleontology, 53(1–2): 1–72.

Dragastan, O., Herbig, H.G., 2007. Halimeda (green siphonous algae) from the Paleogene south of the central High Atlas (Morocco)–Taxonomy, phylogeny and paleoenvironment. Micropaleontology, 53(1–2): 1–72.

Dreyer, T., Corregidor, J., Arbues, P., Puigdefàbregas, C., 1999. Architecture of the tectonically influenced Sobrarbe deltaic complex in the Ainsa Basin, northern Spain. Sed. Geol., 127, 127–169.

Drooger, C.W., 1993. Radial foraminifera; morphometrics and evolution. Proceedings of the Royal Academy of Sciences and Arts of the Netherlands, Science series, 41, 1–242.

Dubinsky, Z., Berman-Frank, I., 2001. Uncoupling primary production from population growth in photosynthesizing organisms in aquatic ecosystems. Aquatic Sciences, 63, 4–17.

Dutton, A., Lohmann, K.C., Leckie, R.M., 2005. Insights from the Paleogene tropical Pacific: Foraminiferal stable isotope and elemental results from Site 1209, Shatsky Rise. Paleoceanography, 20, PA3004, doi: 10.1029/2004PA001098.

Einchenseer, H., 2003. Stratigraphic styles influenced by thrust tectonics: Architecture and facies of lowstand wdges and transgressive to highstand carbonate banks (upper Paleocene to lower Eocene, central-southern Pyrenees). Geological Field Trip 4. AAPG International Conference and Exhibition 2003, Barcelona, Spain, 77 p.

Einchenseer, H., Luterbacher, H., 1992. The marine paleogene of the tremp region (NE Spain)-depositional sequences, facies history, biostratigraphy and controlling factors. Facies, 27, 119–151, doi: 10.1007/BF02536808.

Eisele, M., Frank, N., Wienberg, C., Hebbeln, D., López-Correa, M., Douville, E., Freiwald, A., 2011. Productivity controlled cold-water coral growth periods during the last glacial off Mauritania. Mar. Geol., 280, 143–149.

Enríquez, S., Schubert, N., 2014. Direct contribution of the seagrass Thalassia testudinum to lime mud production. Nature Communications, 5, 1–12. DOI: 10.1038/ncomms4835.

Esteban, M., 1996. An overview of Miocene reefs from Mediterranean areas: general trends and facies models. In: Franseen, E., Esteban, M., Ward, W.C., Rouchy, J.M. (eds), Models for Carbonate Stratigraphy from Miocene Reef Complexes of the Mediterranean regions. SEPM, Concepts in Sedimentology and Paleontology Series, 5, 3–53.

Eva, A.N., 1980. Pre-Miocene seagrass communities in the Caribbean: Paleontology, 23, 231–236.

Fagerstrom, J.A., 1987. The Evolution of Reef Communities. Wiley Interscience, John Wiley and Sons, New York.

Filippelli, G.M., 2008. The global phosphorus cycle: past, present, and future. Elements, 4, 89–95.

Flügel, E., 2004. Microfacies of Carbonate Rocks. Analysis, Interpretation and Application. Springer-Verlag, Germany.

Föllmi, K.B., Hofmann, H., Chiaradia, M., de Kaenel, E., Frijia, G., Parente, M., 2015. Miocene phosphate-rich sediments in Salento (southern Italy). Sediment. Geol., 327, 55–71, doi: http://dx.doi.org/10.1016/j.sedgeo.2015.07.009.

Fornós, J.J., Ahr, W.M., 1997. Temperate carbonates on a modern, low energy, isolated ramp: the Balearic platform, Spain: J. Sediment. Res., 67, 364–373.

Fornós, J.J., Ahr, W.M., 2006. Present-day temperate carbonate sedimentation on the Balearic Platform, western Mediterranean: compositional and textural variation along a low-energy isolated ramp, in Pedley, H.M., and Carannante, G., eds., Cool- Water Carbonates: Depositional Systems and Palaeoenvironmental Controls. Geol. Soc. London, Spec. Publ., 255, p. 121–135.

Franseen, E.K., Goldstein, R., Farr, M., 1997. Substrate-slope and temperature controls on carbonate ramps: revelations from Upper Miocene outcrops, SE Spain. Spec. Publ. 56, 271–292. doi:10.3748/wjg.v17.i23.2860

Freiwald, A., 2003. Reef-Forming Cold-Water Corals. In: Wefer, G., Billet, D., Hebbeln, D., Jorgensen, B.B., Schlüter, M., Weering, T.C.E.V. (eds), Ocean Margin Systems. Springer-Verlag, Berlin Heidelberg, pp. 365–385.

Frost, S.H., 1977. Oligocene reef coral biogeography Caribbean and western Tethys. Mem. B.R.G.M., Paris, 342–352.

Frost, S.H., 1981. Oligocene reef coral biofacies of the Vicentin, northeast Italy. In: Toomey, D.F. (ed.), European Fossil Reef Models. SEPM Spec. Publ., pp. 483–539.

Frost, S.H., Harbour, J.L., Realini, M.J., Harris, P.M., 1983. Oligocene Reef Tract Development, Southwestern Puerto Rico. Sedimenta, 9, 141 pp.

Furla, P., Allemand, D., Shick, J.M., Ferrier-Pagès, C., Richier, S., Plantivaux, A., Merle, P.L., Tambutté, S., 2005. The symbiotic anthozoan: a physiological chimera between alga and animal. Integrative and Comparative Biology, 45, 595–604

Gatt, P.A., Gluyas, J.G., 2012. Climatic controls on facies in Palaeogene Mediterranean subtropical carbonate platforms. Petroleum Geoscience, 18, 355–367, doi: 10.1144/1354–079311–032.

Geister, J., Ungaro, S., 1977. The Oligocene coral formations of the Colli Berici. Eclogae Geol. Helv. 70, 811 – 823.

Ghosh, A.M., Sarkar, S., 2013. Diversification of the Family Sporolithaceae: A case of successful survival in the perspective of Cretaceous–Tertiary mass extinctions in India. Natl. Acad. Sci. Lett. 36:215–224. DOI 10.1007/s40009-013-0122-6

Granier, B., 2012. The contribution of calcareous green algae to the production of limestones: a review. In: Basso D. & Granier B. (eds), Calcareous algae and global change: from identification to quantification. *Geodiversitas* 34 (1): 35–60. http://dx.doi.org/10.5252/g2012n1a3

Gregg, M., 1989. Scaling turbulent dissipation in the thermocline. J. Geophys. Res., 94, 9686–9698 doi: 10.1029/JC094iC07p09686.

Gumati, Y.D., 1992. Lithostratigraphy of oil-bearing Tertiary bioherms in the Sirte basin, Libya. J. Petrol. Geol., 15, 305–318.

Halfar, J., Mutti, M., 2005. Global dominance of coralline red-algal facies: A response to Miocene oceanographic events. Geology, 33, 481–484, doi: 10.1130/G21462.1.

Hallock, P., 1979. Trends in test shape with depth in large, symbiont-bearing foraminifera. J. Foraminifer. Res. 9, 61–69. doi:10.2113/gsjfr.9.1.61

Hallock, P., 1981. Algal symbiosis: a mathematical analysis. Marine Biology, 62, 249–255.

Hallock, P., 1985. Why are larger foraminifera large? Paleobiology, 11-2, 195-208.

Hallock, P., 1987. Fluctuations in the trophic resource continuum: A factor in global diversity cycles? Paleoceanography, 2, 457–471.

Hallock, P., 1988a. Diversification in algal symbiont-bearing foraminifera: a response to oligotrophy? Revue de Paleobiologie, Vol. Spec. no. 2 (Benthos '86): 789–797.

Hallock, P., 1988b. Interoceanic differences in foraminifera with symbiotic algae: A result of nutrient supplies? Proc. Sixth International Coral Reef Symposium, Townsville, Australia, 3, 251–255.

Hallock, P., 1999. Symbiont-bearing Foraminifera. In: Sen Gupta, B.K. (ed.), Modern Foraminifera. Kluwer Academic Publishers, Dordrecht, The Netherlands, pp. 123–139.

Hallock, P., 2001. Coral reefs, carbonate sedimentation, nutrients, and global change. In: Stanley, G. D. (ed.), The History and Sedimentology of Ancient Reef Ecosystems. Kluwer Academic/Plenum Publishers, pp. 387–427.

Hallock, P., 2011. Foraminifera. In: Hopley D. (ed.), Encyclopedia of modern coral reef. Springer BV, pp. 416-421.

Hallock, P., Glenn, E.C., 1986. Larger Foraminifera: A tool for paleoenvironmental analysis of Cenozoic carbonate depositional facies. Palaios 1, 55–64.

Hallock, P., Hansen, H. J., 1979. Depth adaptation in Amphistegina: change in lamellar thickness. Bull. geol. Soc. Denmark, vol 27, pp. 99-104.

Hallock, P., Pomar, L., 2008. Cenozoic evolution of larger benthic foraminifers: Paleoceanographic evidence for changing habitats. Proc. 11th Internat. Coral Reef Symp., Ft. Lauderdale, Florida, 16–20.

Hallock, P., Premoli-Silva, I., Boersma, A., 1991a. Similarities between planktonic and larger foraminiferal evolutionary trends through Paleogene paleoceanographic changes. Palaeogeogr., Palaeoclimatol., Palaeoecol., 83, 49–64.

Hallock, P., Röttger, R., Wetmore, K., 1991b. Hypotheses on form and function in foraminifera. *Biology of the Foraminifera*, J. J. Lee and O. R. Anderson, eds., Academic Press, pp. 41–72.

Hallock, P., Sheps, K., Chapronière, G., Howell, M., 2006. Larger benthic foraminifers of the Marion Plateau, northeastern Australia (ODP Leg 194): comparison of faunas from bryozoan (Sites 1193 and 1194) and red algal (Sites 1196–1198) dominated carbonate platforms. In: Anselmetti, F.S., Isern, A.R., Blum, P., Betzler, C. (eds), Proc. ODP, Sci. Results, pp. 1–31.

Hallock, P., Schlager, W., 1986. Nutrient excess and the demise of coral reefs and carbonate platforms. Palaios, 1, 389–398.

Hearn, C., Atkinson, M., Falter, J., 2001. A physical derivation of nutrient-uptake rates in coral reefs: effects of roughness and waves. Coral Reefs, 20, 347–356, doi: 10.1007/s00338-001-0185-6.

Heckel, P.H., 1974. Carbonate buildups in the geologic record: a review. In: Laporte, L.F. (ed.), Reefs in Time and Space. Tulsa, OK, SEPM Special Publication, 18, 90–154.

Hein, M., Sand-Jansen, K., 1997. CO_2 increases oceanic primary production. Nature, 388, 526–527.

Hendry, J.P., Taberner, C., Marshall, J.D., Pierre, C., Carey, P.F., 1999. Coral reef diagenesis records pore-fluid evolution and paleohydrology of a siliciclastic basin margin succession (Eocene South Pyrenean foreland basin, northeastern Spain. Geol. Soc. Am. Bull., 111, 395–411.

Henriet, J.P., Hamoumi, N., Da Silva, A.C., Foubert, A., Lauridsen, B.W., Rüggeberg, A., Van Rooij, D., 2014. Carbonate mounds: from paradox to World Heritage. Mar. Geol. 352, 89–110. http://dx.doi.org/10.1016/j.margeo.2014.01.008.

Hernández-Molina, F.J., Paterlini, M., Somoza, L., Violante, R., Arecco, M.A., de Isasi, M., Rebesco, M., Uenzelmann-Neben, G., Neben, S. & Marshall, P., 2010. Giant mounded drifts in the Argentine Continental Margin: Origins, and global implications for the history of thermohaline circulation. Mar. Petrol. Geol., 27, 1508–1530, doi: http://dx.doi.org/10.1016/j.marpetgeo.2010.04.003.

Hernández-Molina, F.J., Paterlini, M., Violante, R., Marshall, P., de Isasi, M., Somoza, L. & Rebesco, M., 2009. Contourite depositional system on the Argentine Slope: An exceptional record of the influence of Antarctic water masses. Geology, 37, 507–510, doi: 10.1130/g25578a.1.

Hernández-Molina, F.J., Serra, N., Stow, D.A.V., Llave, E., Ercilla, G., Van Rooij, D., 2011. Along-slope oceanographic processes and sedimentary products around the Iberian margin. Geo-Marine Letters, 31, 315–341, doi: 10.1007/s00367-011-0242-2.

Hinz, K., Neben, S., Schreckenberger, B., Roeser, H.A., Block, M., Souza, K.G.D., Meyer, H., 1999. The Argentine continental margin north of 48°S: sedimentary successions, volcanic activity during breakup. Mar. Petrol. Geol., 16, 1–25, doi: http://dx.doi.org/10.1016/S0264-8172(98)00060-9.

Höntzsch, S., Scheibner, C., Brock, J.P., Kuss, J., 2013. Circum-Tethyan carbonate platform evolution during the Palaeogene: the Prebetic platform as a test for climatically controlled facies shifts. Turkish J. Earth Sci., 22, 891–918, doi: 10.3906/yer-1207-8.

Hottinger, L., 1983. Neritic macroid genesis, an ecological approach. In: Peryt, T.M. (ed.), Coated Grains. Springer-Verlag, New York, pp. 27–37.

Hottinger, L., 1997. Shallow benthic foraminiferal assemblages as signals for depth of their deposition and their limitations. B. Soc. Géol. Fr., 168, 491–505.

Hottinger, L., 1998. Shallow benthic foraminifera at the Paleocene-Eocene Boundary. Strata série 1, 9, 6–64.

Houlbrèque, F., Ferrier-Pagès, C., 2009. Heterotrophy in Tropical Scleractinian Corals. Biological Reviews, 84: 1–17

Huston, M., 1985. Variations in coral growth with depth at Discovery Bay, Jamaica. Coral Reefs, 4, 19–25.

Immenhauser, A., 2009. Estimating palaeo-water depth from the physical rock record. Earth-Science Reviews, 96, 107–139, doi: 10.1016/j.earscirev.2009.06.003

Inall, M.E., Shapirob, G.I., Sherwin, T.J., 2001. Mass transport by non-linear internal waves on the Malin Shelf. Cont. Shelf Res., 21, 1449–1472.

Insalaco, E., 1998. The descriptive nomenclature and classification of growth fabrics in fossil scleractinian reefs. Sediment. Geol., 118, 159–186, doi: 10.1016/S0037-0738(98)00011-6.

Ivany, L.C., Portell, R.W, and Jones, D.S., 1990. Animal-plant relationships and paleobiogeography of an Eocene seagrass community from Florida: PALAIOS, v. 5, p. 244–258.

James, N.P., 1983. Reef environment. In: Scholle, P.A., Bebout, D.G., Moore, C.H. (eds), Carbonate Depositional Environments. Am. Ass. Petrol. Geol. Memoir 33, Tulsa, OK, pp. 345–440.

James, N.P., 1984. Reefs. In: Walker, R.G. (ed.), Facies Models. Geological Association of Canada, pp. 229–244.

James, N.P., Bone, Y., van der Borch, C. C., Gostin, V.A., 1992. Modern carbonate and terrigenous clastic sediments on a cool water, high energy, mid-latitude shelf: Lapedece, southernAustralia: Sedimentology, v. 39, p. 877–903.

James, N.P., Boreen, T.D., Bone, Y., Feary, D.A., 1994. Holocene carbonate sedimentation on the west Eucla Shelf, Great Australian Bight: a shaved shelf: Sediment. Geol., 90, 161–177.

Janson, X., Eberli, G., Bonnaffe, F., Gaumet, F., De Casanove, V., 2007. Seismic expression of a Miocene prograding carbonate margin, Mut Basin, Turkey. AAPG Bulletin, 91, 685–713.

Janson, X., Van Buchem, F.S.P., Dromart, G., Eichenseer, H.T., Dellamonica, X., Boichard, R., Bonnaffe, F., Eberli, G., 2010. Architecture and facies differentiation within a Middle Miocene carbonate platform, Ermenek, Mut Basin, southern Turkey. In: Van Buchem, F.S.P., Gerdes, K.D., Esteban, M. (eds), Mesozoic and Cenozoic carbonate systems of the Mediterranean and the Middle East: stratigraphic and diagenetic reference models. Geol. Soc., London, Spec. Publ., pp. 265–290.

Jaramillo-Vogel, D., Strasser, A., Frijia, G., Spezzaferri, S., 2013. Neritic isotope and sedimentary records of the Eocene–Oligocene greenhouse–icehouse transition: The Calcare di Nago Formation (northern Italy) in a global context. Palaeogeogr. Palaeoclimatol. Palaeoecol., 369, 361–376. doi:10.1016/j.palaeo.2012.11.003

Johnson, K.G., Jackson, J.B.C., Budd, A.F., 2008. Caribbean Reef Development Was Independent of Coral Diversity over 28 Million Years. Science, 319, 1521–1523, doi: 10.1126/science.1152197.

Johnson, Z.I., Zinser, E.R., Coe, A., McNulty, N.P., Woodward, E.M.S., Chisholm, S.W., 2006. *Prochlorococcus* is the numerically dominant phytoplankter in the oligotrophic oceans, accounting for up to half of the photosynthetic biomass and production in some regions. Science, 311, 1737–1740.

Jones, R.W., Racey, A., 1994. Cenozoic stratigraphy of the Arabian Peninsula and Gulf. In: Simmons, M.D. (ed.), Micropalaeontology and Hydrocarbon Exploration in the Middle East. Chapman & Hall, pp. 273–307.

Jorry, S.J., Hasler, C.A., Davaud, E., 2006. Hydrodynamic behaviour of Nummulites: implications for depositional models. Facies, 52, 221–235, doi: 10.1007/s10347-005-0035-z.

Kahng, S.E., Copus, J.M., Wagner, D., 2014. Recent advances in the ecology of mesophotic coral ecosystems (MCEs). Curr. Opin. Environ. Sustain. 7, 72–81. doi:10.1016/j.cosust.2013.11.019

Kahng, S.E., Garcia-Sais, J.R., Spalding, H.L., Brokovich, E., Wagner, D., Weil, E., Hinderstein, L., Toonen, R.J., 2010. Community ecology of mesophotic coral reef ecosystems. Coral Reefs, 29, 255–275, doi: 10.1007/s00338-010-0593-6.

Kanwisher, J.W., Wainwright, S.A., 1967. Oxygen balance in some reef corals. Biol. Bull., 133, 378–390, doi: http://www.jstor.org/stable/1539833.

Kennett, J.P., (ed.), The Miocene Ocean: Paleoceanography and biogeography. CENOP, GSA Memoir 163, 337 pp.

Kennett, J.P., Stott, L.D., 1991. Abrupt deep-sea warming, palaeoceanographic changes and benthic extinctions at the end of the Palaeocene. Nature, 353, 225–229, doi: 10.1038/353225a0.

Kiessling, W., 2006. Towards an unbiased estimate of fluctuations in reef abundance and volume during the Phanerozoic. Biogeosciences, 3, 15–27, doi: 10.5194/bg-3-15-2006.

Kiessling, W., 2009. Geologic and Biologic Controls on the Evolution of Reefs. Annual Review of Ecology, Evolution, and Systematics, 40, 173–192, doi: doi:10.1146/annurev.ecolsys.110308.120251.

Kiessling, W., Baron-Szabo, R.C., 2004. Extinction and recovery patterns of scleractinian corals at the Cretaceous–Tertiary boundary. Palaeogeogr., Palaeoclimatol., Palaeoecol., 214, 195–223.

Kiessling, W., Flügel, E., Golonka, J., 1999. Paleo Reef Maps: Evaluation of a comprehensive database on Phanerozoic reefs. Am. Ass. Petrol. Geol. Bull., 83, 1552–1587.

Kiessling, W., Flügel, E., Golonka, J., 2002. Phanerozoic Reef Patterns. SEPM Special Publication, 775 p.

Kiessling, W., Simpson, C., 2011. On the potential for ocean acidification to be a general cause of ancient reef crises. Global Change Biology, 17, 56–67.

Knoll, A.H., Lipps, J.H., 1993. Evolutonary history of prokariotes and protists. In: Lipps, J.H. (ed.), Fossil Procariotes and Protists. Blackwell Sci. Publ., Boston, pp. 19–29.

Langer, M.R., 1993. Epiphytic foraminifera. Mar. Micropaleontol. 20, 235–265. doi:10.1016/0377-8398(93)90035-V

Larsen, A.R., 1976. Studies of recent *Amphistegina*, taxonomy and some ecological aspects. Isr. Journ. Earth-Sci. 25, 1–26.

Larsen, A.R., Drooger, C.W., 1977. Relative thickness of the test in the Amphistegina species of the Gulf of Elat. Utr. Micropal. Bull. 15, 225–240.

Leichter, J.J., Shellenbarger, G., Genovese, S.J., Wing, S.R., 1998. Breaking internal waves on a Florida (USA) coral reef: a plankton pump at work? Mar. Ecol. Prog. Ser., 166, 83–97.

Leichter, J.J., Stewart, H.L., Miller, S.L., 2003. Episodic nutrient transport to Florida coral reefs. Limnol. Oceanogr, 48, 1394–1407.

Leichter, J.J., Stokes, M.D., Genovese, S.J., 2008. Deep water macroalgal communities adjacent to the Florida Keys reef tract. Mar. Ecol. Prog. Ser., 356, 123–138, doi: 10.3354/meps07230.

Leichter, J.J., Wing, S.R., Miller, S.L., Denny, M.W., 1996. Pulsed delivery of subthermocline water to Conch Reef (Florida Keys) by internal tidal bores. Limnol. Oceanogr., 41, 1490–1501.

Lennert-Cody, C.R., Franks, P.J.S., 1999. Plankton patchiness in high-frequency internal waves. Mar. Ecol. Prog. Ser., 59–66.

Liebau, A., 1984. Grundlagen der Ökobathymetrie. Paläontologische Kursbücher, 2, 149–184.

Liu, Z., Pagani, M., Zinniker, D., DeConto, R., Huber, M., Brinkhuis, H., Shah, S.R., Leckie, R.M., Pearson, A., 2009. Global Cooling During the Eocene–Oligocene Climate Transition. Science, 323, 1187–1190, doi: 10.1126/science.1166368.

Lüning, K., 1990. Seaweeds. Their environment, biogeography, and ecophysiology. John Wiley & Sons, Inc.

Manker, J.P., Carter, B.D., 1987. Paleoecology and paleogeography of an extensive rhodolith facies from the lower Oligocene of south Georgia and north Florida. Palaios, 592, 181–188, doi: http://www.jstor.org/stable/3514647.

Mann, K.H., Lazier, J.R.N., 2006. Dynamics of marine ecosystems: biological-physical interactions in the oceans. Wiley-Blackwell.

Markello, J.R., Koepnick, R.B., Waite, L.E., Collins, J.F., 2008. The Carbonate Analogs Through Time (CATT) Hypothesis and the Global Atlas of Carbonate Fields—A Systematic and Predictive Look at Phanerozoic Carbonate Systems. In: Lukasik, J., Simo (Toni), J.A. (eds), Controls on Carbonate Platform and Reef Development, pp. 15–45.

Marshall, J.F., Davies, P.J., 1988. *Halimeda* bioherms of the northern Great Barrier Reef. Coral Reefs, 6, 139-148, doi: 10.1007/bf00302010.

Martín, J., Braga, J.-C., 1994. Messinian events in the Sorbas Basin in southeastern Spain and their implications in the recent history of the Mediterranean. Sediment. Geol. 90, 257–268. doi:10.1016/0037-0738(94)90042-6

Martin, J., Braga, J.-C., Betzler, C., Brachert, T., 1996. Sedimentary model and high-frequency cyclicity in a Mediterranean, shallow-shelf, temperate-carbonate environment (uppermost Miocene, Agua Amarga Basin, Southern Spain). Sedimentology, 43, 263–277. doi:10.1046/j.1365-3091.1996.d01-4.x

Martín, J.M, Braga, J.-C., Sánchez-Almazo, I., 1999. The Messinian record of the outcropping marginal Alboran Basin deposits: significance and implications. In: Zahn, R., Comas, M.C., and Klaus, A. (eds), Proc. ODP, Sci. Res., pp. 543 – 551.

Mateu-Vicens, G., Hallock, P., Brandano, M., 2008. A depositional model and paleoecological reconstruction of the lower Tortonian distally steepened ramp of Menorca (Balearic Islands, Spain). Palaios, 23, 465–481, doi: 10.2110/palo.2007.p07-061r.

Mateu-Vicens, G., Hallock, P., Brandano, M., 2009. Test shape variability of *Amphistegina* D'Orbigny 1826 as a paleobathymetric proxy: application to two Miocene examples. In: Demchuk T, Gary A (eds), Geologic problems solving with microfossils. SEPM Spec. Publ., pp. 67–82.

Mateu-Vicens, G., Khokhlova, A., Sebastián-Pastor, T., 2014. Epiphytic foraminiferal indices as bioindicators in Mediterranean seagrass meadows. J. Foramin. Res., 44, 325 – 339, doi: 10.2113/gsjfr.44.3.325.

Mateu-Vicens, G., Pomar, L., Ferràndez-Cañadell, C., 2012. Nummulitic banks in the upper Lutetian "Buil level", Ainsa basin, South Central Pyrenean Zone: the impact of internal waves. Sedimentology, 59, 527–552, doi: 10.1111/j.1365-3091.2011.01263.x.

Maurin, N., Amblard, C., Bourdier, G., 1997. Phytoplanktonic excretion and bacterial reassimilation in an oligomesotrophic lake: molecular weight fractionation. J. Plankton Res., 8, 1045–1068.

Meyers, S.P., 2000. Developments in aquatic microbiology. Int. Microbiol., 3, 203–211.

Mienis, F., van Weering, T., de Haas, H., de Stigter, H., Huvenne, V., Wheeler, A., 2006. Carbonate Mound development at the SW Rockall Trough margin based on high resolution TOBI and seismic recording. Mar. Geol., 233.

Morsilli, M., Bosellini, F.R., Pomar, L., Hallock, P., Papazzoni, C.A., Aurell, M., 2012. Mesophotic coral buildups in a prodelta setting (Late Eocene, southern Pyrenees, Spain): a mixed carbonate siliciclastic system. Sedimentology, 59, 766–794, doi: 10.1111/j.1365-3091.2011.01275.x.

Muñoz, J.-A., Beamud, E., Fernández, O., Arbués, P., Dinarès-Turell, J., Poblet, J., 2013. The Ainsa Fold and thrust oblique zone of the central Pyrenees: Kinematics of a curved contractional system from paleomagnetic and structural data. Tectonics, 32, 1142–1175, doi: 10.1002/tect.20070.

Nebelsick, J.H., Bassi, D., Lempp, J., 2013. Tracking paleoenvironmental changes in coralline algal-dominated carbonates of the Lower Oligocene Calcareniti di Castelgomberto formation (Monti Berici, Italy). Facies 59, 133–148. doi:10.1007/s10347-012-0349-6.

Nebelsick, J.H., Rasser, M.W., Bassi, D., 2005. Facies dynamics in Eocene to Oligocene circumalpine carbonates. Facies 51, 197–216. doi:10.1007/s10347-005-0069-2

Nielsen, T.G., Løkkegaard, B., Richardson, K., Pedersen, F.B., Hansen, L., 1993. Structure of plankton communities in the Dogger Bank area (North Sea) during a stratified situation. Mar. Ecol. Prog. Ser., 95, 115–131.

Nikolaev, S.D., Oskina, N.S., Blyum, N.S., Bubenshchikova, N.V., 1998. Neogene–Quaternary variations of the 'Pole–Equator' temperature gradient of the surface oceanic waters in the North Atlantic and North Pacific. Global Planet. Change, 18, 85–111.

Nisancioglu, K.H., Raymo, M.E. & Stone, P.H., 2003. Reorganization of Miocene deep water circulation in response to the shoaling of the Central American Seaway. Paleoceanography, 18, n/a-n/a, doi: 10.1029/2002PA000767.

Nunes, F., Norris, R.D., 2006. Abrupt reversal in ocean overturning during the Palaeocene/Eocene warm period. Nature, 439, 60–63, doi: 10.1038/nature04386.

Pagani, M., Zachos, J.C., Freeman, K.H., Tipple, B., Bohaty, S., 2005. Marked decline in atmospheric carbon dioxide concentrations during the Paleogene. Science, 309, 600–603.

Pak, D.K., Miller, K.G., 1992. Paleocene to Eocene benthic foraminiferal isotopes and assemblages; implications for deepwater circulation. Paleoceanography, 7, 405–422, doi: 10.1029/92PA01234.

Partensky, F., Hess, W.R., Vaulot, D., 1999. *Prochlorococcus*, a marine photosynthetic prokaryote of global significance. Microbiol. Mol. Biol. R., 63, 106–127.

Pawelek, T., 2009. From thin sections to discovery: The Upper Satal in the dentral Sirte basin (North-central Libya) – a success history. Geotectonic Res., 96: 87–100.

Pearson, P.N., Palmer, M.R., 2000. Atmospheric carbon dioxide concentrations over the past 60 million years. Nature, 406, 695–699.

Pearson, P.N., McMillan, I.K., Wade, B.S., Jones, T.D., Coxall, H.K., Bown, P.R., Lear, C.H., 2008. Extinction and environmental change across the Eocene–Oligocene boundary in Tanzania. Geology, 36, 179–182, doi: 10.1130/g24308a.1.

Pedley, M., 1998. A review of sediment distribution and processes in Oligo–Miocene ramps of southern Italy and Malta (Mediterranean divide). In: Wright, V.P., Burchette, T.P. (eds), Carbonate Ramps. Geol. Soc. London, Spec. Publ., pp. 163–179.

Peduzzi, P., Herndl, G.J., 1992. Zooplankton activity fueling the microbial loop: Differential growth response of bacteria from oligotrophic and eutrophic waters. Limnol. Oceanogr., 37, 1087–1092.

Perrin, C., 2000. Changes of palaeozonation patterns within Miocene coral reefs, Gebel Abu Shaar, Gulf of Suez, Egypt. Lethaia, 33, 253–268.

Perrin, C., 2002. Tertiary: the emergence of modern reef ecosystems. In: Kiessling, W., Flügel, E., Golonka, J. (eds), Phanerozoic Reef Patterns. SEPM Special Publication, 72, 587–621.

Perrin, C., Bosellini, F.R., 2012. Paleobiogeography of scleractinian reef corals: Changing patterns during the Oligocene–Miocene climatic transition in the Mediterranean. Earth-Science Reviews, 111, 1–24, doi: http://dx.doi.org/10.1016/j.earscirev.2011.12.007.

Perrin, C., Kiessling, W., 2012. Latitudinal Trends in Cenozoic Reef Patterns and their Relationship to Climate. In: Mutti, M., Piller, W., Betzler, C. (eds), Carbonate Systems during the Oligocene–Miocene Climatic Transition. Wiley-Blackwell, Oxford, UK., Int. Assoc. Sedimentol. Spec. Publ., 42, 17–34.

Perrin C., Plaziat J.C., Rosen, B. R., 1998. Miocene coral reefs and reef corals of the southwestern Gulf of Suez and north-western Red Sea: distribution, diversity and regional environmental controls. Purser B.H., Bosence D.W.J. (eds), Sedimentation and Tectonics of Rift Basins: Red Sea–Gulf of Aden. Chapman & Hall, London. ISBN 0412 73490 7.

Pingree, R.D., Mardell, G.T., New, A.L., 1986. Propagation of internal tides from the upper slopes of the Bay of Biscay. Nature Geosci., 312, 154–158, doi: 10.1038/321154a.

Pisera, A., Busquets, P., 2002. Eocene siliceous sponges from the Ebro Basin (Catalonia, Spain). Geobios, 35, 321.

Plaziat, J.C., Perrin, C., 1992. Multikilometer-sized reefs built by foraminifera (*Solenomeris*) from the early Eocene of the Pyrenean domain (S. France, N. Spain): Paleoecologic relations with coral reefs. Palaeogeogr., Palaeoclimatol., Palaeoecol., 96, 195– 231.

Poblet, J., Muñoz, J.A., Travé, A., Serra-Kiel, J., 1998. Quantifying the kinematics of detachment folds using three-dimensional geometry: Application to the Mediano anticline (Pyrenees, Spain). Geol. Soc. Am. Bull., 110, 111–125, doi: doi: 10.1130/0016-7606(1998)110<0111:QTKODF>2.3.CO;2.

Pochon, X., Montoya-Burgos, J.I., Stadelmann, B., Pawlowski, J., 2006. Molecular phylogeny, evolutionary rates, and divergence timing of the symbiotic dinoflagellate genus *Symbiodinium*. Molecular Phylogenetics and Evolution, 38, 20–30, doi: 10.1016/j.ympev.2005.04.028.

Polzin, K.L., Toole, J.M., Ledwell, J.R., Schmitt, R.W., 1997. Spatial variability of turbulent mixing in the abyssal ocean. Science, 276, 93–96. doi:10.1126/science.276.5309.93

Polzin, K.L., Toole, J.M., Schmitt, R.W., 1995. Finescale Parameterizations of Turbulent Dissipation. J. Phys. Oceanogr. 25, 306–328. doi:10.1175/1520-0485(1995)025<0306:FPOTD>2.0.CO;2

Pomar, L., 1991. Reef geometries, erosion surfaces and high-frequency sea-level changes, upper Miocene reef complex, Mallorca, Spain. Sedimentology, 38, 243–270, doi: DOI: 10.1111/j.1365-3091.1991.tb01259.x.

Pomar, L., 1993. High-resolution sequence stratigraphy in prograding carbonates: application to seismic interpretation. In: Louks, B., Sarg, R.J. (eds), Carbonate Sequence Stratigraphy: Recent Developments and Applications. A.A.P.G. Mem. 57, 389–407.

Pomar, L., 2001 a. Types of carbonate platforms, a genetic approach. Basin Research, 13, 313–334, doi: 10.1046/j.0950-091x.2001.00152.x.

Pomar, L., 2001 b. Ecological control of sedimentary accommodation: evolution from a carbonate ramp to rimmed shelf, Upper Miocene, Balearic Islands. Palaeogeogr., Palaeoclimatol., Palaeoecol., 175: 249–272

Pomar, L., Bassant, P., Brandano, M., Ruchonnet, C., Janson, X. 2012 a. Impact of carbonate producing biotas on platform architecture: insights from Miocene examples of the Mediterranean region. Earth-Science Reviews, 113, 186–211, doi: doi:10.1016/j.earscirev.2012.03.007.

Pomar, L., Brandano, M., Westphal, H., 2004. Environmental factors influencing skeletal-grain sediment associations: a critical review of Miocene examples from the Western-Mediterranean. Sedimentology, 51, 627-651, doi: DOI: 10.1111/j.1365-3091.2004.00640.x.

Pomar, L., Hallock, P., 2007. Changes in coral-reef structure through the Miocene in the Mediterranean: adaptative vs. environmental influence. Geology, 35, 899–902, doi: 10.1130/G24034A.1.

Pomar, L., Hallock, P., 2008. Carbonate Factories: A Conundrum in Sedimentary Geology. Earth-Science Reviews, 87, 134–169, doi: 10.1016/j.earscirev.2007.12.002.

Pomar, L., Mateu-Vicens, G., Morsilli, M., Brandano, M., 2014. Carbonate ramp evolution during the Late Oligocene (Chattian), Salento Peninsula, southern Italy. Palaeogeogr., Palaeoclimatol., Palaeoecol., 404, 109–132, doi: http://dx.doi.org/10.1016/j.palaeo.2014.03.023.

Pomar, L., Morsilli, M., Hallock, P., Bádenas, B., 2012 b. Internal waves, an under-explored source of turbulence events in the sedimentary record. Earth-Science

Reviews, 111, 56–81, doi: 10.1016/j.earscirev.2011.12.005.

Pomar, L., Obrador, A., Westphal, H., 2002. Sub-wavebase cross-bedded grainstones on a distally steepened carbonate ramp, upper Miocene, Menorca, Spain. Sedimentology, 49, 139–169, doi: 10.1046/j.1365-3091.2002.00436.x.

Pomar, L., Ward, W.C., 1994. Response of a Late Miocene Mediterranean reef platform to high-frequency eustasy. Geology, 22, 131-134, doi: doi: 10.1130/0091-7613(1994)022<0131:ROALMM>2.3.CO;2.

Pomar, L., Ward, W.C., 1995. Sea-level changes, carbonate production and platform architecture: the Llucmajor Platform, Mallorca, Spain. In: Haq, B.U. (ed.), Sequence Stratigraphy and Depositional Response to Eustatic, Tectonic and Climatic Forcing. Kluwer Academic Press, pp. 87–112.

Pomar, L., Ward, W.C., 1999. Reservoir-scale heterogeneity in depositional packages and diagenetic patterns on a reef-rimmed platform, Upper Miocene, Mallorca, Spain. American Association of Petroleum Geologists Bulletin, 83, 1759–1773.

Pomar, L., Ward, W.C., Green, D.G., 1996. Upper Miocene Reef Complex of the Llucmajor area, Mallorca, Spain. In: Franseen, E., Esteban, M., Ward, W.C., Rouchy, J.M. (eds), Models for Carbonate Stratigraphy from Miocene Reef Complexes of the Mediterranean regions. SEPM, Concepts in Sedimentology and Paleontology Series, 5, 191–225.

Pujalte, V., Schmitz, B., Baceta, J.I., 2014. Sea-level changes across the Paleocene–Eocene interval in the Spanish Pyrenees, and their possible relationship with North Atlantic magmatism. Palaeogeogr. Palaeoclimatol. Palaeoecol. 393, 45–60. doi:10.1016/j.palaeo.2013.10.016

Putnam, H.M., Stat, M., Pochon, X., Gates, R.D., 2012. Endosymbiotic flexibility associates with environmental sensitivity in scleractinian corals. Proc. R. Soc. B, 279, 4352–4361.

Racey, A., Al-Sayigh, A.R.S., Hanna, S., 2001. Biostratigraphy and Microfacies of the Jafnayn Formation (Late Palaeocene–Early Eocene) of northern Oman. International Conference on the Geology of Oman, Sultan Qaboos University, Muscat, 2001, Abstract. GeoArabia, v. 6, no. 2, p. 320–321.

Rasser, M.W., 2000. Coralline red algal limestones of the late Eocene Alpine Foreland basin in Upper Austria: component analysis, Facies and Palecology. Facies 42, 59– 92.

Rasser, M., Piller, W., 2004. Crustose algal frameworks from the Eocene Alpine foreland. Palaeogeogr., Palaeoclimatol., Palaeoecol., 206, 21–39, doi: 10.1016/j.palaeo.2003.12.018.

Raven, J.A., Hurd, C.L., 2012. Ecophysiology of photosynthesis in macroalgae. Photosynth Res, 113, 105–125.

Reich, S., Di Martino, E., Todd, J.A., Wesselingh, F.P., Renema, W., 2015. Indirect paleo-seagrass indicators (IPSIs): A review. Earth-Science Reviews 143, 161–186

Reiss, Z., Hottinger, L., 1984. The Gulf of Aqaba: Ecological Micropaleontology. Ecological Studies. vol 50. Springer-Verlag, Berlin.

Renema, W., 2005. Depth estimation using diameter-thickness ratios in larger benthic foraminifera. Lethaia 38, 137–141. doi:10.1080/00241160510013259

Ribes, M., Coma, R., Atkinson, M.J., Kinzie, R.A., 2003. Particle removal by coral reef communities: picoplankton is a major source of nitrogen. Mar. Ecol. Prog. Ser., 257, 13–23, doi: 10.3354/meps257013.

Richardson, K., Visser, A.W., Pedersen, F.B., 2000. Subsurface phytoplankton blooms fuel pelagic production in the North Sea. J. Plankton Res., 22, 1663–1671, doi: 10.1093/plankt/22.9.1663.

Riding, R., 2002. Structure and composition of organic reef and carbonate mud mounds: concepts and categories. Earth-Science Reviews, 58, 163–231, 137 Figs., doi: 10.1016/S0012-8252(01)00089-7.

Riebesell, U., 2004. Effects of CO_2 enrichment on marine phytoplankton. J. Oceanogr., 60, 719–729.

Riebesell, U., Wolf-Gladrow, D.A., Smetacek, V., 1993. Carbon dioxide limitation of marine phytoplankton growth rates. Nature, 361, 249–251.

Riegl, B., Piller, W.E., 2000. Reefs and coral carpets in the northern Red Sea as models for organism-environment feedback in coral communities and its reflection in growth fabrics. In: Insalaco, E., Skelton, P.W., Palmer, T.J. (eds), Carbonate platform systems: components and interactions. Geol. Soc., London, Spec. Publ., pp. 71–88.

Riordan, N.K., James, N.P., Bone, Y., 2011. Oligo–Miocene seagrass-influenced carbonate sedimentation along the temperate marine palaeoarchipelago, Padthaway Ridge, South Australia. Sedimentology, 59, 393– 418.

Roberts, H.H., Phipps, C.V., Effendi, L., 1987. *Halimeda* bioherms of the eastern Java Sea, Indonesia. Geology, 15, 371-374, doi: 10.1130/0091-7613(1987)15<371:hbotej>2.0.co;2.

Roberts, J.M., Wheeler, A.J., Freiwald, A., 2006. Reefs of the Deep: The Biology and Geology of Cold-Water Coral Ecosystems. Science, 312, 543–547, doi: 10.1126/science.1119861.

Rögl, F., Steininger, F. Müller, C., 1978. Middle Miocene salinity crisis and paleogeography of the Paratethys (Middle and Eastern Europe). Initial Reports Deep Sea Drill. Proj. 42, 985 – 990.

Romero, J., Caus, E., Rosell, J., 2002. A model for the palaeoenvironmental distribution of larger foraminifera based on late Middle Eocene deposits on the margin of the South Pyrenean basin (NE Spain). Palaeogeogr., Palaeoclimatol., Palaeoecol., 179, 43–56.

Rosen, B.R., 2000. Algal symbiosis, and the collapse and recovery of reef communities: Lazarus corals across the K–T boundary. In: Culver, S.J., Rawson, P.F. (eds), Biotic Response to Global Change: The Last 145 Million Years. Cambridge University Press, Cambridge, pp. 164–180.

Rossi, D., Semenza, E., 1958. Le scogliere oligoceniche dei Colli Berici. Ann. Univ. Ferrara (n.s.). Sez. IX. Sci. geol. Miner. 3, 49 – 70.

Rowan, R., 2004. Thermal adaptation in reef coral symbiont. Nature, 430, 742.

Royer, D.L., Pagani, M., Beerling, D.J., 2012. Geobiological constraints on Earth system sensitivity to CO_2 during the Cretaceous and Cenozoic. Geobiology 10, 298–310. doi:10.1111/j.1472-4669.2012.00320.x

Ruchonnet, C., 2006. Climatic and oceanographic evolution of the Mediterranean basin during the late Serravallian/early Tortonian (middle/late Miocene): the record from the Ragusa Platform (SE Sicily, Italy). Terre and Environnement, Université de Genève, 63, 156.

Ryan, J.P., Chavez, F.P., Bellingham, J.G., 2005. Physical-biological coupling in Monterey Bay, California: topographic influences on phytoplankton ecology. Mar. Ecol. Prog. Ser., 287, 23–32.

Salas, R., 1995. The basin margin in the Igualada area. In: Perejón, A., Busquets, P. (eds), Bioconstructions of the Eocene South Pyrenean Foreland Basin (Vic and Igualada areas) and of the Upper Cretaceous South Central Pyrenees (Tremp area). VII International Symposium on Fossil Cnidaria and Porifera, Field Trip C Guidebook, pp. 30–35.

Sanders, D., 1998. Tectonically controlled terrestrial to neritic deposition (Northern Calcareous Alps, Tyrol, Austria). Facies 39:139–178.

Sanders, D., Baron-Szabo, R.C., 2005. Scleractinian assemblages under sediment input: their characteristics and relation to the nutrient input concept. Palaeogeogr., Palaeoclimatol., Palaeoecol., 216, 139–181.

Sandstrom, H., Elliott, J.A., 1984. Internal tidae and solitons on the Scotian shelf: A nutrient pump at work. J. Geophys. Res., 89, 6415–6426.

Santisteban, C., Taberner, C., 1988. Sedimentary models of siliciclastic deposits and coral reef interactions. In: Doyle, L.J., Roberts, H.H. (eds), Carbonate–Clastic Transitions. Developments in Sedimentology, pp. 35–76.

Santodomingo, N., Renema, W. & Johnson, K.G., 2016. Understanding the murky history of the Coral Triangle: Miocene corals and reef habitats in East

Kalimantan (Indonesia). Coral Reefs, 1-17, doi: 10.1007/s00338-016-1427-y.

Scheibner, C., Reijmer, J.J.G., Marzouk, A.M., Speijer, R.P., Kuss, J., 2003. From platform to basin: the evolution of a Paleocene carbonate margin (Eastern Desert, Egypt). Int. J. Earth Sci., 92, 624–640.

Scheibner, C., Speijer, R.P., 2007. Decline of coral reefs during late Paleocene to early Eocene global warming. eEarth Discuss., 2, 133–150.

Scheibner, C., Speijer, R.P., 2008. Decline of coral reefs during late Paleocene to early Eocene global warming. eEarth, 3, 19–26, doi: 10.5194/ee-3-19-2008.

Sclater, J.G., Meinke, L., Bennet, A. & Murphy, C., 1985. The depth of the ocean trhough the Neogene. In: Kennett, J.P. (ed.), The Miocene Ocean: Paleogeography and Biogeography. GSA Memoir, pp. 1-19.

Scotti, A., Pineda, J., 2004. Observation of very large and steep internal waves of elevation near the Massachusetts coast. Geophys. Res. Lett., 31, L22307.

Serra-Kiel, J., Hottinger, L., Caus, E., Drobne, K., Ferrandez, C., Jauhri, A. K., Less, Gy., Pavlovec, R., Pignatti, J., Samsò, J. M., Schaub, H., Sirel, E., Strougo, A., Tambareau, Y., Tosquella, J., Zakrevskaya, E.J., 1998. Larger foraminiferal biostratigraphy of the Tethyan Paleocene and Eocene. Bull. Soc. géol. Fr. 169, 281–299.

Serra-Kiel, J., Travé, A., 1995. Lithostratigraphic and chronostratigraphic framework of the Bartonian sediments in the Vic and Igualada areas. In: Perejón, A., Busquets, P. (eds), Bioconstructions of the Eocene South Pyrenean Foreland Basin (Vic and Igualada areas) and of the Upper Cretaceous South Central Pyrenees (Tremp area). VII International Symposium on Fossil Cnidaria and Porifera, Field Trip C Guidebook, pp. 11–14.

Serra-Kiel, J., Travé, A., Mató, E., Saula, E., Ferràndez, C., Busquets, P., Tosquella, J., Vergés, J., 2003. An inventory of the Marine and Transitional Middle/Upper Eocene Units of the Southeastern Pyrenean Foreland Basin (NE Spain). Geol. Acta 1, 177 – 200. doi:10.1344/105.000001609

Shabafrooz, R., Mahboubi, A., Vaziri-Moghaddam, H., Ghabeishavi, A., Moussavi-Harami, R., 2014. Depositional architecture and sequence stratigraphy of the Oligo–Miocene Asmari platform; Southeastern Izeh Zone, Zagros Basin, Iran. Facies, 61, 1–32, doi: 10.1007/s10347-014-0423-3.

Spring, D., Hansen, O., 2004. The influence of platform morphology and sea level on the development of a carbonate sequence: the Harash Formation, Eastern Sirt Basin, Libya. Geological Society, London, Special Publications; 1998; v. 132; p. 335-353. DOI: 10.1144/GSL.SP.1998.132.01.19

Stanley Jr., G.D., 2003. The evolution of modern corals and their early history. Earth-Science Reviews, 60, 195–225.

Stanley Jr., G.G., 2006. Photosymbiosis and the evolution of modern coral reefs. Science, 312, 857–858.

Stanley, D.J. (ed.), 1972. The Mediterranean Sea: a natural sedimentation laboratory. Dowden, Hutchinson & Ross, Inc., Stroudsburg, Pa, 765pp.

Taberner, C., Bosence, D.W.J., 1995. An Eocene biodetrital mud-mound from the southern Pyrenean foreland basin, Spain: an ancient analogue for Florida Bay mounds? In: Monty, C.L.V., Bosence, D.W.J., Bridges, P.H., Pratt, B.R. (eds), Carbonate Mud-Mounds - Their Origin and Evolution. IAS Spec. Publ., pp. 423–437.

Taberner, C., Dinarès-Turell, J., Giménez, J., Docherty, C., 1999. Basin infill architecture and evolution from magnetostratigraphy cross-basin correlations in the southeastern Pyrenean foreland basin. Geol. Soc. Am. Bull., 11, 1155–1174.

Taylor, J., 1992. The energetics of breaking events in a resonantly forced internal wave field. J. Fluid Mechanics, 239, 309– 340, doi: 10.1017/S0022112092004427.

Teichberg, M., Fricke, A., Bischof, K., 2013. Increased physiological performance of the calcifying green macroalga *Halimeda opuntia* in response to experimental nutrient enrichment on a Caribbean coral reef. Aquatic Botany, 104: 25-33, http://dx.doi.org/10.1016/j.aquabot.2012.09.010

Ter Kuile, B., Erez, J., 1984. In situ growth late experiments on the symbiont-bearing foraminifera *Amphistegina lobifer*a and *Amphisorus hemprichii*. J. Foramin. Res., 14, 262–76.

Tripati, A., Elderfield, H., 2005. Deep-sea temperature and circulation changes at the Paleocene–Eocene Thermal Maximum. Science, 308, 1894–1898.

Tucker, M.E., Wright, V.P., 1990. Carbonate Sedimentology. Blackwell Sci. Public.

Van Buchem, F.S.P., Allan, T.L., Laursen, G.V., Lotfpour, M., Moallemi, A., Monibi, S., Motiei, H., Pickard, N.A.H., Tahmasbi, A.R., Vedrenne, V., Vincent, B., 2010. Regional stratigraphic architecture and reservoir types of the Oligo–Miocene deposits in the Dezful Embayment (Asmari and Pabdeh Formations) SW Iran. In: Van Buchem, F.S.P., Gerdes, K.D., Esteban, M. (eds), Mesozoic and Cenozoic Carbonate Systems of the Mediterranean and the Middle East: Stratigraphic and Diagenetic Reference Models. Geol. Soc., London, Spec. Publ., 329, 219–263.

Van Dam, J.A., 1997. The small mammals from the upper Miocene of the Teruel-Alfambra region (Spain): paleobiology and paleoclimatic reconstructions. Universiteit Uthrech.

Van Dam, J.A., 2006. Geographic and temporal patterns in the late Neogene (12–3†Ma) aridification of Europe: The use of small mammals as paleoprecipitation proxies. Palaeogeogr., Palaeoclimatol., Palaeoecol., 238, 190–218.

Van Dam, J.A., Weltje, G.J., 1999. Reconstruction of the Late Miocene climate of Spain using rodent palaeocommunity successions: an application of end-member modelling. Palaeogeogr., Palaeoclimatol., Palaeoecol., 151, 267–305.

Vandenberghe, N., Hilgen, F.J., Speijer, R.P., Ogg, J.G., Gradstein, F.M., Hammer, O., Hollis, C.J., Hooker, J.J., 2012. Chapter 28 – The Paleogene Period. In: Gradstein, F.M., Ogg, J.G., Schmitz, M., Ogg, G. (eds), The Geologic Time Scale. Elsevier, Boston, pp. 855–921.

Vannucci, G., Quaranta, F., Piazza, M., Fravega, P., 2003. The Oligocene Reefal facies of Bric San Bernardino (Millesimo, NW Italy). Atti Ticinensi di Scienze della Terra, 44, 35–44.

Vaulot, D., Marie, D., Olson, R.J., Chisholm, S.W., 1995. Growth of *Prochlorococcus*, a photosynthetic prokaryote, in the Equatorial Pacific Ocean. Science, 268, 1480–1482.

Verdugo, P., Alldredge, A.L., Azam, F., Kirchman, D.L., Passow, U., Santschi, P.H., 2004. The oceanic gel phase: a bridge in the DOM–POM continuum. Marine Chemistry, 92, 67– 85.

Veron, J.E.N., 1995. Corals in Space and Time; the Biogeography and Evolution of the Scleractinians. Cornell University Pres, Sidney.

Vescogni, A., Bosellini, F., Cipriani, A., Gürler, G., Ilgar, A., Paganelli, E., 2016. The Dağpazarı carbonate platform (Mut Basin, Southern Turkey): Facies and environmental reconstruction of a coral reef system during the Middle Miocene Climatic Optimum. Palaeogeogr., Palaeoclimatol., Palaeoecol., 410, 213–232. http://dx.doi.org/10.1016/j.palaeo.2014.05.040.

Viebahn, J.P., von der Heydt, A. S., Le Bars, D., Dijkstra, H. A., 2016. Effects of Drake Passage on a strongly eddying global ocean. Paleoceanography, v. 31, p. 564–581. DOI: 10.1002/2015PA002888

Vissier de, J.P., 1991. Clay mineral stratigraphy of Miocene to recent marine sediments in the Central Mediterranean. Geologica Ultraiectina, 75. 245 pp.

Wall, M., Putchim, L., GM., S., Jantzen, C., Khokiattiwong, S., Richter, C., 2015. Large-amplitude internal waves benefit corals during thermal stress. Proc. R. Soc. B., 282, 20140650, doi: 10.1098/rspb.2014.0650.

Wall, M., Schmidt, G.M., Janjang, P., Khokiattiwong, S., Richter, C., 2012. Differential Impact of Monsoon and Large Amplitude Internal Waves on Coral Reef Development in the Andaman Sea. PLoS ONE, 7, e50207, doi: 10.1371/journal.pone.0050207.

Wheeler, A., Beyer, A., Freiwald, A., de Haas, H., Huvenne, V., Kozachenko, M., Olu-Le Roy, K., Opderbecke, J., 2007. Morphology and environment of cold-water coral carbonate mounds on the NW European margin. Int. J. Earth Sci., 96, 37–56, doi: 10.1007/s00531-006-0130-6.

White, M., Dorschel, B., 2010. The importance of the permanent thermocline to the cold water coral carbonate mound distribution in the NE Atlantic. Earth Planet. Sc. Lett., 296, 395–402, doi: 10.1016/j.epsl.2010.05.025.

Wilson, J.L., 1975. Carbonate Facies in Geologic History. Springer-Verlag, New York, N.Y.

Wilson, M.E.J., 2008. Global and regional influences on equatorial shallow-marine carbonates during the Cenozoic. Palaeogeogr., Palaeoclimatol., Palaeoecol., 265, 262–274, doi: http://dx.doi.org/10.1016/j.palaeo.2008.05.012.

Wolanski, E., Colin, P., Naithani, J., Deleersnijder, E., Golbuu, Y., 2004. Large amplitude, leaky, island-generated internal waves around Palau, Micronesia. Estuar. Coast. Shelf S., 60, 705–716.

Wood, R., 1998. The ecological evolution of reefs. Annu. Rev. Ecol. Syst. 1998. 29:179–206

Wood, R., 1999. Reef Evolution. Oxford University Press, New York.

Yang, Y., Gao, K., 2003. Effects of CO_2 concentrations on the freshwater microalgae, *Chlamydomonas reinhardtii*, *Chlorella pyrenoidosa*, and *Scenedesmus obliquus* (Chlorophyta). J. Appl. Phycol., 15, 1–11.

Yordanova, E.K., 2004. Morphoclines of living operculinid foraminifera based on quantitative characters. Micropaleontology. doi:10.2113/50.2.149

Yordanova, E.K., Hohenegger, J., 2007. Studies on settling, traction and entrainment of larger benthic foraminiferal tests: implications for accumulation in shallow marine sediments. Sedimentology, 54, 1273–1306, doi: 10.1111/j.1365-3091.2007.00881.x.

Zachos, J.C., Dickens, G.R. & Zeebe, R.E., 2008. An early Cenozoic perspective on greenhouse warming and carbon-cycle dynamics. Nature, 451, 279-283.

Zachos, J.C., McCarren, H., Murphy, B., Röhl, U., Westerhold, T., 2010. Tempo and scale of late Paleocene and early Eocene carbon isotope cycles: Implications for the origin of hyperthermals. Earth Planet. Sc. Lett., 299, 242–249.

Zachos, J.C., Pagani, M., Sloan, L., Thomas, E., Billups, K., 2001. Trends, rhythms, and aberrations in global climate 65 Ma to Present. Science, 292, 686–693, doi: 10.1126/science.1059412

Zamagni, J., Košir, A., Mutti, M., 2009. The first microbialite—coralmounds in the Cenozoic (Uppermost Paleocene) from the Northern Tethys (Slovenia): environmentally triggered phase shifts preceding the PETM? Palaeogeogr., Palaeoclimatol., Palaeoecol., 274, 1–17.

Zamagni, J., Mutti, M., Kosir, A., 2008. Evolution of shallow benthic communities during the late Palaeocene–earliest Eocene transition in the Northern Tethys (SW Slovenia): Facies, v. 54, p. 25–43.

Zamagni, J., Mutti, M., Košir, A., 2012. The evolution of mid Paleocene–early Eocene coral communities: How to survive during rapid global warming. Palaeogeogr., Palaeoclimatol., Palaeoecol., 317–318, 48–65, doi: http://dx.doi.org/10.1016/j.palaeo.2011.12.010.

CASE STUDIES

Age/*name*	**Platform type**	**Coral buildups**	**Reef type sensu Riding (2002)**	**Buildup position**	**Light zone**	**Buildup main components**	**Minor components**	**Authors**		**References**
								Direct field work	**Field rev.**	
PALEOCENE										
Lower Danian *Ma–Da sequence*	Homoclinal ramp	m-thick biostromes	Cluster	Outer ramp	Mesophotic	Solenomeris Red algae	corals	Yes		Baceta, 1996; Baceta et al., 2005, 2011; Aguirre et al., 2007
Middle Danian *Da-1 sequence*	Low angle ramp with bulge	5-10m thick bioherms	Cluster	Bulging mid-outer ramp	Mesophotic	Corals Red algae	Foraminifers Bryozoans Solenoporaceans peyssonnelids	Yes		Baceta et al., 2005
Upper Danian *Da-2, Lizarraga reef*	Rimmed shelf	180m-thick stack	Cluster	Platform margin	Mesophotic	Corals Red algae peyssonnelids	Heterozoan carbonates	Yes		Baceta et al., 2005; Aguirre et al., 2007
U. Selandian-m. Thanetian *Sel/Th-1 sequence*	Low angle ramp	5–35m thick few 100'm wide	Cluster	Mid- to outer-ramp	Mesophotic	Red algae peyssonnelids	corals bryozoans LBF	Yes		Baceta et al., 2005, 2011; Aguirre et al., 2007
Late Thanetian *Th-2 sequence*	Low angle ramp	Few-m thick	Cluster			Red algae Microbial carbonates	Corals Encrusting foraminifers	Yes		Einchenseer, 1987 Baceta et al. (2011
EOCENE										
Early Ypresian (Ilerdian) *Merli*	LBF-dominated ramp	45–60m thick	Cluster	Tectonic highs	Mesophotic	Corals Solenomeris	Red algae *Discocyclina*	No	Yes	Einchenseer, 1987, 2003; Einchenseer and Luterbacher, 1992
Lutetian *Grustan*	LBF-dominated ramps	Discrete coral bearing mounds	Spaced cluster	Mid- to distal ramp	Mesophotic	LBF	Corals	No	Yes	Barnolas et al., 1991; Arbues et al., 2011;
Lutetian	LBF-	Discrete	Spaced	Mid- to distal	Mesophotic	Mud	Corals	Yes		This paper

Meson Ligüerre	dominated ramps	coral bearing mounds	cluster	ramp		oysters				
Late Lutetian *Buil Level*	LBF-dominated ramps	Discrete coral bearing mud mounds	Corals on top of the mound	Mid- to distal ramp	Mesophotic	Nummulites, other LBF	corals	Yes		Mateu-Vicens et al., 2012; this paper
Bartonian-Priabonian *Ebro Foreland Basin*	Siliciclastic ramps – Prodelta clays Sandy lobes	Few 10's m thick Few 100'sm wide	Cluster	Associated to monospecific LBF banks: *Nummulites, Discocyclina*	Mesophotic	Corals	Red algae, LBF	no	Yes	Busquets et al., 1985; Santisteban and Taberner, 1988; Alvarez et al., 1994; Taberner and Bosence, 1995; Hendry et al., 1999; Romero et al., 2002
Priabonian *Yeste-Rasal*	Prodelta clays	20-30m tick, up to 50m few 100's m wide	Cluster		Mesophotic	Corals	Red algae foraminifers	Yes		Morsilli et al., 2012
OLIGOCENE										
Rupelian *Castelgomberto Lumignano*	Low angle ramp	Few m thick	Cluster	Middle- outer ramp	Mesophotic	Corals	Foraminifers Red algae	Yes		Geister and Ungaro (1977; Bassi and Nebelsick (2010), Bortot (2012), Nebelsick et al. (2013)
Early Chattian *Castro Limestone*	Ramp at the margin of a continental block	10'sm tick	Cluster	Middle ramp	Mesophotic	Corals Large Rotalid foraminifers	Red algae	Yes		Pomar et al. (2014)
Early Chattian *Asmari Fm*	Low angle ramp	50–60 m thick 100–200 m wide	Cluster	Middle ramp	Mesophotic	Corals, Red algae	Large Rotalid foraminifers	No	No	Van Buchem et al. (2010) Shabafrooz et al. (2014)
Late Chattian *Portobadisco Calcarenite*	Low angle ramp	Few m thick	Cluster	Middle ramp	Mesophotic	Corals Rotalid foraminifers	Red algae	Yes		Pomar et al. (2014)

MIOCENE										
Burdigalian *Latium-Abruzzi*	Low angle ramp	m-sized	Cluster	Inner-middle ramp	Euphotic-mesophotic (seagrass canopy)	Corals Red algae	LBF	No	No	Brandano, 2001; Brandano and Corda, 2002; Brandano, 2003; Pomar et al., 2004, 2012 a
Burdigalian *Sedini*	Low-angle to distally steepened ramp	m-sized	Cluster	Inner-middle ramp	Euphotic-mesophotic (seagrass canopy)	Red algae & corals	LBF, barnacles, bryozoans	No	No	Benisek et al., 2009, 2010
Burdigalian-Langhian *Ermenek and Mut*	Low-angle to distally steepened ramp	10's m thick	Cluster	Toe of slope to middle ramp	Mesophotic to euphotic (seagrass canopy)	Red algae & corals	LBF, epiphytic sbf	No	No	Bassant, 1999; Bassant et al., 2004, 2005; Janson, 2002; Janson et al., 2007, 2010; Pomar et al., 2012 a
Early Tortonian *Ragusa*	Low-angle ramp	no	Isolated colonies	Inner ramp	Mesophotic to euphotic (seagrass canopy)	Sbf, red algae	Corals	No	No	Ruchonnet, 2006
Early Tortonian *Migjorn*	distally steepened ramp	no	Resedimented isolated colonies	-	-	-		Yes		Pomar, 2001 b; Pomar et al., 2002
Upper Tortonian-lower Messinian *Llucmajor*	Reef rimmed platform	100 m thick 20 km progradation	Framework	Platform margin	Euphotic	Corals	Red algae, foraminifers Green algae	Yes		Pomar, 1991, 1993; Pomar and Ward, 1994, 1995, 1999; Pomar et al., 1996; 2012 a

Most Cenozoic coral buildups were small and developed in the mesophotic zone

Strengthening of thermal gradients is essential for plankton catchers such as corals

Large coral buildups only developed during cooling episodes in tropical settings

Eocene LBF diversification and abundance coincide with warming and low pCO_2.

Eurythermal red algae predominated in the mesophotic zone when $\delta^{13}C$ was high

Seagrass epiphytic production dominated the shallow seas for most of the Cenozoic

Chlorozoan sediment association developed after the Late Miocene

Before Late Miocene, corals and red algae (rhodozoan) thrived in low light conditions